

**DINUCLEAR COMPLEXES OF COPPER, SILVER
AND GOLD BRIDGED BY
PHOSPHORUSPYRIDYL AND
PHOSPHORUSNAPHTHYRIDYL
LIGANDS**

by

Barry Warwick B.Sc. (Hons), (Natal)

**A thesis submitted in partial fulfillment of the requirements for the degree of Master of
Science in the Faculty of Science, University of Natal, Pietermaritzburg**

Department of Chemistry

University of Natal

Pietermaritzburg

January 1995

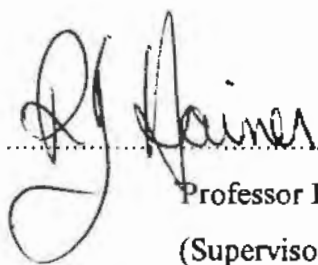
DECLARATION

I hereby certify that this research is the result of my own investigation which has not already been accepted in substance for any degree and is not being submitted in candidature for any other degree.

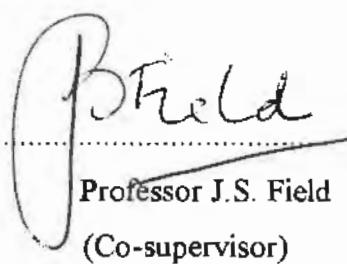
Signed: 

B. Warwick

I hereby certify that this statement is correct.

Signed: 

Professor R.J. Haines
(Supervisor)

Signed: 

Professor J.S. Field
(Co-supervisor)

Department of Chemistry
University of Natal
Pietermaritzburg
January 1995

CONTENTS

Acknowledgements	i
Abbreviations	ii
Summary	iii
CHAPTER 1: The Coordination Chemistry of 2,6-Bis(diphenylphosphino)pyridine, Phenylbis(2-pyridyl)phosphine and 2,7-Bis(diphenylphosphino)naphthyridine.	1
1.1 The Coordination Chemistry of 2,6-Bis(diphenylphosphino)pyridine {(Ph ₂ P) ₂ py}.	1
1.1.1 Monodentate (Ph ₂ P) ₂ py	2
1.1.2 Chelating (Ph ₂ P) ₂ py	3
1.1.3 Bridging (Ph ₂ P) ₂ py	3
1.1.3.1 Mode 6	4
1.1.3.2 Mode 7	4
1.1.3.3 Mode 8	6
1.1.4 Conclusion	10
1.2 The Coordination Chemistry of Phenylbis(2-pyridyl)phosphine {PhP(py) ₂ }.	11
1.2.1 Coordination of PhP(py) ₂ to Cu(I), Ag(I) and Au(I)	13
1.2.2 Coordination of PhP(py) ₂ to Pd(II)	14
1.2.3 Coordination of PhP(py) ₂ to Rh(I)	15
1.2.4 Coordination of PhP(py) ₂ to Mo(0) and Mo(II)	16
1.2.5 Coordination of PhP(py) ₂ to Co(II)	18
1.2.6 Conclusion	18

1.3	The Coordination Chemistry of 2,7-Bis(diphenylphosphino)naphthyridine {(Ph ₂ P) ₂ napy} and 2,7-Bis(diphenylphosphino)-4-methyl-naphthyridine {(Ph ₂ P) ₂ menapy}	20
CHAPTER 2: Dinuclear 2,6-Bis(diphenylphosphino)pyridine Ligand-Bridged Complexes of Cu(I) and Ag(I).		23
2.1	Aims	23
2.2	Synthesis of 2,6-Bis(diphenylphosphino)pyridine	23
2.3	Synthesis and Characterisation of 2,6-Bis(diphenylphosphino)pyridine Derivatives of Copper(I)	24
2.3.1	Reaction of [Cu(MeCN) ₄](PF ₆) with (Ph ₂ P) ₂ py: Synthesis and Crystal Structure of [Cu ₂ {μ-(Ph ₂ P) ₂ py} ₃](PF ₆) ₂ (1)	24
2.3.2	Reaction of [Cu(η ² -bipy)(MeCN) ₂](PF ₆) with (Ph ₂ P) ₂ py: Synthesis and Crystal Structure of [Cu ₂ {μ-(Ph ₂ P) ₂ py} ₂ (η ² -bipy) ₂](PF ₆) ₂ (2)	27
2.4	Synthesis and Characterisation of 2,6-Bis(diphenylphosphino)pyridine Derivatives of Silver(I)	30
2.4.1	Reaction of [Ag(COD) ₂](BF ₄) with (Ph ₂ P) ₂ py: Synthesis and Crystal Structure of [Ag ₂ {μ-(Ph ₂ P) ₂ py} ₃](PF ₆) ₂ (3)	30
2.4.2	Reaction of [Ag(η ² -bipy)(COD)](BF ₄) with (Ph ₂ P) ₂ py: Synthesis and Characterisation of [Ag ₂ {μ-(Ph ₂ P) ₂ py} ₂ (η ² -bipy) ₂](BF ₄) ₂ (4)	33
2.5	Photophysical Studies on the [Cu ₂ {μ-(Ph ₂ P) ₂ py} ₃](PF ₆) ₂ (1) and [Ag ₂ {μ-(Ph ₂ P) ₂ py} ₃](BF ₄) ₂ (3) Complexes	35
2.5.1	Introduction	35
2.5.2	Photophysical Studies on the [Cu ₂ {μ-(Ph ₂ P) ₂ py} ₃](PF ₆) ₂ (1) Complex	37
2.5.3	Photophysical Studies on the [Ag ₂ {μ-(Ph ₂ P) ₂ py} ₃](BF ₄) ₂ (3) Complex	38
2.6	Conclusion	40
2.7	Experimental	41
2.7.1	Synthesis of [Cu ₂ {μ-(Ph ₂ P) ₂ py} ₃](PF ₆) ₂ (1)	41
2.7.2	Synthesis of [Cu ₂ {μ-(Ph ₂ P) ₂ py} ₂ (η ² -bipy) ₂](PF ₆) ₂ (2)	41

2.7.3 Synthesis of $[\text{Ag}_2\{\mu\text{-(Ph}_2\text{P)}_2\text{py}\}_3](\text{BF}_4)_2$ (3)	42
2.7.4 Synthesis of $[\text{Ag}_2\{\mu\text{-(Ph}_2\text{P)}_2\text{py}\}_2(\eta^2\text{-bipy})_2](\text{BF}_4)_2$ (4)	42
2.7.5 Single Crystal X-ray Diffraction Study of $[\text{Cu}_2\{\mu\text{-(Ph}_2\text{P)}_2\text{py}\}_3](\text{PF}_6)_2$ (1)	44
2.7.6 Single Crystal X-ray Diffraction Study of $[\text{Cu}_2\{\mu\text{-(Ph}_2\text{P)}_2\text{py}\}_2(\eta^2\text{-bipy})_2](\text{PF}_6)_2$ (2)	44
2.7.7 Single Crystal X-ray Diffraction Study of $[\text{Ag}_2\{\mu\text{-(Ph}_2\text{P)}_2\text{py}\}_3](\text{BF}_4)_2$ (3)	44

CHAPTER 3: Dinuclear Phenylbis(2-pyridyl)phosphine

Ligand-Bridged Complex of Cu(I). 76

3.1 Aims	76
3.2 Synthesis of Phenylbis(2-pyridyl)phosphine	76
3.3 Synthesis and Characterisation of $[\text{Cu}_2\{\mu\text{-PhP(py)}_2\}_2(\text{MeCN})_2](\text{PF}_6)_2$ (5)	77
3.3.1 Reaction of $[\text{Cu}(\text{MeCN})_4](\text{PF}_6)$ with PhP(py)_2 : Synthesis of $[\text{Cu}_2\{\mu\text{-(Ph}_2\text{P)}_2\text{py}\}_2(\text{MeCN})_2](\text{PF}_6)_2$ (5)	77
3.3.2 Crystal Structure of $[\text{Cu}_2\{\mu\text{-PhP(py)}_2\}_2(\text{MeCN})_2](\text{PF}_6)_2 \cdot 2\{(\text{CH}_3)_2\text{CO}\}$	77
3.4 Reaction of PhP(py)_2 with Silver(I) and Gold(I)	78
3.5 Conclusion	78
3.6 Experimental	80
3.6.1 Synthesis of $[\text{Cu}_2\{\mu\text{-PhP(py)}_2\}_2(\text{MeCN})_2](\text{PF}_6)_2$ (5)	80
3.6.2 Reaction of PhP(py)_2 with $[\text{Ag}(\text{COD})_2](\text{BF}_4)$	80
3.6.3 Reaction of PhP(py)_2 with $[\text{Au}(\text{MeCN})_2](\text{BF}_4)$	80
3.6.4 Single Crystal X-ray diffraction study of $[\text{Cu}_2\{\mu\text{-PhP(py)}_2\}_2(\text{MeCN})_2](\text{PF}_6)_2 \cdot 2\{(\text{CH}_3)_2\text{CO}\}$	83

CHAPTER 4: Dinuclear 2,7-Bis(diphenylphosphino)-

4-methylnaphthyridine Ligand-Bridged Complexes of Cu(I), Ag(I) and Au(I). 90

4.1	Aims	90
4.2	Synthesis of 2,7-Bis(diphenylphosphino)-4-methylnaphthyridine	90
4.3	Reactions Involving $[\text{Cu}(\text{MeCN})_4](\text{PF}_6)$ as Precursor	92
4.3.1	Reaction of $[\text{Cu}(\text{MeCN})_4](\text{PF}_6)$ with $(\text{Ph}_2\text{P})_2\text{menapy}$ Synthesis and Characterisation of $[\text{Cu}_2\{\mu-(\text{Ph}_2\text{P})_2\text{menapy}\}_2(\text{H}_2\text{O})_4](\text{PF}_6)_2$ (6)	92
4.3.2	Reaction of $[\text{Cu}(\text{MeCN})_4](\text{PF}_6)$ with a mixture of $(\text{Ph}_2\text{P})_2\text{menapy}$ and $\text{Ph}_2\text{POmenapyPPh}_2$: Synthesis and Crystal Structure of $[\text{Cu}_2(\mu-\text{Ph}_2\text{PmenapyPPh}_2)_2(\text{MeCN})_2](\text{PF}_6)_2$ (7)	93
4.4	Reaction of $[\text{Ag}(\text{COD})_2](\text{BF}_4)$ with $(\text{Ph}_2\text{P})_2\text{menapy}$: Synthesis and Characterisation $[\text{Ag}_2\{\mu-(\text{Ph}_2\text{P})_2\text{menapy}\}_2(\text{H}_2\text{O})_4](\text{BF}_4)_2$ (8)	94
4.5	Reaction of $(\text{Ph}_2\text{P})_2\text{menapy}$ with Gold(I)	96
4.6	Conclusion	97
4.7	Experimental	98
4.7.1	Synthesis of 2-Amino-7-hydroxy-4-methyl-1,8-naphthyridine	98
4.7.2	Synthesis of 2,7-Dihydroxy-4-methyl-1,8-naphthyridine	98
4.7.3	Synthesis of 2,7-Dichloro-4-methyl-1,8-naphthyridine	98
4.7.4	Synthesis of 2,7-Bis(diphenylphosphino)-4-methyl- 1,8-naphthyridine $\{(\text{Ph}_2\text{P})_2\text{menapy}\}$	99
4.7.5	Synthesis of $[\text{Cu}_2\{\mu-(\text{Ph}_2\text{P})_2\text{menapy}\}_2(\text{H}_2\text{O})_4](\text{PF}_6)_2$ (6)	99
4.7.6	Synthesis of $[\text{Cu}_2(\mu-\text{Ph}_2\text{PmenapyPPh}_2)_2(\text{MeCN})_2](\text{PF}_6)_2$ (7)	100
4.7.7	Synthesis of $[\text{Ag}_2\{\mu-(\text{Ph}_2\text{P})_2\text{menapy}\}_2(\text{H}_2\text{O})_4](\text{BF}_4)_2$ (8)	100
4.7.8	Reaction of $(\text{Ph}_2\text{P})_2\text{menapy}$ with $[\text{Au}(\text{MeCN})_2](\text{SbF}_6)$	100
APPENDIX A: General Experimental Details		103
1	Instrumentation	103
2	Experimental Techniques	103
3	Crystal Structure Determinations	104
APPENDIX B: Sources of Chemicals		106
REFERENCES		107

ACKNOWLEDGEMENTS

I wish to thank Professors R.J. Haines and J.S. Field for their guidance and input throughout the course of this investigation.

I am also grateful to the following persons:

- Professor M.M. Zulu of the University of Zululand for his guidance and help with the emission measurements done in Chapter 2;
- Miss Niyum Ramesar for her contribution to all X-ray crystal structure determinations with regard to data collection and computation;
- Mr Martin Watson and Mrs Zöe Hall for the recording of NMR spectra and for running GCMS samples;
- Mr Dave Crawley for technical assistance and for the drawing of diagrams;
- Mr Hashim Desai for elemental analysis and technical assistance, and Mr Raj Somaru for elemental analysis;
- Mr Paul Forder for the construction and repair of glassware;
- The Faculty of Science Mechanical Instrument Workshop for the repair of mechanical instrumentation;
- The Foundation for Research and Development and the University of Natal for financial support;
- My research colleagues in both laboratories for often triggering ideas that did and did not work;
- A special thank you to Campbell Parry for his help with the mounting and selection of single crystals.

I wish to thank my family for their support.

A special thank you to Lucille for encouraging me and standing by me throughout; your patience is appreciated.

LIST OF ABBREVIATIONS AND SYMBOLS

Abbreviation	Description
Ph	phenyl
py	pyridine
bipy	2,2'-bipyridine
napy	1,8-naphthyridine
menapy	4-methyl-1,8-naphthyridine
dppm	bis(diphenylphosphino)methane
Ppy ₃	tris(2-pyridyl)phosphine
Ph ₂ Ppy	2-(diphenylphosphino)pyridine
(Ph ₂ P) ₂ py	2,6-bis(diphenylphosphino)pyridine
PhP(py) ₂	phenylbis(2-pyridyl)phosphine
(Ph ₂ P) ₂ napy	2,7-bis(diphenylphosphino)naphthyridine
(Ph ₂ P) ₂ menapy	2,7-bis(diphenylphosphino)-4-methylnaphthyridine
Ph ₂ POmenapyPPh ₂	2-diphenylphosphineoxide-7-diphenylphosphine-4-methylnaphthyridine
(Ph ₂ PO) ₂ menapy	2,7-bis(diphenylphosphineoxide)-4-methylnaphthyridine
COD	1,5-cyclooctadiene
NBD	norbornadiene
MeCN	acetonitrile
THF	tetrahydrofuran
δ	chemical shift in parts per million
λ	wavelength
{ ¹ H}	proton noise decoupled
NMR	nuclear magnetic resonance
nm	nanometre
cm ⁻¹	reciprocal centimetre
Å	angstrom
ν	frequency
°C	degree celsius
g	gram
IR	infrared
ml	millilitre
mg	milligram
mmol	millimole
max	maximum

SUMMARY

Chapter 1 serves as an introduction to the synthesis and characterisation of copper(I), silver(I) and gold(I) complexes of the 2,6-bis(diphenylphosphino)pyridine $\{(\text{Ph}_2\text{P})_2\text{py}\}$, phenylbis(2-pyridyl)phosphine $\{\text{PhP}(\text{py})_2\}$ and 2,7-bis(diphenylphosphino)-4-methylnaphthyridine $\{(\text{Ph}_2\text{P})_2\text{menapy}\}$ ligands. A review of all the transition metal complexes of these ligands is presented. Particular attention is given to the modes of coordination that these ligands may adopt when coordinating to a transition metal.

Chapter 2 describes the reactions of the $(\text{Ph}_2\text{P})_2\text{py}$ ligand with $[\text{Cu}(\text{MeCN})_4](\text{PF}_6)$, $[\text{Cu}(\eta^2\text{-bipy})(\text{MeCN})_2](\text{PF}_6)$, $[\text{Ag}(\text{COD})_2](\text{BF}_4)$ and $[\text{Ag}(\eta^2\text{-bipy})(\text{COD})](\text{BF}_4)$ which result in the formation of the dinuclear ligand-bridged complexes $[\text{Cu}_2\{\mu\text{-(Ph}_2\text{P)}_2\text{py}\}_3](\text{PF}_6)_2$ (**1**), $[\text{Cu}_2\{\mu\text{-(Ph}_2\text{P)}_2\text{py}\}_2(\eta^2\text{-bipy})_2](\text{PF}_6)_2$ (**2**), $[\text{Ag}_2\{\mu\text{-(Ph}_2\text{P)}_2\text{py}\}_3](\text{BF}_4)_2$ (**3**) and $[\text{Ag}_2\{\mu\text{-(Ph}_2\text{P)}_2\text{py}\}_2(\eta^2\text{-bipy})_2](\text{BF}_4)_2$ (**4**) respectively. The X-ray crystal structures of **1** and **3** reveal that the three $(\text{Ph}_2\text{P})_2\text{py}$ ligands bridge the two metal atoms coordinating solely through their phosphorus atoms with the result that each metal atom has a trigonal geometry. The nitrogen atoms of the pyridines are left free resulting in a fairly open cavity in the centre of the complex cation. The cavity sizes are calculated to be 4.9 and 5.3 Å for the copper and silver complexes respectively. It is suggested that these open cavities should be able to bind metal ions such as Cu^+ and Ag^+ . Absorption and emission spectra were recorded for both complexes **1** and **3** and the effects of the addition of Cu^+ and Ag^+ ions on the emission spectra are discussed. These studies reveal that the emission spectra are indeed perturbed upon the addition of metal ions. The X-ray crystal structure of **2** has been determined confirming the presence of two bridging $(\text{Ph}_2\text{P})_2\text{py}$ ligands and a 2,2'-bipyridyl ligand chelating at each copper atom. Thus each copper atom has a tetrahedral geometry. Based on characterisation data the structure of **4** is proposed to be similar to the structure of **2** with a tetrahedral geometry around each silver atom.

Chapter 3 describes the reaction of the ligand $\text{PhP}(\text{py})_2$ with $[\text{Cu}(\text{MeCN})_4](\text{PF}_6)$, $[\text{Ag}(\text{COD})_2](\text{BF}_4)$ and $[\text{Au}(\text{MeCN})_2](\text{SbF}_6)$. The reaction with $[\text{Cu}(\text{MeCN})_4](\text{PF}_6)$ afforded the dinuclear complex $[\text{Cu}_2\{\mu\text{-PhP}(\text{py})_2\}_2(\text{MeCN})_2](\text{PF}_6)_2$ (**5**) as a crystalline solid. Single crystals

were obtained and a X-ray crystal structure revealed the first example of $\text{PhP}(\text{py})_2$ coordinating in a bridging fashion that has been characterised in this way. The ligand coordinates to the one copper atom through its phosphorus atom and to the other copper atom through its two nitrogen atoms. The coordination around each copper atom is completed by an acetonitrile ligand resulting in a tetrahedral geometry around each copper atom. The reaction of the ligand with silver(I) and gold(I) precursors resulted in ill-defined products that could not be isolated and characterised.

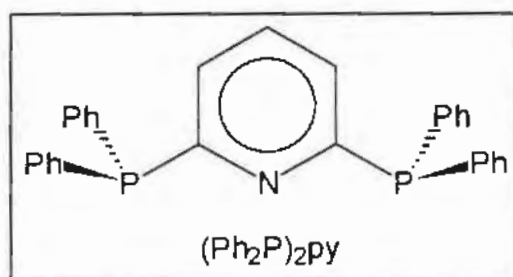
Chapter 4 describes the synthesis of the novel $(\text{Ph}_2\text{P})_2\text{menapy}$ ligand and its reactions with $[\text{Cu}(\text{MeCN})_4](\text{PF}_6)$, $[\text{Ag}(\text{COD})_2](\text{BF}_4)$ and $[\text{Au}(\text{MeCN})_2](\text{SbF}_6)$. The ligand proved difficult to isolate as a pure solid and is extremely reactive towards oxygen. Reaction of the ligand with copper(I) and silver(I) precursors afforded crystalline solids which were characterised as $[\text{Cu}_2\{\mu-(\text{Ph}_2\text{P})_2\text{menapy}\}_2(\text{H}_2\text{O})_4](\text{PF}_6)_2$ (**6**) and $[\text{Ag}_2\{\mu-(\text{Ph}_2\text{P})_2\text{menapy}\}_2(\text{H}_2\text{O})_4](\text{BF}_4)_2$ (**8**). The structures of these two complexes are thought to consist of the two metal atoms bridged by two naphthyridyl ligands each bonded to the metal *via* the phosphorus atoms with the coordination at each metal being completed by two water molecules. This would result in a tetrahedral arrangement around each metal atom. To reduce the uncertainty of the proposed structures attempts at growing single crystals of both **6** and **8** were attempted. Single crystals were obtained in both cases but they proved to be too small for X-ray crystal structure analysis. Reaction of a mixture of the oxidised ligand 2-diphenylphosphineoxide-7-diphenylphosphine-4-methylnaphthyridine ($\text{Ph}_2\text{POmenapyPPh}_2$) and $(\text{Ph}_2\text{P})_2\text{py}$ resulted in the formation of a mixture of **6** and $[\text{Cu}_2(\mu\text{-Ph}_2\text{POmenapyPPh}_2)_2(\text{MeCN})_2](\text{PF}_6)_2$ (**7**). A single crystal X-ray diffraction study has been performed on **7** which shows that the oxidised ligands bridge the two copper atoms; coordination at the one copper is through the phosphorus atom while the ligand chelates at the second copper *via* the oxygen and the adjacent naphthyridine nitrogen atom. The coordination at each copper atom is completed by an acetonitrile ligand resulting in a tetrahedral geometry. Reaction of the ligand with the gold(I) precursor afforded ill-defined products that could not be isolated.

CHAPTER 1

The Coordination Chemistry of 2,6-Bis(diphenylphosphino)pyridine, Phenylbis(2-pyridyl)phosphine and 2,7-Bis(diphenylphosphino)naphthyridine.

Much of the work described in this thesis involves the synthesis and characterisation of complexes of the metals of the copper triad containing the ligands 2,6-bis(diphenylphosphino)pyridine¹, phenylbis(2-pyridyl)phosphine² and 2,7-bis(diphenylphosphino)naphthyridine³. These three ligands all have in common P-C(sp²)-N linkages with the sequence of the linkages being different in each case. It is therefore of interest to compare the potential coordination modes of these three ligands. Also, the survey of their potential coordinating modes in this chapter serves as an introduction to the study of their coordination behaviour reported in subsequent chapters.

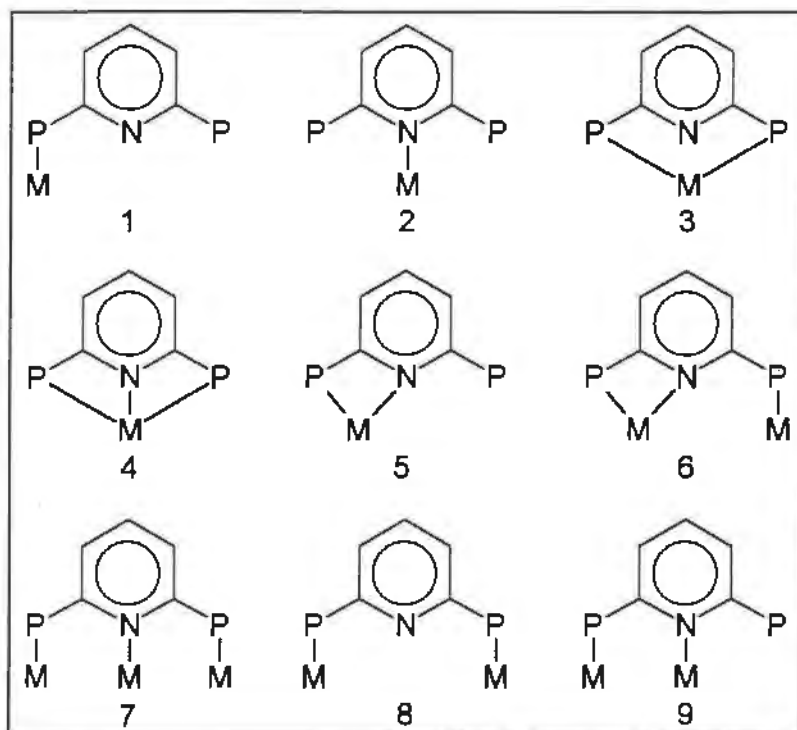
1.1 The Coordination Chemistry of 2,6-Bis(diphenylphosphino)pyridine $\{(Ph_2P)_2py\}$



To date the coordination chemistry of $(Ph_2P)_2py$ has not been studied anywhere near as extensively as the 2-diphenylphosphinopyridine (Ph_2Ppy) ⁴ and bis(diphenylphosphino)methane $(dppm)$ ⁵ ligands. $(Ph_2P)_2py$ is related to the latter two ligands and similar modes of coordination would be expected although $(Ph_2P)_2py$ has greater coordination possibilities due to its being a potential tridentate as opposed to a bidentate ligand.

In principle there are nine different modes of coordination that the $(Ph_2P)_2py$ ligand could adopt (Scheme 1), two monodentate modes (1 and 2), three chelating modes (3, 4 and 5) and four bridging modes (6, 7, 8, and 9). A tenth coordination mode with the two phosphorus

atoms coordinated to a metal atom and the nitrogen atom of the pyridine ring coordinated to a different metal atom could be included but the rigidity of the ligand makes this mode of coordination highly unlikely.



Scheme 1. Possible modes of coordination of the $(\text{Ph}_2\text{P})_2\text{py}$ ligand.

1.1.1 Monodentate $(\text{Ph}_2\text{P})_2\text{py}$

As noted above there are two ways in which the $(\text{Ph}_2\text{P})_2\text{py}$ ligand can coordinate to a transition metal in a monodentate fashion. It can either coordinate through one of the phosphorus atoms or alternatively through the nitrogen atom of the pyridine ring. Although examples of the latter mode of coordination exist for the Ph_2Ppy ⁶ ligand there are no examples of $(\text{Ph}_2\text{P})_2\text{py}$ coordinating in this way. The fact that there are no examples of this mode of coordination can be most likely ascribed to the limited amount of research that has been carried out involving the $(\text{Ph}_2\text{P})_2\text{py}$ ligand.

Examples of complexes containing the $(\text{Ph}_2\text{P})_2\text{py}$ ligand coordinating in a monodentate fashion through a phosphorus atom do exist although none of these complexes has been verified X-ray crystallographically⁷. For example by refluxing $(\text{Ph}_2\text{P})_2\text{py}$ with $\text{M}(\text{CO})_6$ ($\text{M} = \text{Cr}, \text{Mo}, \text{W}$) in

diglyme the corresponding monometallic complexes $M[(Ph_2P)_2py](CO)_5$ with one uncoordinated phosphorus are formed as intermediates *en route* to the corresponding dinuclear complexes. The monodentate coordination mode of the ligand in these complexes was established by means of $^{31}P\{^1H\}$ NMR spectroscopy, the spectrum exhibiting two singlets at δ 21 and -3 corresponding to the coordinated and uncoordinated phosphorus atoms respectively. The only other example of $(Ph_2P)_2py$ coordinating in a monodentate fashion is that of $Pd[(Ph_2P)_2py]_2Cl_2$ ⁸. Again the identity of this complex was determined by $^{31}P\{^1H\}$ NMR spectroscopy, two singlets at δ 28 and -1.6 which correspond to the coordinated and uncoordinated phosphorus atoms respectively being observed. This complex exists in equilibrium with the trimer $Pd_3[\mu-(Ph_2P)_2py]_3Cl_6$ when excess $(Ph_2P)_2py$ is added.

1.1.2 Chelating $(Ph_2P)_2py$

There are three possible ways in which $(Ph_2P)_2py$ can function as a chelating ligand. Firstly both phosphorus atoms could coordinate to the same metal atom, secondly the two phosphorus atoms and the nitrogen atom could coordinate to the same metal atom, and thirdly one phosphorus atom and the nitrogen atom could coordinate to the same metal atom.

There are no examples of $(Ph_2P)_2py$ coordinating in any of these chelating modes. This can be attributed to the inflexibility of the ligand arising from the location of the pyridine ring. Chelation would result in the geometries around each donor atom being highly strained making the resulting complex unstable. The last chelating mode would seem to be the most likely as there are examples of Ph_2Ppy chelating in this way⁹.

1.1.3 Bridging $(Ph_2P)_2py$

The most common modes of coordination adopted by the $(Ph_2P)_2py$ ligand are the bridging modes of coordination. There are four possible ways in which $(Ph_2P)_2py$ can coordinate to metal atoms in a bridging fashion as shown in 6, 7, 8 and 9. Of these four possible bridging modes only mode 9 has not been reported in the chemical literature. Examples of all the other bridging modes are known and have been verified by single crystal X-ray crystal structure

determinations. These complexes will now be discussed.

1.1.3.1 Mode 6

The complex cation $[\text{Rh}_2\{\mu\text{-(Ph}_2\text{P)}_2\text{py}\}_2(\mu\text{-CO})(\mu\text{-I})]^+$ (Fig. 1) is the only example of a complex containing the $(\text{Ph}_2\text{P})_2\text{py}$ ligand in which part of the ligand is coordinating in a chelating fashion through the one phosphorus atom and the nitrogen atom forming a four membered PCNM ring at one rhodium while the second phosphorus atom serves to link the second rhodium atom¹⁰. The Rh...Rh separation is 2.568 (2) Å. This complex can be divided into two fragments *viz* a chelate ring portion and a bridging portion, these resembling the coordination of the Ph_2Ppy ligand in $\text{Ru}(\text{Ph}_2\text{Ppy})(\text{CO})_2\text{Cl}_2$ ⁹ and $\text{Rh}_2(\mu\text{-Ph}_2\text{Ppy})(\mu\text{-CO})\text{Cl}_2$ ¹¹ respectively.

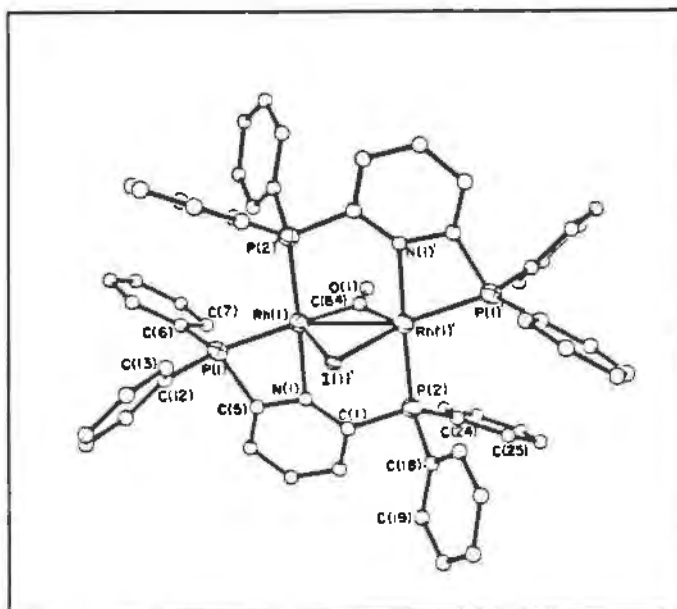


Figure 1. Perspective drawing of $[\text{Rh}_2\{\mu\text{-(Ph}_2\text{P)}_2\text{py}\}_2(\mu\text{-CO})(\mu\text{-I})]^+$.

1.1.3.2 Mode 7

In the complex $\text{Rh}_4[\mu\text{-(Ph}_2\text{P)}_2\text{py}]_2(\mu\text{-CO})(\text{CO})_2(\mu\text{-Cl})_2\text{Cl}_2$ ¹² (Fig. 2) each $(\text{Ph}_2\text{P})_2\text{py}$ ligand bridges three rhodium atoms. The ligands are *trans* to one another and are separated by a one Rh-Rh unit translation. The Rh(2)-Rh(2)' separation is 2.594 (2) Å and is indicative of the

presence of a metal-metal bond. The Rh(1)-Rh(2) separation is 2.921 (2) Å which is significantly longer than the Rh(2)-Rh(2)' distance, but is shorter than nonbonded Rh...Rh separations. A related complex $\text{Rh}_4[\mu-(\text{Ph}_2\text{P})_2\text{py}]_2(\mu-\text{SO}_2)(\text{CO})_2(\mu-\text{Cl})_2\text{Cl}_2$ where the bridging carbonyl has been replaced by a bridging sulfur dioxide has been reported, although this complex has not been characterised structurally¹³.

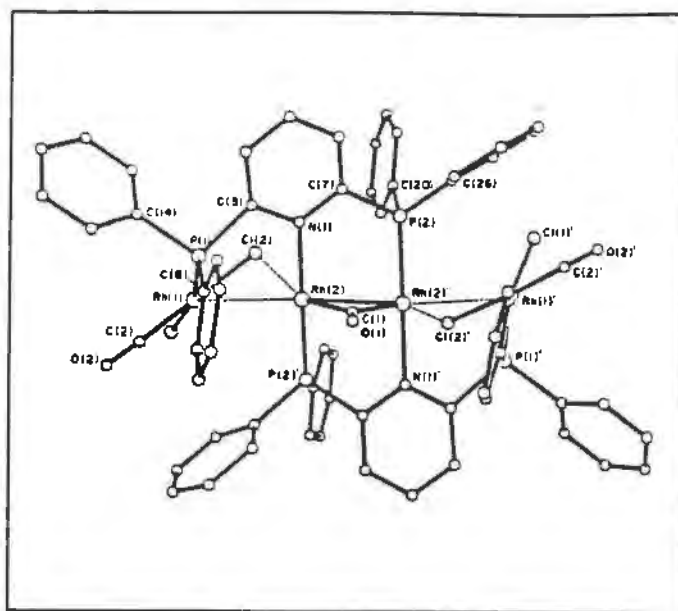


Figure 2. Perspective drawing of $\text{Rh}_4[\mu-(\text{Ph}_2\text{P})_2\text{py}]_2(\mu-\text{CO})(\text{CO})_2(\mu-\text{Cl})_2\text{Cl}_2$.

The complex $\text{Rh}_2\text{Sn}_2(\text{CO})_2\text{Cl}_6[\mu-(\text{Ph}_2\text{P})_2\text{py}]_2$ ¹⁴ (Fig. 3) is the only example in the literature of a complex containing the $(\text{Ph}_2\text{P})_2\text{py}$ ligand coordinated to two different types of metal in the same complex. The Rh(1) atom is six-coordinate, Rh(2) is five coordinate and the Sn(1) atom is five coordinate. The Rh(1)-Sn(1) and Rh(2)-Sn(1) distances are nearly equal being 2.601 (2) and 2.588 (2) Å respectively. There is a considerable difference between the Sn(1)-N(1) and Sn(1)-N(2) distances of 2.62 (1) and 2.42 (1) Å respectively. The longer of these is very long compared with the Sn-N distances in structurally characterised tin(II) phthalocyanine complexes (2.25 (1), 2.24 (1), 2.25 (1) and 2.27 (1) Å). Nevertheless it would still appear that both nitrogens are bonded to Sn(1) particularly as both pyridine rings tilt towards Sn(1).

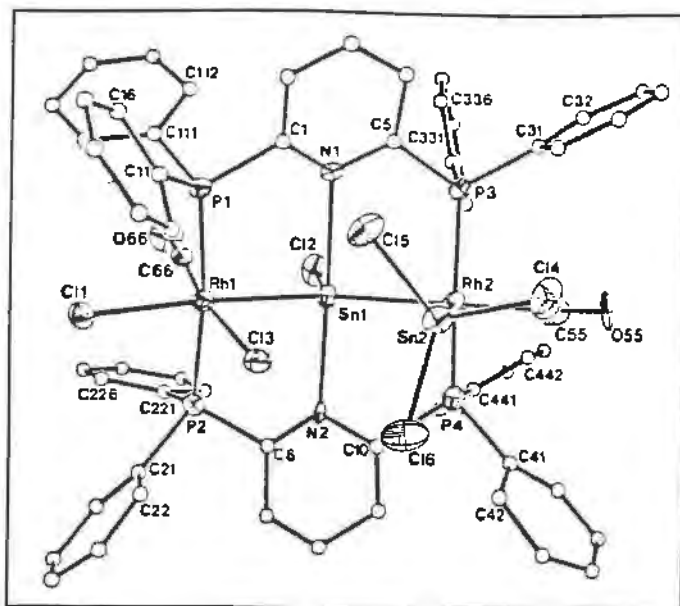


Figure 3. Perspective drawing of $\text{Rh}_2\text{Sn}_2(\text{CO})_2\text{Cl}_6[\mu\text{-(Ph}_2\text{P)}_2\text{py}]_2$.

1.1.3.3 Mode 8

This particular bridging mode is well characterised. All of the structures described below have in common metal atoms separated by distances significantly greater than expected for a direct metal-metal interaction.

The first example is the complex $\text{Pd}_3\text{Cl}_6[\mu\text{-(Ph}_2\text{P)}_2\text{py}]_3$ ¹² which contains an internal, non-planar, 18-membered ring (Fig. 4). Two of the palladium ions are bound by *cis*-disposed pairs of chlorine atoms and phosphorus atoms, while the remaining palladium is bonded to *trans*-disposed pairs of chlorine and phosphorus atoms.

The two rhodium atoms, the four phosphorus atoms, and the two nitrogen atoms in $[\text{Rh}_2\{\mu\text{-(Ph}_2\text{P)}_2\text{py}\}_2(\text{CO})_2(\text{CH}_3\text{OH})\text{Cl}][\text{PF}_6]^{13}$ (Fig. 5) form a nearly planar framework. Each of the two rhodium atoms is four-coordinate and planar with *trans*-disposed phosphorus atoms. The coordination at Rh(1) is completed by a carbonyl group and a chloride ligand *trans* to each other while that at Rh(2) is completed by a carbonyl and a methanol group also *trans* to each other. The Rh(1)-Rh(2) separation is 5.425 (2) Å.

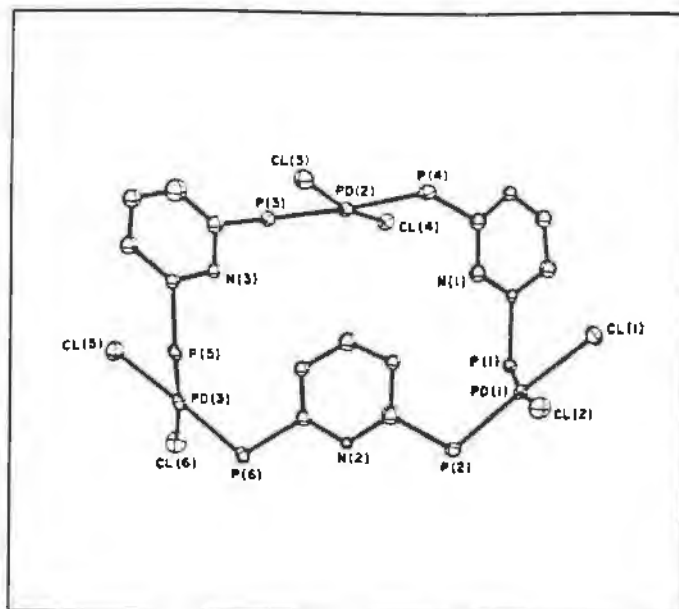


Figure 4. Perspective drawing of $\text{Pd}_3\text{Cl}_6[\mu\text{-(Ph}_2\text{P)}_2\text{py}]_3$.

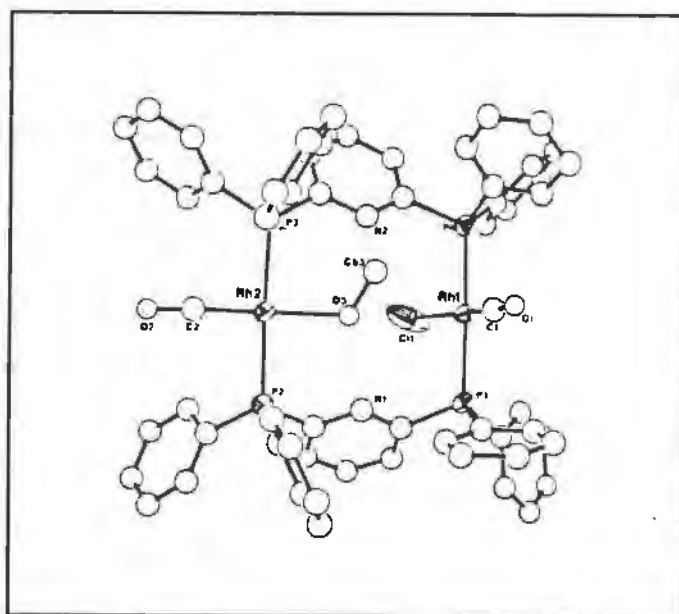


Figure 5. Perspective drawing of $[\text{Rh}_2\{\mu\text{-(Ph}_2\text{P)}_2\text{py}\}_2(\text{CO})_2(\text{CH}_3\text{OH})\text{Cl}]^+$.

The platinum atoms in the complex $\text{Pt}_2[\mu\text{-(Ph}_2\text{P)}_2\text{py}]_2\text{Cl}_4$ ⁸ (Fig. 6) have square-planar coordination. The nonbonded Pt-Pt separation is 8.2 Å. The PpyP portions of the ring are planar and parallel to each other the separation between the planes being 3.01 Å. Each of the nitrogen lone pairs is directed into space above the other pyridine ring.

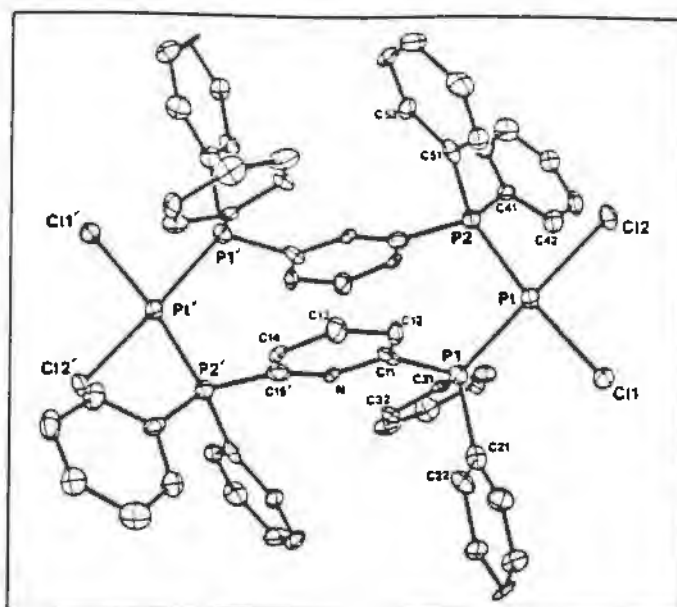


Figure 6. Perspective drawing of $\text{Pt}_2[\mu\text{-(Ph}_2\text{P)}_2\text{py}]_2\text{Cl}_4$.

The structure of the complex $\text{Pt}_2[\mu\text{-(Ph}_2\text{P)}_2\text{py}]_2\text{I}_4$ ⁸ is similar to that of $\text{Pt}_2[\mu\text{-(Ph}_2\text{P)}_2\text{py}]_2\text{Cl}_4$ but there are significant differences (Fig. 7). The platinum atoms have planar geometry. The Pt-P distances are longer than in the chloro complex and this is a consequence of the greater *trans*

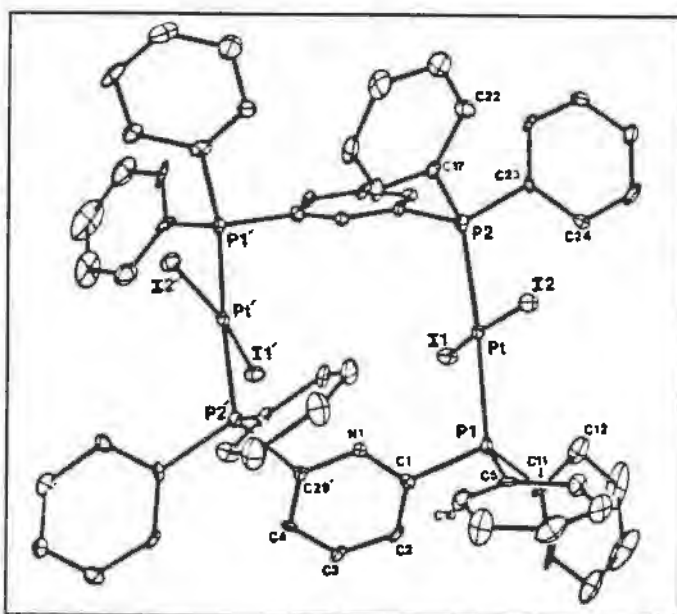


Figure 7. Perspective drawing of $\text{Pt}_2[\mu\text{-(Ph}_2\text{P)}_2\text{py}]_2\text{I}_4$.

influence of the iodo compared to the chloro-groups, thus the Pt-P bonds *trans* to phosphorus in $\text{Pt}_2[\mu\text{-(Ph}_2\text{P)}_2\text{py}]_2\text{I}_4$ {Pt-P(1) 2.307 (4) and Pt-P(2) 2.306 (5) Å} is longer than the Pt-P bond

when it is *trans* to Cl in $\text{Pt}_2[\mu-(\text{Ph}_2\text{P})_2\text{py}]_2\text{Cl}_4$ {Pt-P(1) 2.252 (7) and Pt-P(2) 2.278 (7) Å}. The Pt...Pt separation is 5.33 Å. The PpyP units are planar and the two pyridyl planes are inclined at an angle of 71.9°. A fairly open cavity exists in the centre of the molecule.

The coordination around each gold atom in the complex $[\text{Au}_2\{\mu-(\text{Ph}_2\text{P})_2\text{py}\}_3](\text{PF}_6)_2^{15}$ is essentially trigonal planar with P-Au-P angles ranging from 115.8(1) to 122.1(1)° (Fig. 8). The Au...Au separation is 4.866 Å which suggests no metal-metal interaction. This complex contains a quoted cavity with a size of about 4.8-5.0 Å in diameter. This particular complex has interesting photophysical properties and exhibits room-temperature photoluminescence in the solid state as well as in solution. The absorption spectrum of $[\text{Au}_2\{\mu-(\text{Ph}_2\text{P})_2\text{py}\}_3](\text{PF}_6)_2$ in acetonitrile is dominated by a broad absorption band tailing from 250 to 360nm. The absorption band from 300 to 360nm is assigned to the $(5d_{x^2-y^2}, 5d_{xy}) - (6p_z, \pi^*)^{15}$ transitions. Upon excitation of the complex at 300 to 360 nm, two emissions centred at 415 and 520 nm are observed. The higher energy emission is attributed to arise from the intraligand excited state while the low energy emission is considered to arise from two possible states, the spin forbidden $(6p_z, \pi^*) - (5d_{x^2-y^2}, 5d_{xy})$ transition or a metal perturbed intraligand $(\pi, \pi^*) - (\pi^2)$ transition. The emission spectra of this complex is perturbed in the presence of

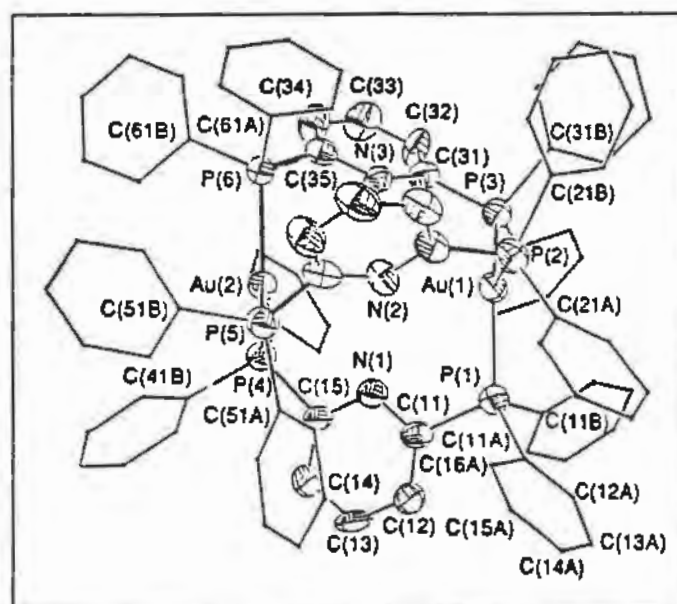


Figure 8. Perspective drawing of $[\text{Au}_2\{\mu-(\text{Ph}_2\text{P})_2\text{py}\}_3]^{2+}$.

$\text{CF}_3\text{CO}_2\text{H}$, AgCF_3SO_3 and $[\text{Cu}(\text{MeCN})_4](\text{PF}_6)$ with a substantial enhancement in intensity of the 520 nm emission and a red shift in its energy in the presence of the Cu^1 cation. This is thought to result from the copper cation being trapped in the cavity that exists in the $[\text{Au}_2\{\mu\text{-(Ph}_2\text{P)}_2\text{py}\}_3](\text{PF}_6)_2$ complex, this property enables this complex to be used as a sensor for the copper cation.

Other examples of $(\text{Ph}_2\text{P})_2\text{py}$ coordinating by bridging through the phosphorus atoms only (mode 9) are known and are now described. No X-ray crystal structures have been reported for any of these complexes. Treatment of $\text{Rh}_2(\text{CO})_4(\mu\text{-Cl})_2$ with $(\text{Ph}_2\text{P})_2\text{py}$ in benzene has been found to yield a mixture of compounds consisting of the *cis* and *trans* rotameric isomers of $\text{Rh}_2\{\mu\text{-(Ph}_2\text{P)}_2\text{py}\}_2(\text{CO})_2\text{Cl}_2$ and an ionic, chloro-bridged complex identified as $[\text{Rh}_2(\mu\text{-Cl})(\text{CO})_2\{\mu\text{-(Ph}_2\text{P)}_2\text{py}\}_2]\text{Cl}^{14}$ (Fig. 9). None of these compounds could be isolated and they were characterised by $^{31}\text{P}\{^1\text{H}\}$ NMR spectroscopy, IR spectroscopy and conductivity studies.

Refluxing $(\text{Ph}_2\text{P})_2\text{py}$ with $\text{M}(\text{CO})_6$ ($\text{M} = \text{Cr, Mo, W}$) in diglyme was shown to yield the bimetallic species $\text{M}_2[(\text{Ph}_2\text{P})_2\text{py}]_2(\text{CO})_{10}^7$. The proposed structures being deduced from elemental analysis and $^{31}\text{P}\{^1\text{H}\}$ NMR spectroscopy.

1.1.4 Conclusion

From the previous discussion it is clear that the bridging modes are the most common modes of coordination that the $(\text{Ph}_2\text{P})_2\text{py}$ ligand will adopt when coordinating to transition metal atoms. This can be attributed to the rigidity of the ligand due to the location of the pyridine ring which would result in strained four-membered PCNM rings if chelation to a transition metal was to occur. Of the bridging modes, mode 8 with the two phosphorus atoms each coordinated to a different metal atom and the nitrogen of the pyridine ring remaining free, is the most common mode of coordination. This results in complexes with open cavities in which there is potential for binding reactions to occur with metal ions as occurs for $\text{Rh}_2\text{Sn}_2(\text{CO})_2\text{Cl}_6[\mu\text{-(Ph}_2\text{P)}_2\text{py}]_2$ and $[\text{Au}_2\{\mu\text{-(Ph}_2\text{P)}_2\text{py}\}_3](\text{PF}_6)_2$.

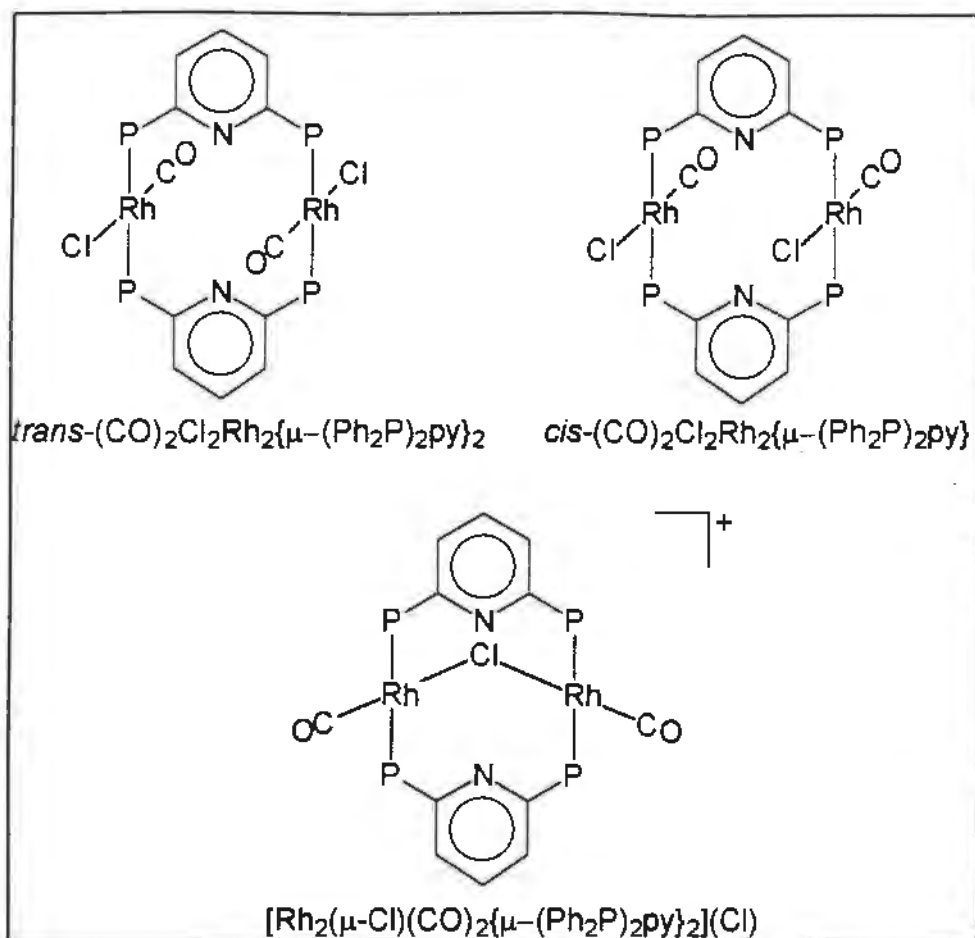
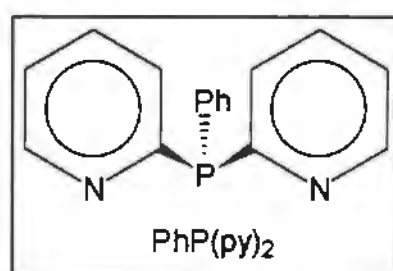


Figure 9. Complexes formed upon reaction of $(Ph_2P)_2py$ with $Rh_2(CO)_4(\mu-Cl)_2$.

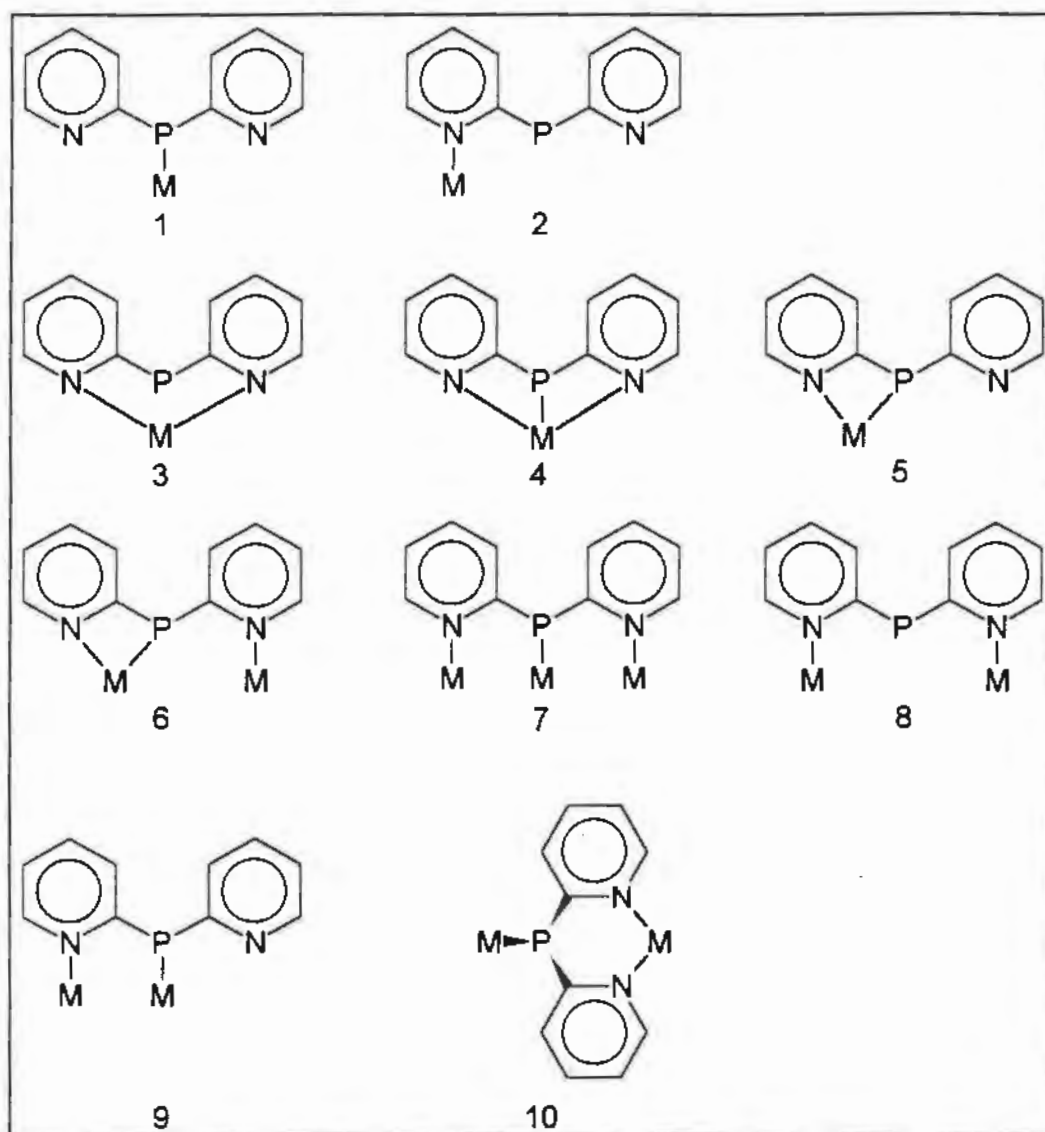
1.2 The Coordination Chemistry of Phenylbis(2-pyridyl)phosphine $\{PhP(py)_2\}$



Although the phosphorus-pyridyl ligand $PhP(py)_2$ is similar to Ph_2Ppy there have been very few reports of its use as a ligand. It is expected to have similar modes of coordination to that of Ph_2Ppy as well as more extensive ones due to it being a potentially tridentate ligand, with the phosphorus atom and the two nitrogen atoms of the pyridine rings all being capable of coordinating to metal atoms. This ligand should also coordinate to transition metals in

interesting ways because it has two pyridine moieties which provide two hard donor atoms for coordination as opposed to one in the Ph_2Ppy ligand.

In principle there are ten different modes of coordination that the $\text{PhP}(\text{py})_2$ ligand can adopt (Scheme 2); two monodentate modes (1 and 2), three chelating modes (3, 4 and 5) and five bridging modes (6, 7, 8, 9 and 10).



Scheme 2. Possible modes of coordination of the $\text{PhP}(\text{py})_2$ ligand.

As indicated above the coordination chemistry of $\text{PhP}(\text{py})_2$ to transition metals has not been studied as extensively as the coordination chemistry of other pyridylphosphine ligands such as Ph_2Ppy and $(\text{Ph}_2\text{P})_2\text{py}$ and this has led to a limited base from which to discuss its differing

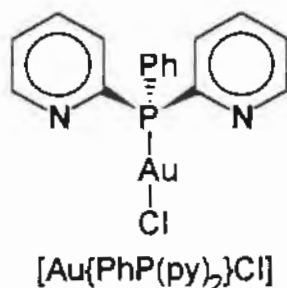
modes of coordination. It is therefore preferable to discuss the reaction of $\text{PhP}(\text{py})_2$ with a particular metal rather than under headings of differing modes of coordination.

It must also be noted from the outset that the structures of most of the complexes containing $\text{PhP}(\text{py})_2$ are merely proposed structures *i.e.* structures that are not confirmed by an X-ray crystal structure determination. As a result there may be some uncertainty about any conclusions that are reached about the coordination geometries of the $\text{PhP}(\text{py})_2$ ligand.

1.2.1 Coordination of $\text{PhP}(\text{py})_2$ to $\text{Cu}(\text{I})$, $\text{Ag}(\text{I})$ and $\text{Au}(\text{I})$

$\text{PhP}(\text{py})_2$ forms colourless 1:1 complexes with both CuCl and AgCl ¹⁶. The structures of these two complexes are uncertain but solubility and spectroscopic studies have provided some clues as to the nature of the coordination of the $\text{PhP}(\text{py})_2$ ligand to the metal atoms in these complexes. It is thought that the copper complex is a coordination polymer due to its insolubility. The silver complex is soluble in chloroform while $^{31}\text{P}\{^1\text{H}\}$ NMR spectroscopy indicates that the phosphorus atom of the $\text{PhP}(\text{py})_2$ coordinates to the silver atom. The structure of the product of an analogous reaction involving Ph_2Ppy was determined X-ray crystallographically and this revealed a tetrameric species with the Ph_2Ppy ligand bonded to the silver atom through the phosphorus atom only. It is thought that the $\text{PhP}(\text{py})_2$ silver complex adopts a similar structure.

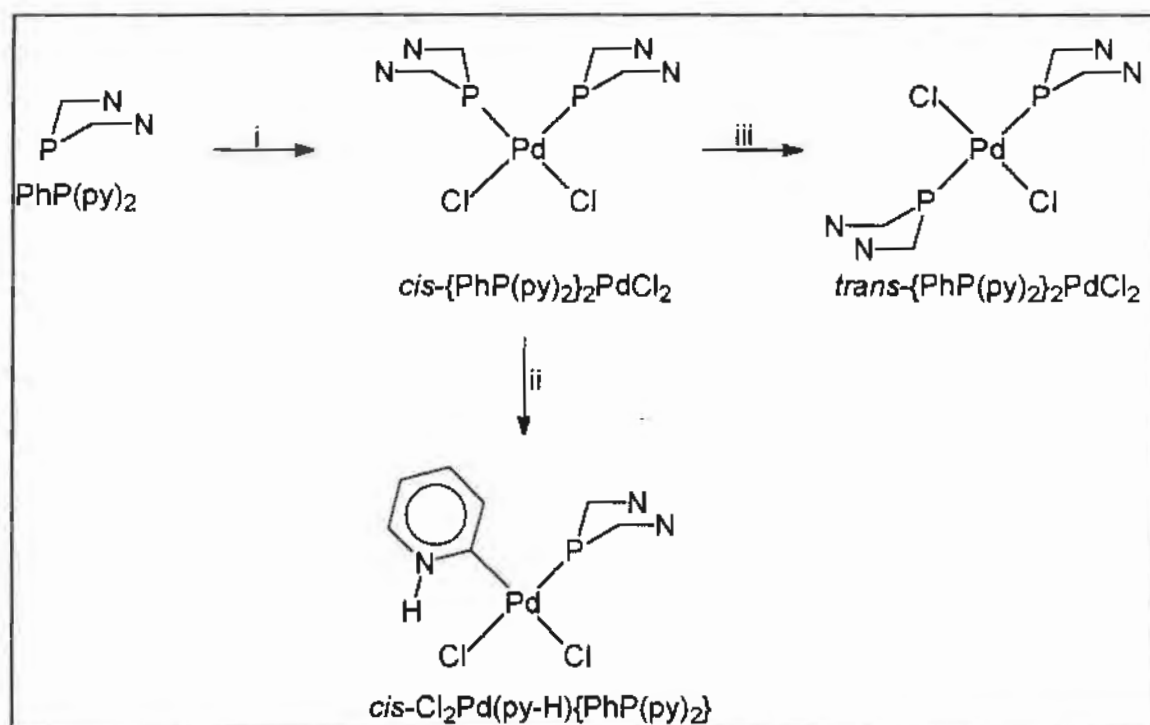
$\text{PhP}(\text{py})_2$ produces a stable 1:1 complex on reaction with $(\text{CO})\text{AuCl}$ ¹⁷. Carbon monoxide is liberated in the process with the ligand coordinating exclusively through the phosphorus. The complex is thought to be a monomer with the gold atom retaining a coordination number of two and having a linear geometry.



All of the complexes formed on reaction of $\text{PhP}(\text{py})_2$ with CuCl , AgCl or AuCl have $\text{PhP}(\text{py})_2$ coordinating in a monodentate fashion with phosphorus as the exclusive coordination site of the ligand. These are examples of coordinating mode 1 (Scheme 2).

1.2.2 Coordination of $\text{PhP}(\text{py})_2$ to $\text{Pd}(\text{II})$

Reaction of $\text{PhP}(\text{py})_2$ with Na_2PdCl_4 in MeOH at 25°C leads to the formation of two products, the major product being $\text{cis}\{-\text{PhP}(\text{py})_2\}_2\text{PdCl}_2$ and the minor one being $\text{cis}\{-\text{PhP}(\text{py})_2\}(\text{py-H})\text{PdCl}_2$ ¹⁸. When the same reaction is run above 50°C in the presence of excess $\text{PhP}(\text{py})_2$ $\text{trans}\{-\text{PhP}(\text{py})_2\}_2\text{PdCl}_2$ is formed (Scheme 3).



Scheme 3. i = $\text{Na}_2\text{PdCl}_4/\text{CH}_3\text{OH}/25^\circ\text{C}$; ii = $\text{CH}_3\text{OH}/\Delta$; iii = excess $\text{PhP}(\text{py})_2/\text{CH}_3\text{OH}/50^\circ\text{C}$.

The $\text{cis}\{-\text{PhP}(\text{py})_2\}_2\text{PdCl}_2$ complex is unusual in that it is the first example of an isolated, nonchelated cis -bis(triarylphosphine)palladium(II) complex. The reason for the formation of the cis instead of the trans complex at temperatures below 50°C is that this structure allows potential for charge transfer to occur between two of the pyridine rings of the $\text{PhP}(\text{py})_2$ ligands coordinated to the palladium. In particular on examining the structure of the $\text{cis}\text{-PhP}(\text{py})_2\text{PdCl}_2$

complex it can be seen that the N(1) and N(4) rings are approximately coplanar, with a dihedral angle of 7.1° and an inter-ring distance of 3.40 \AA (Fig. 10); this arrangement of the two pyridine rings sets up a condition for a possible charge transfer thereby stabilising the complex.

An interesting feature of the *cis*- $\{\text{PhP}(\text{py})_2\}(\text{py-H})\text{PdCl}_2$ complex is that the ring bound directly to the palladium is a C-bonded pyridine ylide, rather than an N-bonded pyridine.

All of the complexes formed by reacting $\text{PhP}(\text{py})_2$ with palladium(II) precursors have the $\text{PhP}(\text{py})_2$ ligand coordinating to the palladium in a monodentate fashion with the phosphorus atom functioning as the sole donor site. These palladium complexes serve as further examples of the $\text{PhP}(\text{py})_2$ ligand coordinating by Mode 1 (Scheme 2).

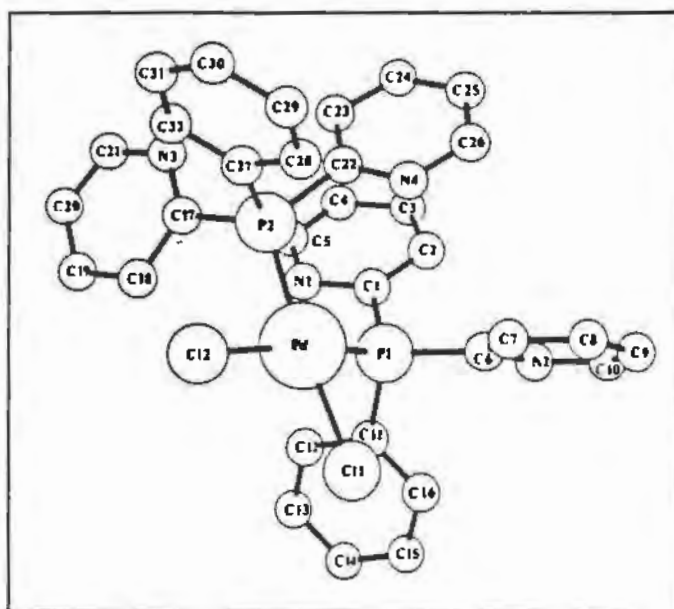
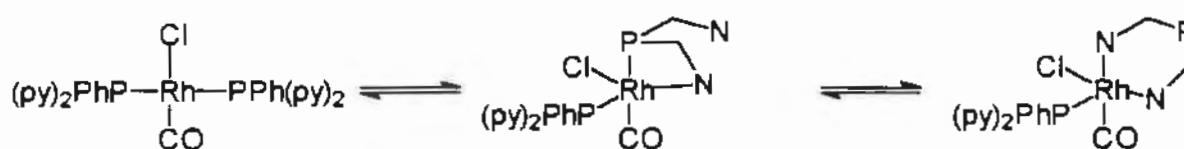


Figure 10. Perspective drawing of *cis*- $\{\text{PhP}(\text{py})_2\}_2\text{PdCl}_2$.

1.2.3 Coordination of $\text{PhP}(\text{py})_2$ to Rh(I)

Reaction of $[\text{Rh}_2\text{Cl}_2(\text{CO})_4]$ with $\text{PhP}(\text{py})_2$ produces *trans*- $[\text{RhCl}(\text{CO})\{\text{PhP}(\text{py})_2\}_2]$ ¹⁹. The complex in the solid state is thought to be square-planar with *trans* disposed phosphines, as spectroscopic data obtained for the $\text{PhP}(\text{py})_2$ complex are similar to the spectroscopic data

obtained for the analogous Ppy_3 complex, for which an X-ray structure analysis revealed a square planar complex with *trans* disposed phosphines. The $\text{PhP}(\text{py})_2$ ligands coordinate to the rhodium atom solely through the phosphorus atom. The structure of $[\text{RhCl}(\text{CO})\{\text{PhP}(\text{py})_2\}_2]$ in solution was found to be different from that in the solid state. $^{31}\text{P}\{^1\text{H}\}$ NMR spectroscopy revealed that an equilibrium is established between the square planar complex and a penta-coordinate complex in which one $\text{PhP}(\text{py})_2$ ligand behaves as a chelating ligand coordinating through the phosphorus and one nitrogen atom. A third complex, also believed to be involved in the equilibrium process, has the $\text{PhP}(\text{py})_2$ ligand coordinating by chelation solely through its nitrogen atoms. The following equilibrium has been proposed to occur in solution.

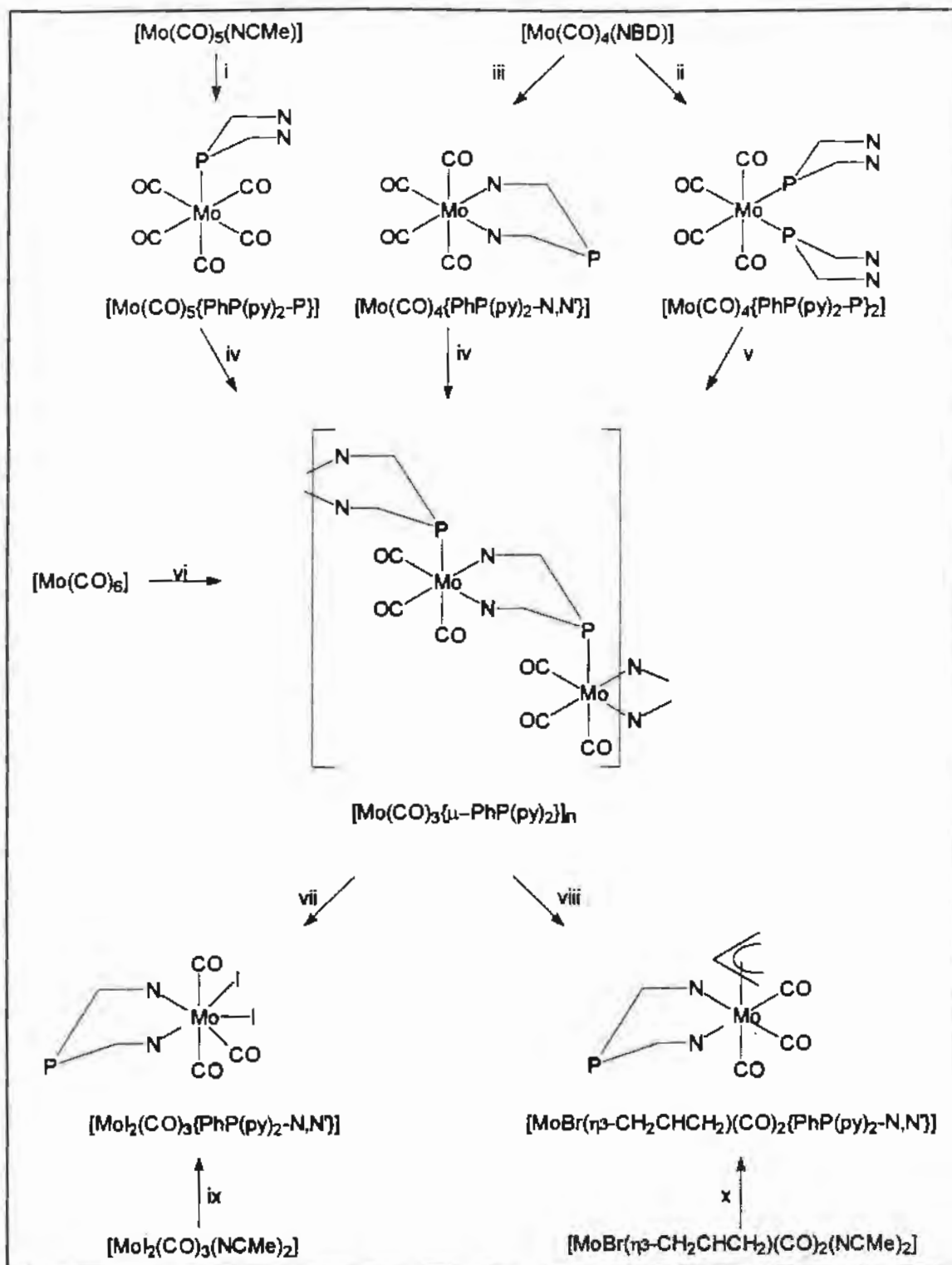


An alternative structure for the species with the $\text{PhP}(\text{py})_2$ ligand coordinating to the rhodium atom through tridentate chelating coordination through the phosphorus and the two nitrogen atoms (Mode 4, Scheme 2) has also been proposed, but this complex can be ruled out due to the formation of two very strained four-membered rings.

These rhodium $\text{PhP}(\text{py})_2$ complexes were the first examples of $\text{PhP}(\text{py})_2$ coordinating in a mode other than a monodentate mode. The complexes formed in solution are examples of chelating modes 3 and 5.

1.2.4 Coordination of $\text{PhP}(\text{py})_2$ to $\text{Mo}(0)$ and $\text{Mo}(\text{II})$

Reaction of $\text{PhP}(\text{py})_2$ with various $\text{Mo}(0)$ and $\text{Mo}(\text{II})$ precursors has been shown to result in complexes with $\text{PhP}(\text{py})_2$ coordinating to the molybdenum atom in a variety of coordinating modes²⁰. The reactions carried out and structures proposed for the complexes obtained are summarised in Scheme 4. This series of reactions serves to illustrate the preference of phosphorus coordination to the softer $\text{Mo}(0)$ metal centre and pyridine coordination to the harder $\text{Mo}(\text{II})$ metal. This is emphasised by the fact that the complex $[\text{Mo}(\text{CO})_4(\text{PhP}(\text{py})_2)]$



Scheme 4. i = PhP(py)₂, -MeCN; ii = 2PhP(py)₂, -NBD; iii = PhP(py)₂, -NBD; iv = CO; v = -CO, -PhP(py)₂; vi = PhP(py)₂, -CO; vii = I₂; viii = CH₂=CHCH₂Br; ix and x = PhP(py)₂, -MeCN.

N,N')] is unstable and decomposes to give the corresponding complexes with the $\text{PhP}(\text{py})_2$ ligand coordinating solely through the phosphorus atom whereas the $[\text{MoI}_2(\text{CO})_3(\text{PhP}(\text{py})_2-N,N')]$ is stable.

The complexes formed by reaction of Mo(0) and Mo(II) precursors with $\text{PhP}(\text{py})_2$ give examples of three different modes of coordination of the ligand, namely monodentate through the phosphorus atom as exhibited by $[\text{Mo}(\text{CO})_5(\text{PhP}(\text{py})_2\text{-P})]$ and $[\text{Mo}(\text{CO})_4(\text{PhP}(\text{py})_2\text{-P})_2]$ (mode 1), chelation through the nitrogen atoms of the pyridine rings as revealed by $[\text{Mo}(\text{CO})_4(\text{PhP}(\text{py})_2-N,N')]$, $[\text{MoI}_2(\text{CO})_3(\text{PhP}(\text{py})_2-N,N')]$ and $[\text{MoBr}(\eta^3\text{-CH}_2\text{CHCH}_2)(\text{CO})_2(\text{PhP}(\text{py})_2-N,N')]$ (mode 3), and bridging by having the phosphorus coordinated to one molybdenum atom and the two nitrogens of the pyridine rings coordinated to one molybdenum atom and the two nitrogens of the pyridine rings coordinated to a different molybdenum atom as found for the $[\text{Mo}(\text{CO})_3\{\mu\text{-PhP}(\text{py})_2\}]_n$ complex (mode 10).

1.2.5 Coordination of $\text{PhP}(\text{py})_2$ to Co(II)

Reaction of $\text{PhP}(\text{py})_2$ with Co(II) results in the formation of the complex $\text{Co}\{\eta^2\text{-PhP}(\text{py})_2\}\text{Cl}_2$ ²¹. This complex has $\text{PhP}(\text{py})_2$ coordinating to the cobalt through its nitrogen atoms only leaving its phosphorus atom free. The coordination around the cobalt is completed by two chlorine atoms resulting in a tetrahedral geometry around the cobalt atom. This is the first example of $\text{PhP}(\text{py})_2$ coordinating in mode 3 (Scheme 2) that has been verified X-ray crystallographically, a perspective drawing of which is shown in figure 11.

1.2.6 Conclusion

The first observation that can be made about the coordination chemistry of $\text{PhP}(\text{py})_2$ is that few studies have been made involving the ligand. It is for this reason that only a few of the possible modes of coordination that this ligand can adopt are represented in the complexes isolated. Of all the possible modes of coordination that the $\text{PhP}(\text{py})_2$ ligand could adopt there seems to be only one, the chelating mode 4, that is very unlikely due to the very strained four membered rings that would result in such a complex. It is therefore safe to assume that after more studies

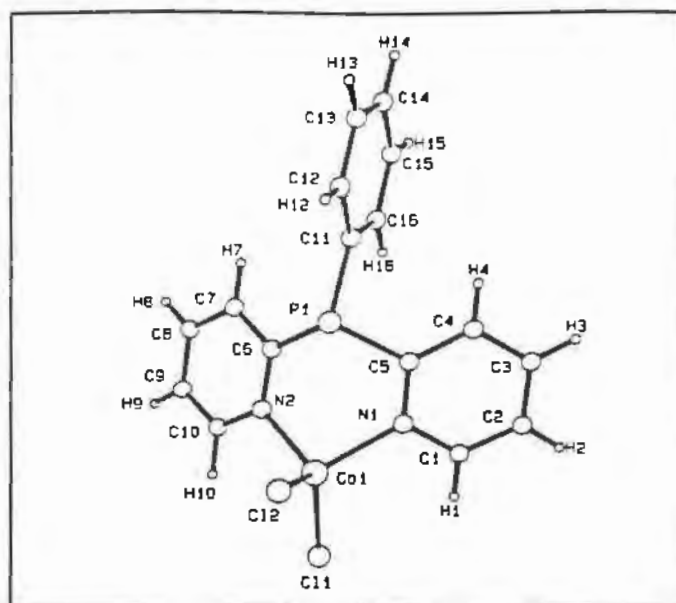
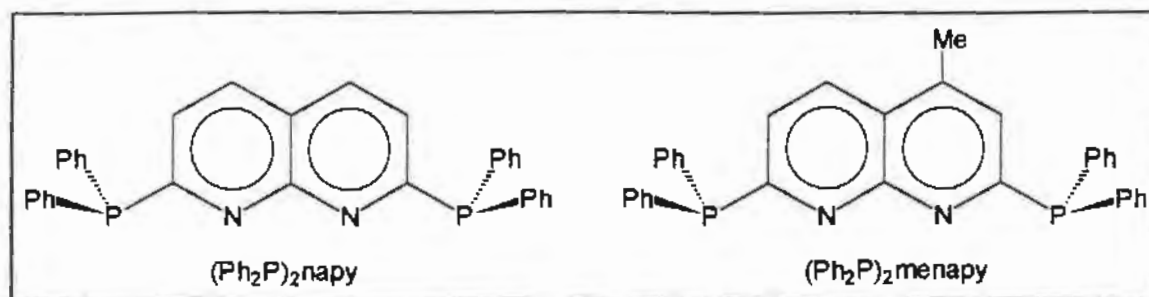


Figure 10. Perspective drawing of $\text{Co}\{\eta^2\text{-PhP(py)}_2\}\text{Cl}_2$.

have been carried out with this ligand, examples of the other possible modes of coordination should appear in the literature.

From the studies that have been carried out it appears that the PhP(py)_2 ligand prefers to adopt the monodentate mode of coordination with coordination to a transition metal taking place solely through the phosphorus atom, although it has been shown that in complexes formed with a harder metal such as Mo(II) and Co(II) the PhP(py)_2 ligand prefers to coordinate to the metal by chelating through the nitrogen atoms of the pyridine rings.

1.3 The Coordination Chemistry of 2,7-Bis(diphenylphosphino)naphthyridine $\{(Ph_2P)_2napy\}$ and 2,7-Bis(diphenylphosphino)-4-methyl-naphthyridine $\{(Ph_2P)_2menapy\}$

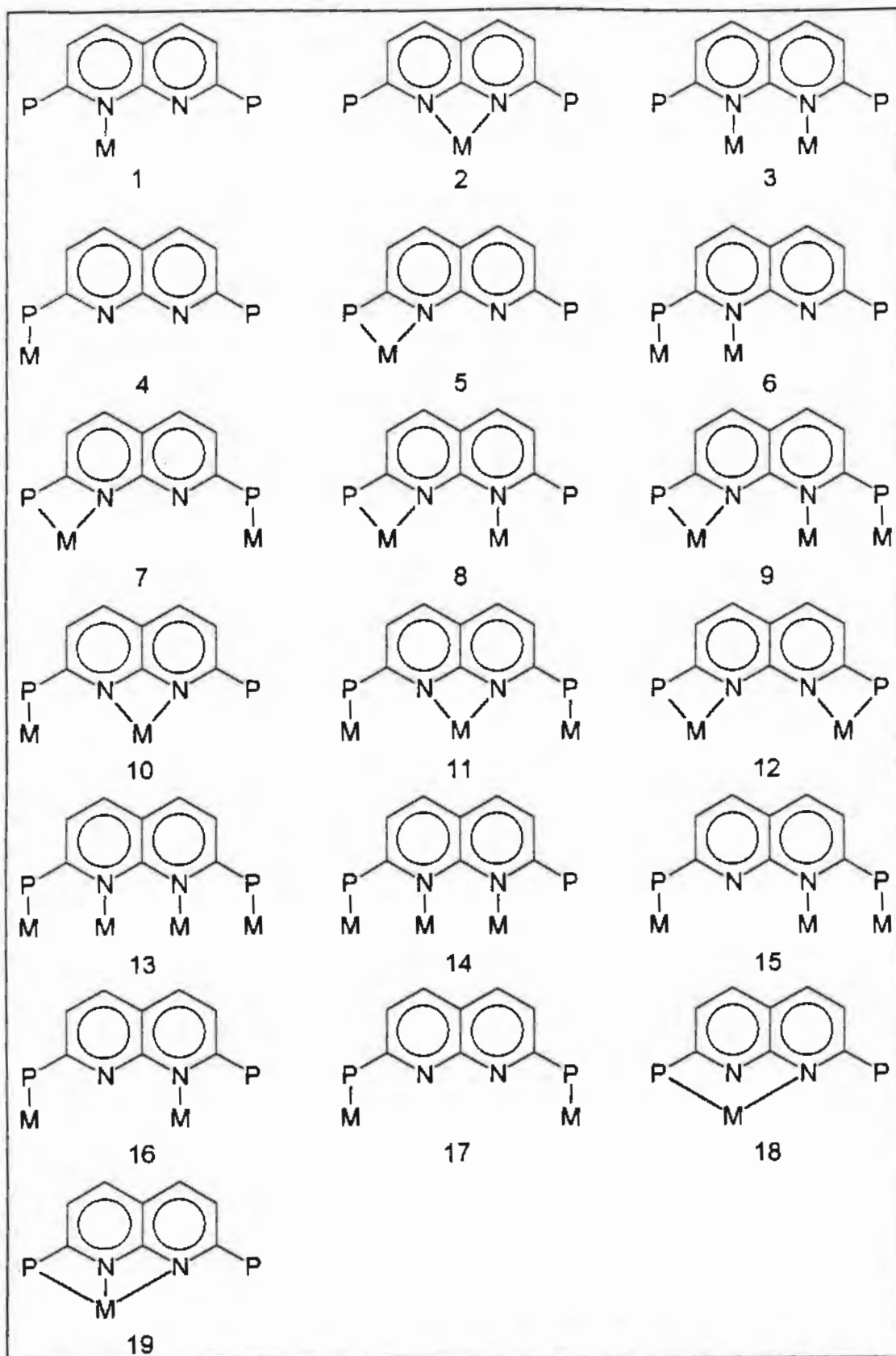


The synthesis of the ligand $(Ph_2P)_2napy$ has only recently been reported with the only report on its use as a ligand being in the same paper by R. Ziessel *et al* (see discussion below) wherein a complex containing the $(Ph_2P)_2napy$ ligand coordinated to rhodium was discussed³. The $(Ph_2P)_2menapy$ ligand has not been reported in the literature but it is expected to exhibit similar coordination behaviour to the $(Ph_2P)_2napy$ ligand.

In principle there are a variety of modes of coordination that the $(Ph_2P)_2napy$ ligand can adopt. However many of these possible modes are not likely due to the rigid nature of the ligand, which is a consequence of all four donor atoms lying in the same plane. For example any mode which includes chelation of the ligand to a single metal atom through the two phosphorus atoms is unlikely; the two donor atoms would simply be too far apart to allow for coordination to the same metal atom.

Scheme 5 presents nineteen possible modes of coordination that the $(Ph_2P)_2napy$ and $(Ph_2P)_2menapy$ ligands could adopt, in principle.

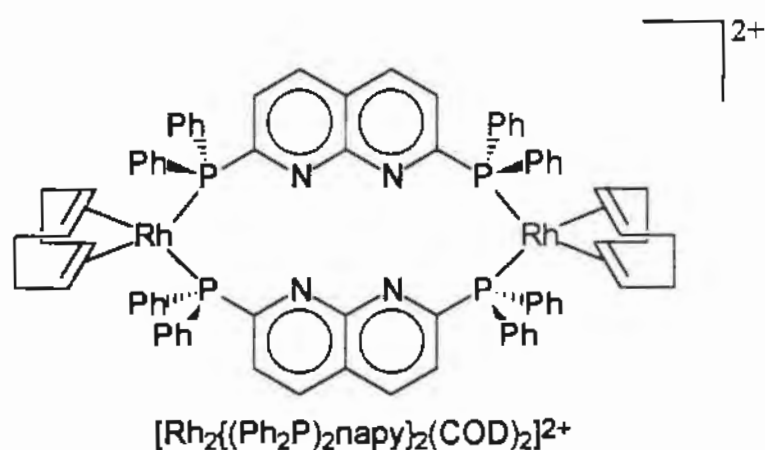
The $(Ph_2P)_2napy$ and $(Ph_2P)_2menapy$ ligands can each be considered as being based on Ph_2Ppy and 1,8-naphthyridine²²⁻²³ (*napy*). It would thus be expected that the modes of coordination adopted by $(Ph_2P)_2napy$ and $(Ph_2P)_2menapy$ will closely resemble those adopted by the Ph_2Ppy and *napy* ligands. *Napy* and 4-methyl-1,8-naphthyridine²⁴⁻²⁵ (*menapy*) ligands are well known ligands and have been reacted with a wide range of transition metals. They have been found to coordinate to transition metals in monodentate²⁶⁻²⁹, chelating³⁰⁻³¹ and bridging³³⁻³⁴



Scheme 5. Possible modes of coordination for the $(\text{Ph}_2\text{P})_2\text{napy}$ and $(\text{Ph}_2\text{P})_2\text{menapy}$ ligands.

modes of coordination. On this basis it is expected that $(\text{Ph}_2\text{P})_2\text{napy}$ and $(\text{Ph}_2\text{P})_2\text{menapy}$ could well coordinate to a transition metal in modes 1, 2 and 3. The ligand Ph_2Ppy is known to coordinate to transition metals in monodentate^{6,36-39}, chelating⁹ and bridging⁴⁰⁻⁴³ modes of coordination. The $(\text{Ph}_2\text{P})_2\text{napy}$ and $(\text{Ph}_2\text{P})_2\text{menapy}$ ligands would thus be expected to coordinate to a transition metal in modes 4, 5 and 6. The remaining modes of coordination that the $(\text{Ph}_2\text{P})_2\text{napy}$ and $(\text{Ph}_2\text{P})_2\text{menapy}$ ligands may adopt can be viewed as combinations of the previously described modes of coordination. Of all of these modes, modes 18 and 19 are probably the most unlikely due to the strained ring systems that would result in complexes containing the $(\text{Ph}_2\text{P})_2\text{napy}$ and $(\text{Ph}_2\text{P})_2\text{menapy}$ ligands bonded in this way.

The only reported example of $(\text{Ph}_2\text{P})_2\text{napy}$ coordinating to a transition metal atom is $[\text{Rh}_2\{(\text{Ph}_2\text{P})_2\text{napy}\}_2(\text{COD})_2](\text{BF}_4)_2$ formed by reaction of $(\text{Ph}_2\text{P})_2\text{napy}$ with $[\text{Rh}(\text{acetone})_2\text{COD}](\text{BF}_4)^3$. The structure of the species was determined from ³¹P-NMR spectroscopy data to be a large ring binuclear complex bridged by two $(\text{Ph}_2\text{P})_2\text{napy}$ ligands which are *cis*-coordinated and bridge the two Rh(I) centres through the two phosphorus atoms of the $(\text{Ph}_2\text{P})_2\text{napy}$ ligand. The Rh...Rh distance of the complex was ascertained using molecular models and was determined to be of the order of 8.4 Å. This complex thus contains a large cavity which, as in the case of similar complexes containing the ligand $(\text{Ph}_2\text{P})_2\text{py}$, should be able to bind metal centres. The $[\text{Rh}_2\{(\text{Ph}_2\text{P})_2\text{napy}\}_2(\text{COD})_2](\text{BF}_4)_2$ complex should in fact be able to bind two metal centres in this cavity due to there being two nitrogen atoms available for coordination.



CHAPTER 2

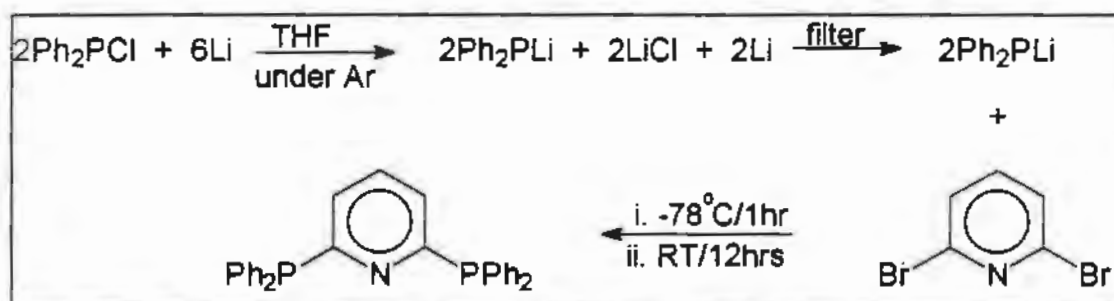
Dinuclear 2,6-Bis(diphenylphosphino)pyridine Ligand-Bridged Complexes of Cu(I) and Ag(I).

2.1 Aims

The aim of the work described in this chapter was to synthesise dinuclear complexes of copper(I) and silver(I) bridged by the ligand $(\text{Ph}_2\text{P})_2\text{py}$, to investigate the type of coordination that the $(\text{Ph}_2\text{P})_2\text{py}$ ligand adopts when bonded to copper(I) or silver(I) and to study the photophysical properties of the complexes formed.

2.2 Synthesis of 2,6-Bis(diphenylphosphino)pyridine

The synthesis of $(\text{Ph}_2\text{P})_2\text{py}$ was based on the method used by Newkome¹ *et al.* and is outlined in Scheme 6.



Scheme 6. Synthesis of the $(\text{Ph}_2\text{P})_2\text{py}$ ligand.

The synthesis of the ligand is performed under an atmosphere of argon, but once it is isolated as a white solid it is relatively air stable and only needs to be kept under an inert atmosphere for storage purposes.

Characterisation data obtained for the ligand were in good agreement with those reported in the literature^{1,7} (see experimental section). The solid state infrared spectrum was, as expected,

dominated by modes resulting from vibrations associated with the phenyl moieties and from P-C bond vibrations. The ^1H NMR spectrum consisted of a broad multiplet from δ 7.6-7.2 corresponding to 21 hydrogens belonging to the phenyl groups and the pyridine moiety, and a doublet at δ 7.0 corresponding to the two hydrogens of the pyridine ring adjacent to the phosphorus atoms. The $^{31}\text{P}\{^1\text{H}\}$ NMR spectrum of $(\text{Ph}_2\text{P})_2\text{py}$ showed a sharp singlet at δ -3.5, which is characteristic of these types of ligands^{2,3,4}. Elemental analysis were in good agreement with the formulation of the ligand.

2.3 Synthesis and Characterisation of 2,6-Bis(diphenylphosphino)pyridine Derivatives of Copper(I)

2.3.1 Reaction of $[\text{Cu}(\text{MeCN})_4](\text{PF}_6)$ with $(\text{Ph}_2\text{P})_2\text{py}$: Synthesis and Crystal Structure of $[\text{Cu}_2\{\mu-(\text{Ph}_2\text{P})_2\text{py}\}_3](\text{PF}_6)_2$ (1)

Reaction of $(\text{Ph}_2\text{P})_2\text{py}$ as a suspension to a stirred solution of $[\text{Cu}(\text{MeCN})_4](\text{PF}_6)$ in acetonitrile in a 3:2 molar ratio was found to afford a product characterised as the dinuclear complex $[\text{Cu}_2\{\mu-(\text{Ph}_2\text{P})_2\text{py}\}_3](\text{PF}_6)_2$ (1). The $(\text{Ph}_2\text{P})_2\text{py}$ ligand dissolves as the reaction takes place to give a colourless solution. Compound 1 is precipitated by addition of diethyl ether to give a white microcrystalline material.

The solid state infrared spectrum of 1 indicates the presence of $(\text{Ph}_2\text{P})_2\text{py}$ and PF_6^- (Table 1). The fact that both phosphorus atoms of the ligand are coordinated is indicated by a $^{31}\text{P}\{^1\text{H}\}$ NMR spectrum which gives a broad peak centred at δ 5.1, which is shifted downfield from the free ligand which shows a sharp singlet at δ -3.5. The ^1H NMR spectrum of 1 is similar to that of the free ligand with a broad series of multiplets ranging from δ 6.9 to 7.6. Elemental analysis was not obtainable for 1 due to the difficulty experienced in drying the solid product. Even when left under reduced pressure for a period of two days solvent was always present in the solid material and this resulted in elemental analysis that was not consistent with the proposed formula for 1.

Single crystals of 1 were obtained, and an X-ray crystal structure analysis confirmed that the

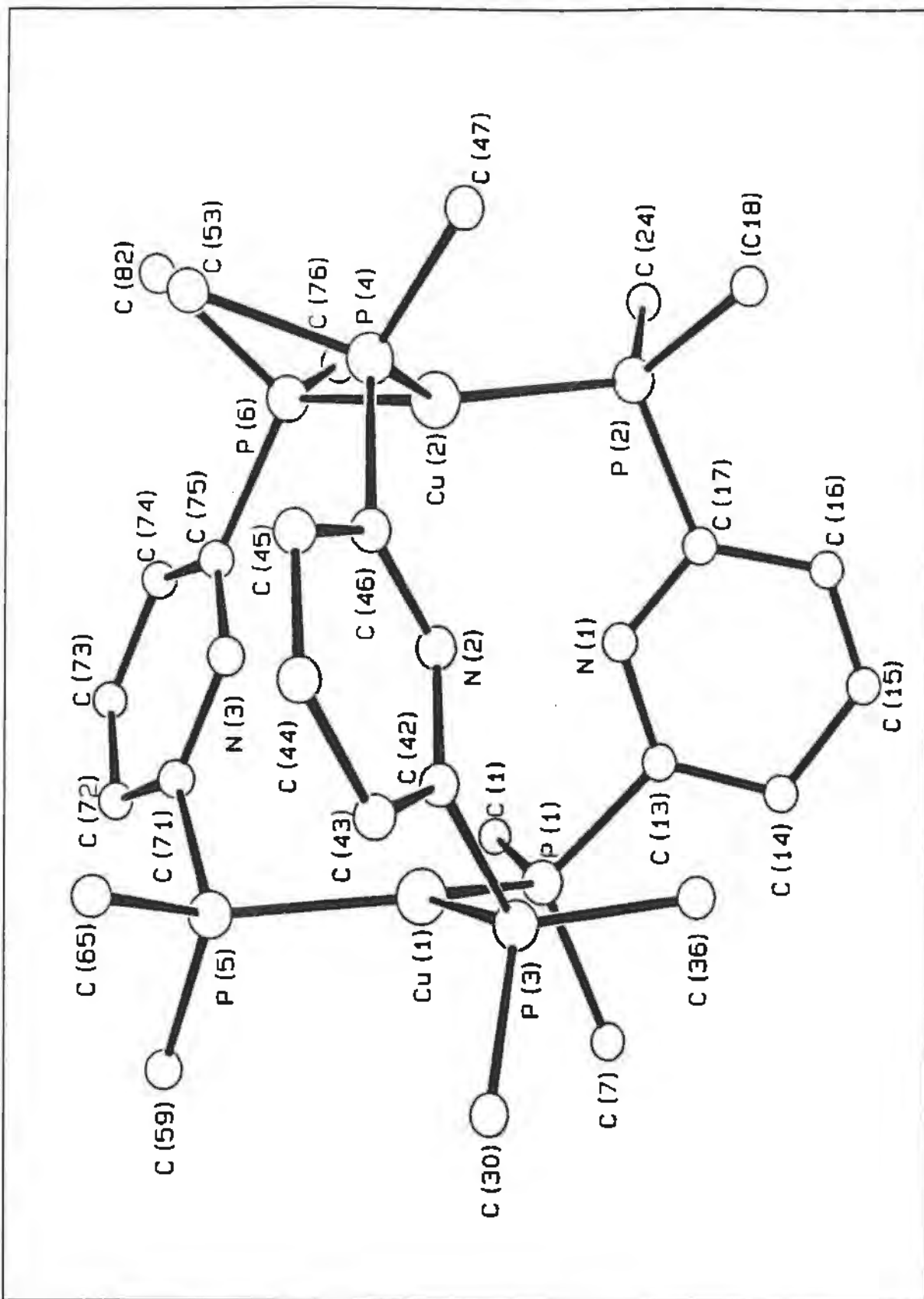


Figure 11. Molecular structure of the $[\text{Cu}_2\{\mu\text{-(Ph}_2\text{P)}_2\text{py}\}_3]^{2+}$ cation. Phenyl rings omitted for clarity.

complex is indeed $[\text{Cu}_2\{\mu\text{-(Ph}_2\text{P)}_2\text{py}\}_3](\text{PF}_6)_2$. The crystal structure consists of well-separated dinuclear $[\text{Cu}_2\{\mu\text{-(Ph}_2\text{P)}_2\text{py}\}_3]^{2+}$ cations and PF_6^- anions. The molecular structure of the cation, showing the atom labelling scheme, is illustrated in Figure 12. The two copper atoms in the dinuclear cation are bridged by three $(\text{Ph}_2\text{P)}_2\text{py}$ ligands with only the phosphorus atoms of the ligand bonding to the copper atoms. Each copper atom has essentially trigonal geometry with P-Cu-P angles ranging from $121.6(2)^\circ$ to $116.5(2)^\circ$. The Cu...Cu distance is $4.744(2) \text{ \AA}$ which indicates that there is no Cu...Cu interaction. The nitrogen atoms of the pyridine rings of the ligand are uncoordinated and are situated such that they point towards the centre of the complex. The Cu-P distances range from $2.231(6)$ to $2.280(4) \text{ \AA}$ which are in the expected range for Cu-P distances^{44,47}. A comprehensive list of interatomic distances and angles is given in Tables 3 and 4.

The phosphorus atoms of the ligand are orientated in a staggered conformation around the two copper atoms. This is illustrated in Figure 13 which shows a perspective view of **1** viewed down the Cu...Cu axis. The carbon and nitrogen atoms have been omitted for clarity. The phosphorus atoms are not orientated in a perfect staggered conformation i.e., with P-Cu-Cu-P torsion angles of 60° but rather have P-Cu-Cu-P torsion angles ranging from 36 to 42° . Presumably this is due to the steric requirements of the ligand which do not allow for further rotation about the P-C(py) bonds.

A marked feature of **1** is the cavity, with a diameter of 4.9 \AA that exists in the centre of the complex. This value was obtained by calculating in the first instance the distances between each pair of pyridine atoms these being $4.17(2)$, $4.29(2)$ and $4.35(2) \text{ \AA}$. The average value ($4.27(2) \text{ \AA}$) was taken as the length of the edges of an equilateral triangle whose median was assumed to be the centre of the cavity. The diameter of the cavity was then assumed to be equal to that of a circle centred on the median and whose circumference passes through all the vertices of the equilateral triangle. The calculated cavity size of 4.9 \AA for **1** is the same size as the cavity that exists in the centre of the analogous gold complex $[\text{Au}_2\{\mu\text{-(Ph}_2\text{P)}_2\text{py}\}_3](\text{ClO}_4)_2$ synthesised by Che and co-workers. This is not surprising considering that the Au-P distances in the gold complex are of similar values (ranging from 2.338 to 2.384 \AA) to those in the copper complex. It is therefore expected that the complex **1** should be able to bind cations into

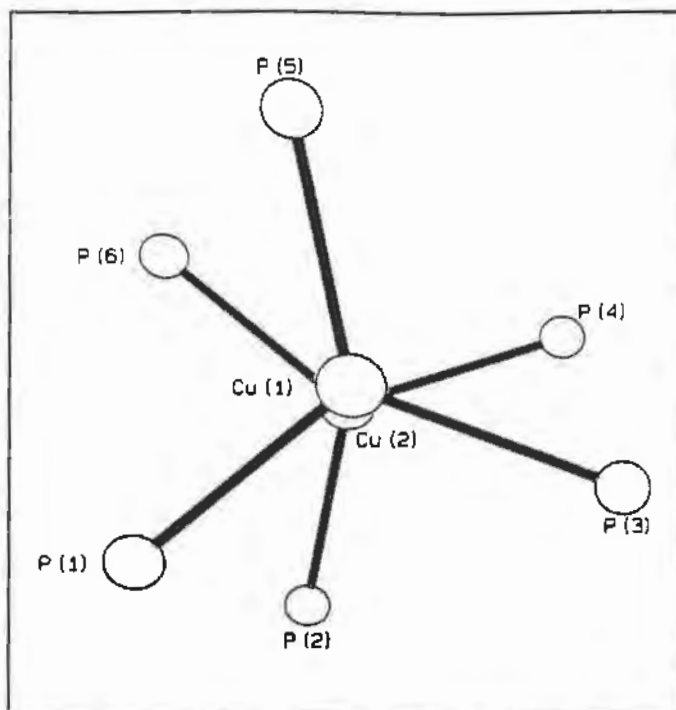


Figure 13. Perspective drawing of $[\text{Cu}_2\{\mu\text{-(Ph}_2\text{P)}_2\text{py}\}_3](\text{PF}_6)_2$ viewed down the Cu...Cu axis.

the cavity as is found for the gold complex which binds Cu(I) ions into its cavity¹⁵. Another complex containing the $(\text{Ph}_2\text{P})_2\text{py}$ ligand and has a cavity capable of binding metal ions is the $\text{Rh}_2\{\mu\text{-(Ph}_2\text{P)}_2\text{py}\}_2(\text{CO})_2\text{Cl}_2$ complex¹⁴. This complex when reacted with SnCl_2 forms the $\text{Rh}_2\text{Sn}_2\{\mu\text{-(Ph}_2\text{P)}_2\text{py}\}_2(\text{CO})_2\text{Cl}_6$ complex in which the Sn(II) ion is trapped into the cavity of the complex.

2.3.2 Reaction of $[\text{Cu}(\eta^2\text{-bipy})(\text{MeCN})_2](\text{PF}_6)$ with $(\text{Ph}_2\text{P})_2\text{py}$: Synthesis and Crystal Structure of $[\text{Cu}_2\{\mu\text{-(Ph}_2\text{P)}_2\text{py}\}_2(\eta^2\text{-bipy})_2](\text{PF}_6)_2$ (2)

The synthesis of the $[\text{Cu}_2\{\mu\text{-(Ph}_2\text{P)}_2\text{py}\}_2(\eta^2\text{-bipy})_2](\text{PF}_6)_2$ complex (2) is a two step process. First the $[\text{Cu}(\eta^2\text{-bipy})(\text{MeCN})_2](\text{PF}_6)$ complex is synthesised by adding a solution of bipy in acetone dropwise to a solution of $[\text{Cu}(\text{MeCN})_4](\text{PF}_6)$ in acetone in a 1:1 mole ratio. The solution changes colour from colourless to red as the bipy is added. The $[\text{Cu}(\eta^2\text{-bipy})(\text{MeCN})_2](\text{PF}_6)$ precursor cannot be isolated as a solid and is added *in situ* to a stirred solution of one mole equivalent of $(\text{Ph}_2\text{P})_2\text{py}$ in acetone. After stirring for two hours a yellow

precipitate separates from the solution. This yellow precipitate is re-crystallised from MeCN/diethyl ether.

The solid state infrared spectrum of **2** indicates the presence of $(\text{Ph}_2\text{P})_2\text{py}$, bipy and the PF_6^- ions (Table 1). The fact that both phosphorus atoms of the ligand are coordinated to the metal atoms is indicated by a $^{31}\text{P}\{^1\text{H}\}$ NMR spectrum which gives a broad peak centred at δ 0.9, which is shifted significantly downfield from the free ligand (*vide supra*). The ^1H NMR spectrum of **2** is similar to that of the free ligand with a broad series of multiplets ranging from δ 6.9 to 8. Elemental analysis is consistent with the proposed formula for **2**.

Single crystals of **2** were obtained, and an X-ray crystal structure analysis confirmed that the complex is indeed $[\text{Cu}_2\{\mu-(\text{Ph}_2\text{P})_2\text{py}\}_2(\eta^2\text{-bipy})_2](\text{PF}_6)_2$. The crystal structure consists of well-separated dinuclear $[\text{Cu}_2\{\mu-(\text{Ph}_2\text{P})_2\text{py}\}_2(\eta^2\text{-bipy})_2]^{2+}$ cations and PF_6^- anions. The molecular structure of the cation, showing the atom labelling scheme, is illustrated in Figure 14. The cation possesses a crystallographically imposed centre of symmetry with the two copper atoms in the dinuclear cation bridged by two $(\text{Ph}_2\text{P})_2\text{py}$ ligands coordinated to the copper atoms through the phosphorus atoms only. A bipyridyl ligand chelates to each of the two copper atoms. The Cu...Cu separation is 6.806 (2) Å which indicates no Cu...Cu interaction. The geometry around each copper atom is pseudo tetrahedral with the smallest angle being the N2-Cu-N3 angle of 79.8 (5)° and the largest angle being the P1-Cu-N2 angle of 113.9 (4)°. The Cu-P1 distance is 2.249 (5) Å and the Cu'-P(2) distance is 2.232 (6) Å both of which lie in the expected range for Cu-P distances⁴⁴⁻⁴⁷. The Cu-N2 distance is 2.107 (13) Å and the Cu-N3 distance is 2.063 (13) Å again distances which are close to literature values⁴⁸⁻⁵⁰. A comprehensive list of interatomic distances and angles is given in Table 8 and 9.

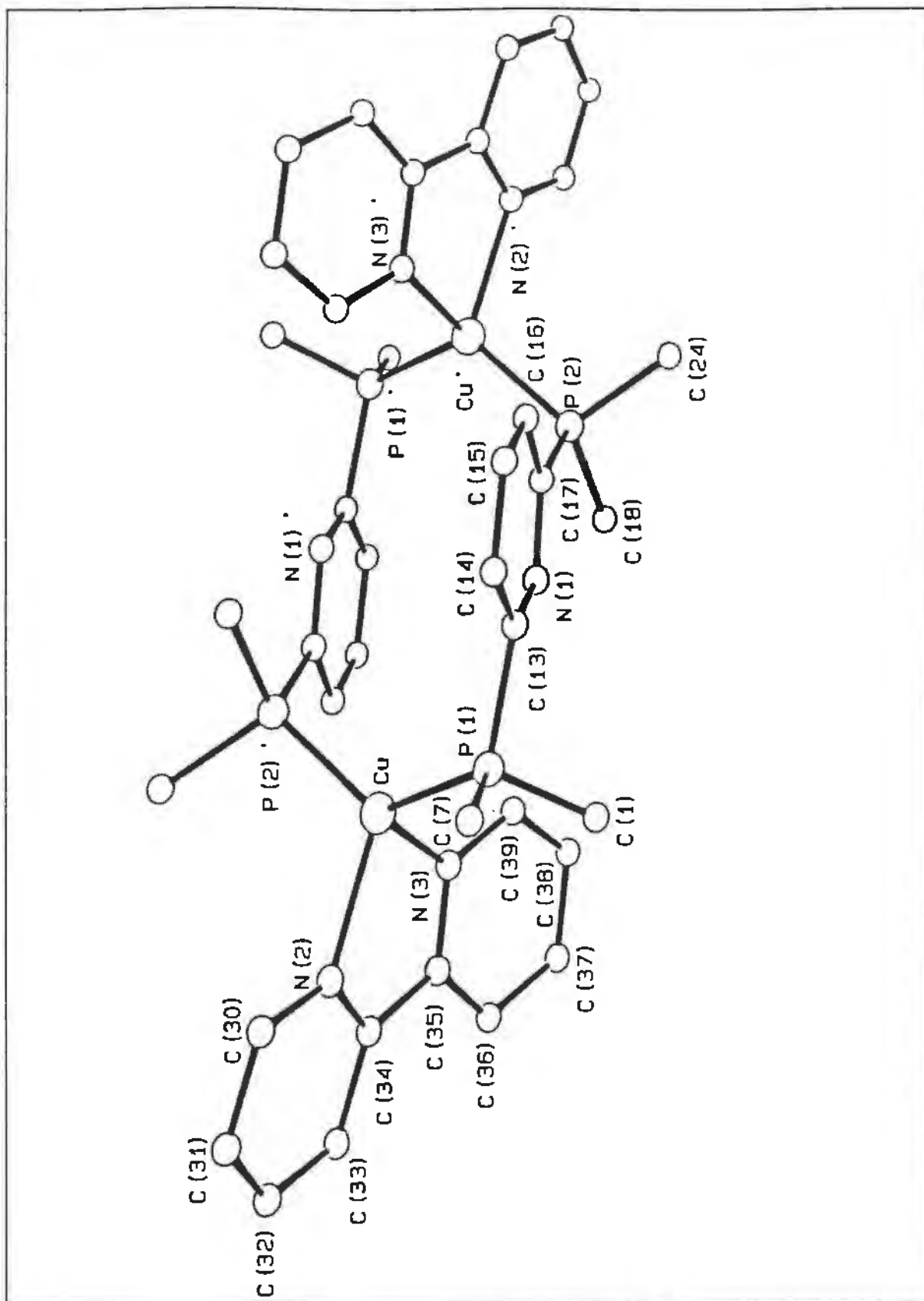


Figure 13. Molecular structure of the $[\text{Cu}_2\{\mu\text{-(Ph}_2\text{P)}_2\text{py}\}_2(\eta^2\text{-bipy})_2]^{2+}$ cation. Phenyl rings omitted for clarity.

2.4 Synthesis and Characterisation of 2,6-Bis(diphenylphosphino)pyridine Derivatives of Silver(I)

2.4.1 Reaction of $[\text{Ag}(\text{COD})_2](\text{BF}_4)$ with $(\text{Ph}_2\text{P})_2\text{py}$: Synthesis and Crystal Structure of $[\text{Ag}_2\{\mu-(\text{Ph}_2\text{P})_2\text{py}\}_3](\text{PF}_6)_2$ (**3**)

Reaction of $(\text{Ph}_2\text{P})_2\text{py}$ as a suspension to a stirred solution of $[\text{Ag}(\text{COD})_2](\text{BF}_4)$ in acetonitrile in a 3:2 molar ratio was found to afford a product characterised as the dinuclear complex $[\text{Ag}_2\{\mu-(\text{Ph}_2\text{P})_2\text{py}\}_3](\text{BF}_4)_2$ (**3**). The $(\text{Ph}_2\text{P})_2\text{py}$ ligand dissolves as the reaction takes place to give a colourless solution. Compound **3** is precipitated by addition of diethyl ether to give a white crystalline material.

The solid state infrared spectrum of **3** indicates the presence of $(\text{Ph}_2\text{P})_2\text{py}$ and BF_4^- (Table 1). The ^{31}P $\{^1\text{H}\}$ NMR spectrum of **3** consists of a series of three broad peaks centred at δ 19.6, 14.3 and 8.8 with the outer two peaks being narrower than the middle peak. This spectrum is consistent with the formulation for **3** as there are two isotopes of silver, namely ^{107}Ag and ^{109}Ag , which have spin $\frac{1}{2}$ and couple with the phosphorus atoms of the ligand. These two isotopes of silver have similar abundancies resulting in effectively three different complexes, two complexes containing only ^{107}Ag or ^{109}Ag and a third complex containing both ^{107}Ag and ^{109}Ag , detectable using ^{31}P $\{^1\text{H}\}$ NMR. This results in a complicated spectrum as is obtained for **3**. The ^1H NMR spectrum of **3** is similar to that of the free ligand with a broad series of multiplets ranging from δ 6.9 to 7.6. Elemental analysis is consistent with the proposed formula for **3**.

Single crystals of **3** were obtained, and an X-ray crystal structure analysis confirmed that the complex is indeed $[\text{Ag}_2\{\mu-(\text{Ph}_2\text{P})_2\text{py}\}_3](\text{BF}_4)_2$. The crystal structure consists of well-separated dinuclear $[\text{Ag}_2\{\mu-(\text{Ph}_2\text{P})_2\text{py}\}_3]^{2+}$ cations and BF_4^- anions. The molecular structure of the cation, showing the atom labelling scheme, is illustrated in Figure 15. The two silver atoms in the dinuclear cation are bridged by three $(\text{Ph}_2\text{P})_2\text{py}$ ligands with only the phosphorus atoms of the ligand bonding to the silver atoms. Each silver atom has essentially trigonal geometry with P-Ag-P angles ranging from 121.9 (2) to 116.0 (2)°. The Ag...Ag distance is 4.657 (2) Å which

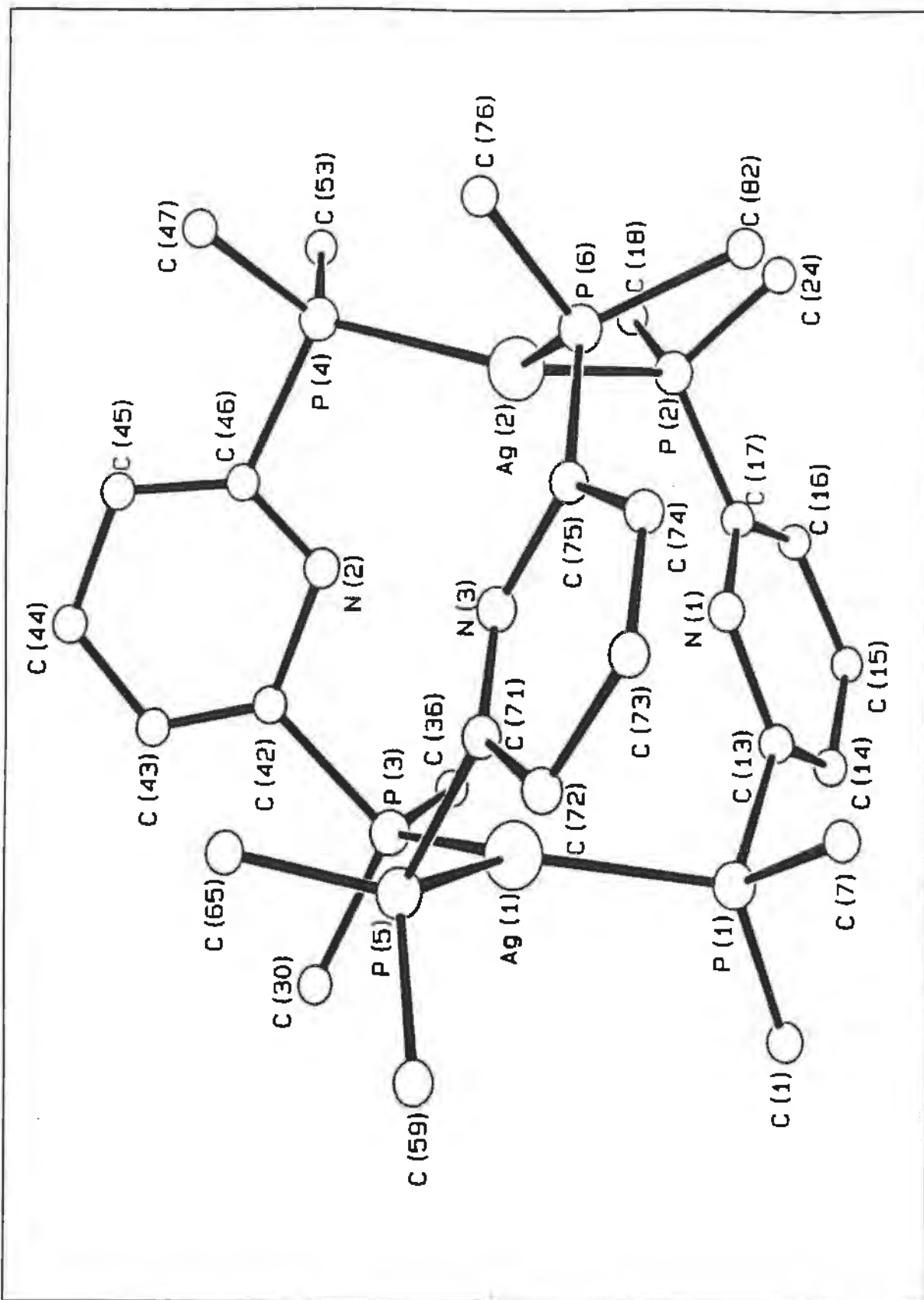


Figure 14. Molecular structure of the $[Ag_2\{\mu-(Ph_2P)_2py\}_3]^{2+}$ cation. Phenyl rings omitted for clarity.

indicates that there is no Ag...Ag interaction. The nitrogen atoms of the pyridine rings of the ligand are uncoordinated and are situated such that they point towards the centre of the complex. The Ag-P distances range from 2.422 (6) to 2.479 (4) Å which are in the expected range for Ag-P distances⁵¹⁻⁵². A comprehensive list of interatomic distances and angles is given in Table 13 and 14.

Complex 3 has a similar structure to complex 1, and if the molecule is viewed down the Ag...Ag axis the staggered conformation of the phosphorus atoms of the ligand can be seen (Fig. 16). The phosphorus atoms are not orientated in a perfectly staggered conformation with P-Ag-Ag-P torsion angles of 60° but rather have P-Ag-Ag-P torsion angles ranging from 36 to 42°. Presumably this is due to the steric requirements of the ligand which do not allow for further rotation about the P-C(py) bonds.

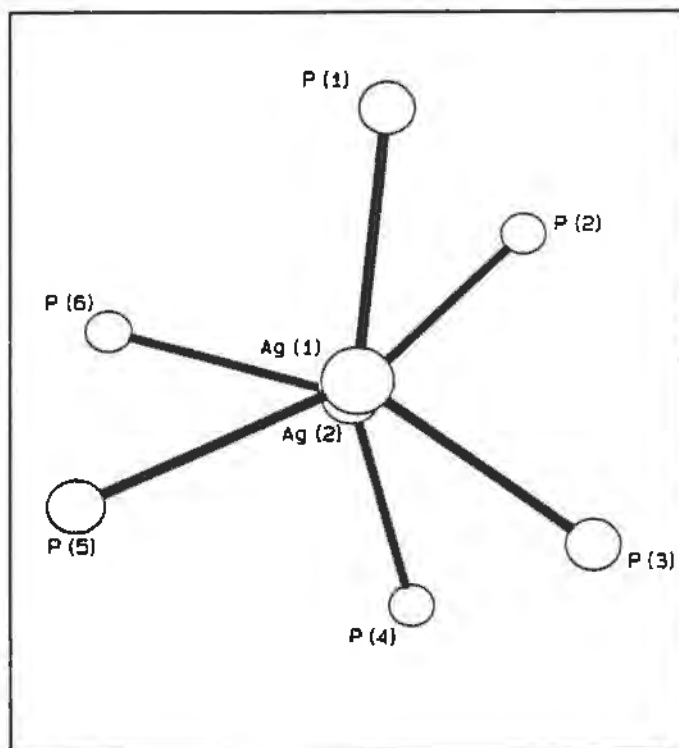


Figure 16. Perspective drawing of $[\text{Ag}_2\{\mu\text{-(Ph}_2\text{P)}_2\text{py}\}_3](\text{BF}_4)_2$ viewed down the Ag...Ag axis.

The size of the cavity that exists in complex 3 has a diameter of 5.3 Å. The cavity size was calculated in the same way as for complex 1 i.e. by first calculating the distance between each pair of nitrogen atoms, these being 4.63 (2), 4.62 (2) and 4.52 (3) Å. These distances are

significantly larger than those of the copper complex and this results in the cavity size of complex **3** being larger than that of complex **1**. The size of the cavity in complex **3** is in fact larger than the cavities that exist in both the gold and the copper complexes. The reason for complex **3** having a larger cavity is largely as a consequence of the Ag-P distances being significantly longer than the Cu-P distances in **1** and the Au-P distances in $[\text{Au}_2\{\mu\text{-(Ph}_2\text{P)}_2\text{py}\}_3](\text{ClO}_4)_2$ ¹⁵. As is the case for the $[\text{Au}_2\{\mu\text{-(Ph}_2\text{P)}_2\text{py}\}_3](\text{ClO}_4)_2$ ¹⁵ and the $\text{Rh}_2\{\mu\text{-(Ph}_2\text{P)}_2\text{py}\}_2(\text{CO})_2\text{Cl}_2$ ¹⁴ complexes, complex **3** would also be expected to be able to bind metal ions into its cavity with the larger cavity size of **3** allowing for larger size ions to be bound into the cavity.

2.4.2 Reaction of $[\text{Ag}(\eta^2\text{-bipy})(\text{COD})](\text{BF}_4)$ with $(\text{Ph}_2\text{P)}_2\text{py}$: Synthesis and Characterisation of $[\text{Ag}_2\{\mu\text{-(Ph}_2\text{P)}_2\text{py}\}_2(\eta^2\text{-bipy})_2](\text{BF}_4)_2$ (**4**)

The synthesis of the $[\text{Ag}_2\{\mu\text{-(Ph}_2\text{P)}_2\text{py}\}_2(\eta^2\text{-bipy})_2](\text{BF}_4)_2$ complex (**4**) is a two step process. First the complex is synthesised by adding a solution of bipy in acetonitrile dropwise to a solution of $[\text{Ag}(\text{COD})_2](\text{BF}_4)$ in acetonitrile in a 1:1 mole ratio. The solution becomes colourless as the reaction takes place. The $[\text{Ag}(\eta^2\text{-bipy})(\text{COD})](\text{BF}_4)$ is then added *in situ* to a stirred suspension of one mole equivalent of $(\text{Ph}_2\text{P)}_2\text{py}$ in acetonitrile. After stirring for six hours a colourless solution forms. Compound **4** is precipitated by addition of diethyl ether to give a white microcrystalline material.

The solid state infrared spectrum of **4** indicates the presence of $(\text{Ph}_2\text{P)}_2\text{py}$, bipy and the BF_4^- ions (Table 1). The fact that both phosphorus atoms of the ligand are coordinated to the metal atoms is indicated by a $^{31}\text{P}\{^1\text{H}\}$ NMR spectrum which gives a broad peak centred at δ 11.0, which is shifted significantly downfield from that of the free ligand which shows a sharp singlet at δ -3.5. A singlet is not expected for a $^{31}\text{P}\{^1\text{H}\}$ NMR where the phosphorus is coordinated to a silver atom as silver couples with phosphorus, resulting in more complicated spectra; however it has been shown that if there is a dissociation of Ag-P bonds on the nmr timescale then only a singlet is seen at room temperature⁵³. The ^1H NMR spectrum of **4** is similar to the free ligand with a broad series of multiplets ranging from δ 7.0 to 8.0. Elemental analysis is consistent with the proposed formula for **4**. Figure 17 shows the

proposed structure of complex 4.

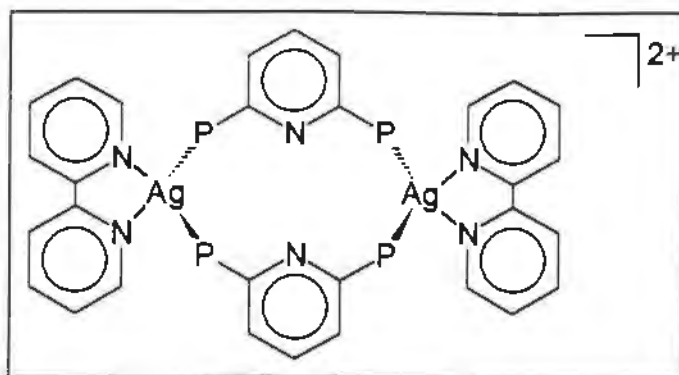
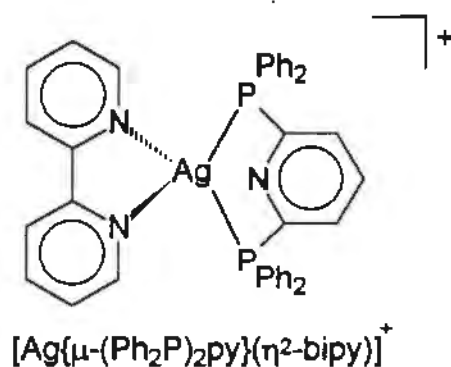


Figure 17. Proposed structure of $[\text{Ag}_2\{\mu\text{-(Ph}_2\text{P)}_2\text{py}\}_2(\eta^2\text{-bipy})_2]^{2+}$.

The characterisation data obtained for 4 is consistent with another possible complex, namely $[\text{Ag}\{\mu\text{-(Ph}_2\text{P)}_2\text{py}\}(\eta^2\text{-bipy})](\text{BF}_4)$, which is a monomer and which has the phosphorus atoms of the $(\text{Ph}_2\text{P})_2\text{py}$ ligand chelating to a silver atom. The reason why this alternative complex has not been chosen as the structure for complex 4 is that the likelihood of the ligand coordinating in this way is very low due to the high angle strain that would result around each donor atom (see section 1.1.2).



2.5 Photophysical Studies on the $[\text{Cu}_2\{\mu\text{-(Ph}_2\text{P)}_2\text{py}\}_3](\text{PF}_6)_2$ (1) and $[\text{Ag}_2\{\mu\text{-(Ph}_2\text{P)}_2\text{py}\}_3](\text{BF}_4)_2$ (3) Complexes

2.5.1 Introduction

It has been shown that many polynuclear Ag(I) and Au(I) complexes with bridging phosphine ligands show intriguing photophysical properties^{15,54-59}. Amongst these complexes is the previously discussed $[\text{Au}_2\{\mu\text{-(Ph}_2\text{P)}_2\text{py}\}_3](\text{ClO}_4)_2$ complex which has recently been synthesised and studied by Che and co-workers¹⁵. This complex has an absorption spectrum in degassed acetonitrile that is dominated by a broad band tailing from 250 to 360 nm; upon excitation at 300 to 360 nm two emissions centred at 415 and 520 nm are observed (Fig. 18). The lower energy emission is much more intense than the higher energy one. The 415 nm emission is assigned to arise from the intraligand excited state while the low energy emission is assigned to arise from a metal to ligand charge transfer (MLCT) transition¹⁵.

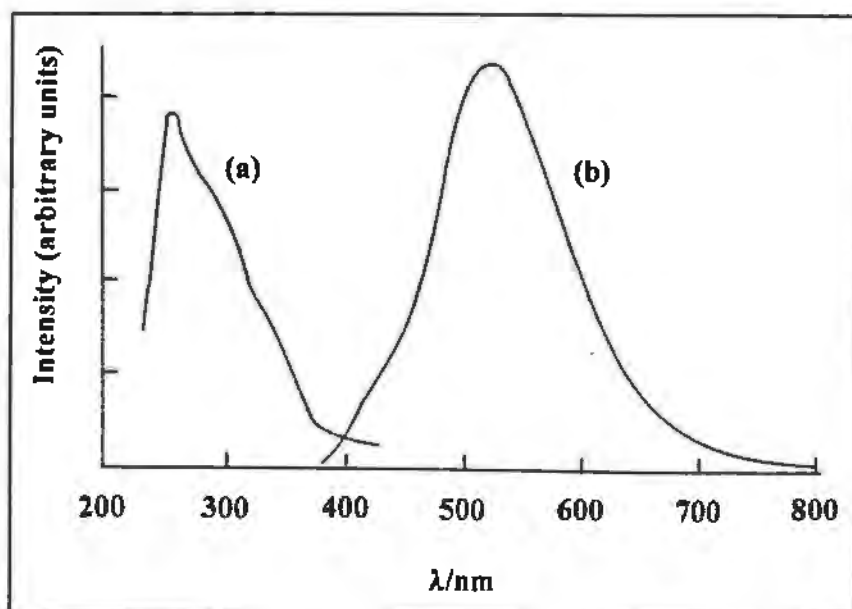


Figure 18. Excitation (a) and emission (b) spectra of $[\text{Au}_2\{\mu\text{-(Ph}_2\text{P)}_2\text{py}\}_3](\text{ClO}_4)_2$ in degassed acetonitrile.

What was of interest with the photophysical studies done on the $[\text{Au}_2\{\mu\text{-(Ph}_2\text{P)}_2\text{py}\}_3](\text{ClO}_4)_2$ complex is that the emission centred at 520 nm is significantly perturbed when Ag^+ , Cu^+ or CF_3COOH is added to a solution containing the gold complex (Fig. 19). Trifluoroacetic acid

was found to quench the emission while the addition of Cu^+ gave a substantial enhancement of the emission intensity and a red shift in its energy. It was suggested by Che that the change in the emission spectrum of $[\text{Au}_2\{\mu-(\text{Ph}_2\text{P})_2\text{py}\}_3](\text{ClO}_4)_2$ upon addition of Cu^+ ions is most likely due to the Cu^+ ion being bound into the cavity between the two gold atoms and bound by the nitrogen atoms of the pyridine rings¹⁵; in fact it was concluded that the Au(I) complex could be used as a sensor for the Cu^+ cation.

The results obtained for the $[\text{Au}_2\{\mu-(\text{Ph}_2\text{P})_2\text{py}\}_3](\text{ClO}_4)_2$ complex led us to examine the photophysical properties 1 and 3. The latter two complexes, being isostructural with the gold complex, would be expected on purely structural grounds to have similar photophysical properties to the gold complex. It would certainly be expected that 1 and 3 should also be able to bind metal ions such as Cu^+ and Ag^+ into their cavities and we wished to determine whether this would result in a change in their emission spectra.

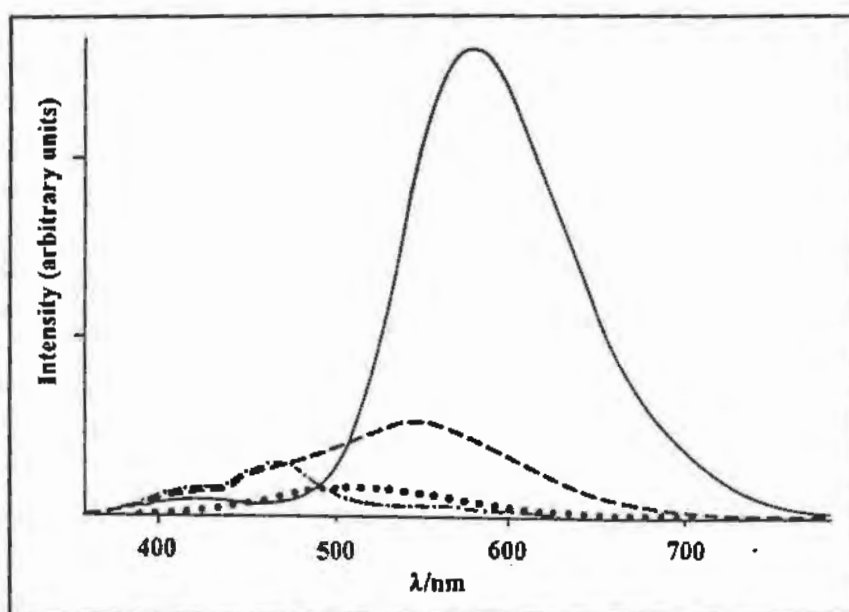


Figure 19. Emission spectra of $[\text{Au}_2\{\mu-(\text{Ph}_2\text{P})_2\text{py}\}_3](\text{ClO}_4)_2$ in degassed acetonitrile (···) and in the presence of CF_3COOH (-·-·-·), Ag^+ (- - -) or Cu^+ (—).

It must be stressed from the outset that the aims of the photophysical studies that were done on 1 and 3 were purely to ascertain whether or not their emission spectra could be used as an indication that a metal ion had been trapped into the cavity of the complex in question as in

the case of the analogous gold complex. Further studies than those done would be required to fully describe the photophysical properties of 1 and 3 and in particular to assign the observed bands to electronic transitions.

2.5.2 Photophysical Studies on the $[\text{Cu}_2\{\mu\text{-(Ph}_2\text{P)}_2\text{py}\}_3](\text{PF}_6)_2$ (1) Complex

The absorption spectrum of 1 in degassed acetonitrile consists of a broad absorption band from 200 to 350 nm. Two absorption maxima occur at 207 and 250 nm. Upon excitation at 330 to 360 nm two emissions centred at 400 and 440 nm are observed. Figure 20 shows both the absorption and emission spectra of 1.

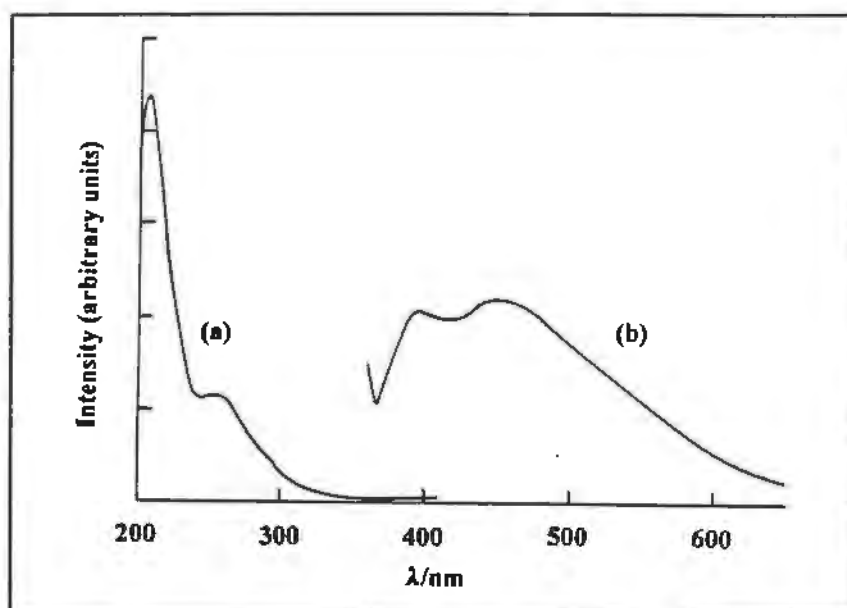


Figure 20. Absorption (a) and emission (b) spectra of $[\text{Cu}_2\{\mu\text{-(Ph}_2\text{P)}_2\text{py}\}_3](\text{PF}_6)_2$ in degassed acetonitrile.

Upon addition of AgCF_3SO_3 , $[\text{Cu}(\text{MeCN})_4](\text{PF}_6)$ or CF_3COOH to a solution of 1 in degassed acetonitrile the emission spectra were found to be significantly perturbed (Fig. 21). In the presence of Ag^+ ions both the emissions centred at 400 and 440 nm are enhanced in intensity with the former being enhanced to the greatest extent. In the presence of Cu^+ ions the emission centred at 400 nm is enhanced while the emission centred at 440 nm is quenched. In the presence of CF_3COOH both emissions are quenched.

Thus, the emission spectrum of **1** is significantly perturbed in the presence of Cu^+ and Ag^+ ions with the largest enhancement occurring in the presence of Ag^+ ions. What is of interest to note is that there is no red shift in the energy of the emissions of **1** when Cu^+ or Ag^+ ions were added as occurred in the case of the gold complex¹⁵. These changes in the emission spectrums can most likely be ascribed to the relevant metal ion being trapped in the cavity that exists in the centre of **1**.

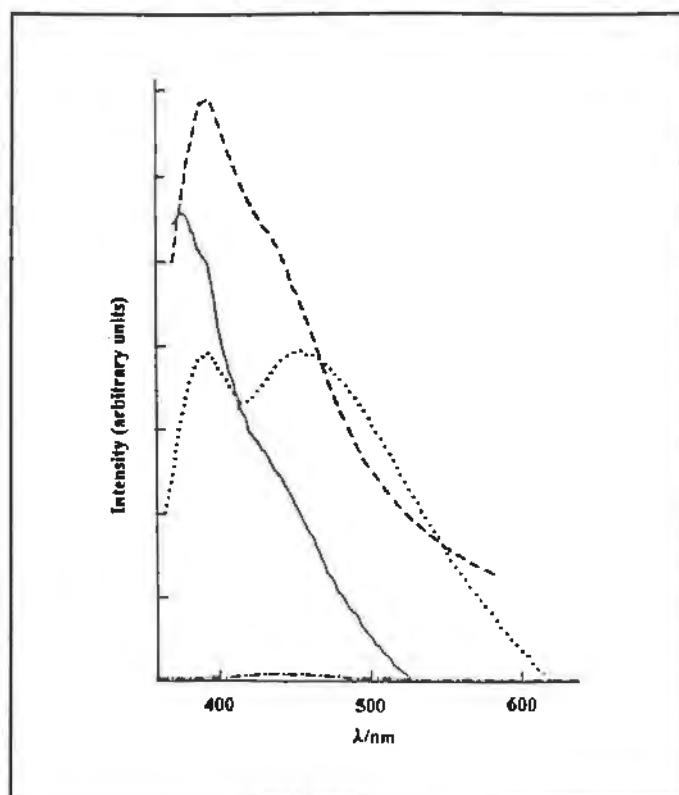


Figure 21. Emission spectra of $[\text{Cu}_2\{\mu\text{-(Ph}_2\text{P)}_2\text{py}\}_3](\text{PF}_6)_2$ in degassed acetonitrile (---) and in the presence of CF_3COOH (-·-·-·), Ag^+ (- - -) or Cu^+ (—).

2.5.3 Photophysical Studies on the $[\text{Ag}_2\{\mu\text{-(Ph}_2\text{P)}_2\text{py}\}_3](\text{BF}_4)_2$ (**3**) Complex

The absorption spectrum of **3** in degassed acetonitrile consists of a broad absorption band from 200 to 350 nm. Two absorption maxima occur at 204 and 255 nm. Upon excitation at 300 to 350 nm two emissions centred at 360 and 470 nm are observed. Figure 22 shows both the absorption and emission spectra of **3**.

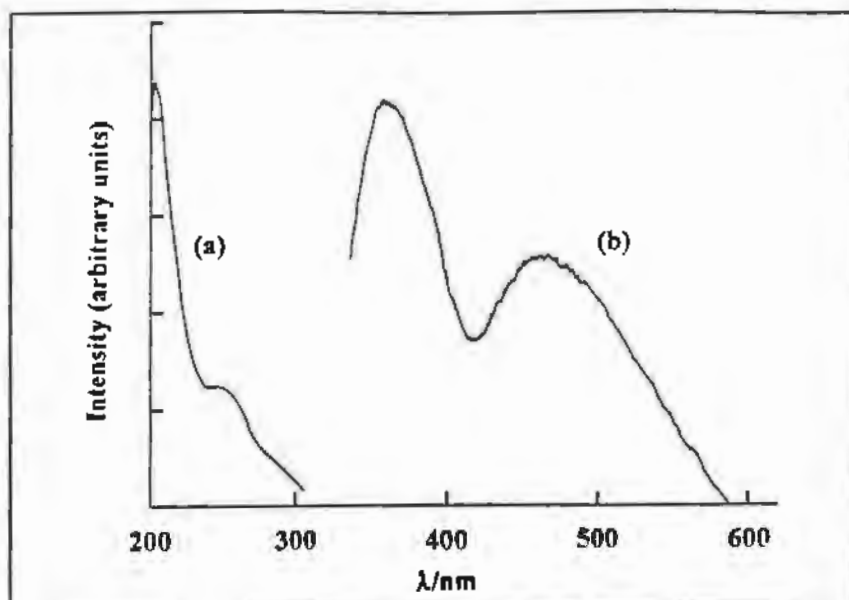


Figure 22. Excitation (a) and emission (b) spectra of $[\text{Ag}_2\{\mu\text{-(Ph}_2\text{P)}_2\text{py}\}_3](\text{BF}_4)_2$ in degassed acetonitrile.

Upon addition of AgCF_3SO_3 , $[\text{Cu}(\text{MeCN})_4](\text{PF}_6)$ or CF_3COOH to a solution of **3** in degassed acetonitrile the emission spectra were found to be perturbed but not to the extent that the emission spectrum of **1** was altered (Fig. 23). In the presence of Ag^+ ions the emission centred at 360 nm was enhanced while the emission centred at 470 nm was of much the same intensity. In the presence of Cu^+ ions the emission spectrum of **3** was hardly changed with both emissions being slightly enhanced. In the presence of CF_3COOH both emissions are quenched. The emission spectrum of **3** is perturbed in the presence of Cu^+ and Ag^+ ions with the largest enhancement occurring in the presence of Ag^+ ions. Again there is no red shift in the energy of the emissions of **3** when Cu^+ or Ag^+ ions were added as occurred in the case of the gold complex¹⁵. These changes in the emission spectrums can most likely be ascribed to the relevant metal ion being trapped in the cavity that exists in the centre of **3**, but as noted above the change in the emission spectrum of **3** was not as great as the change in emission spectrum of **1**. This is most likely due to the fact that the cavity size of **3** is larger than the cavity size of **1** resulting in **3** not being able to bind a metal ion into its cavity as strongly as **1** could.

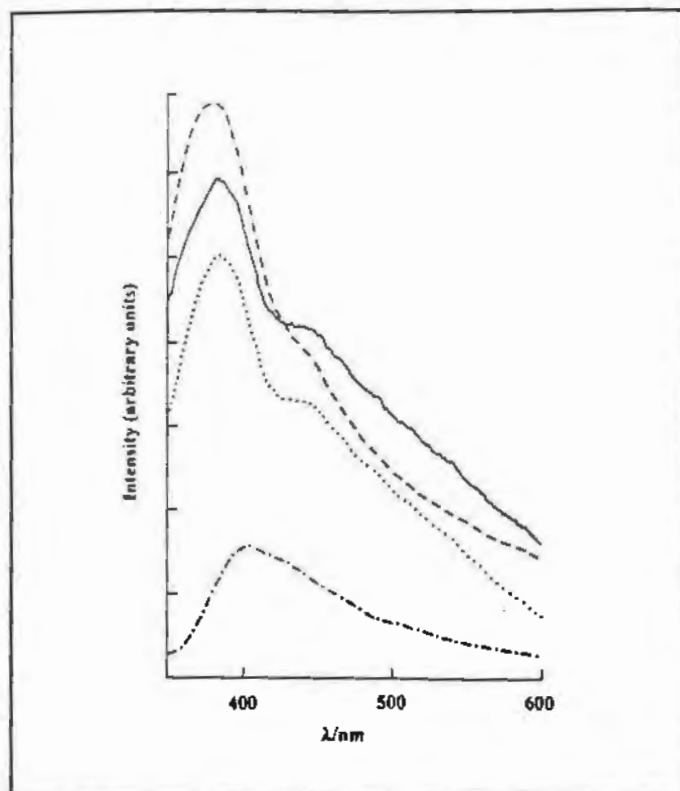


Figure 23. Emission spectra of $[\text{Ag}_2\{\mu\text{-(Ph}_2\text{P)}_2\text{py}\}_3](\text{BF}_4)_2$ in degassed acetonitrile (·····) and in the presence of CF_3COOH (-·-·-·-·), Ag^+ (- - -) or Cu^+ (—).

2.6 Conclusion

The complexes obtained upon reaction of $(\text{Ph}_2\text{P})_2\text{py}$ with copper and silver have provided further evidence for the fact that the $(\text{Ph}_2\text{P})_2\text{py}$ ligand prefers to adopt a bridging mode of coordination when reacted with transition metals. More specifically of all the possible bridging modes, mode 8 (see section 1.1) is the preferred mode of coordination. This type of coordination results in open cavities in the centre of the complexes into which it is proposed that metal ions can be trapped, evidence for which is obtained by the change in emission spectra of both complex 1 and 3 when Cu^+ and Ag^+ ions are added to a solution of 1 or 3 in degassed acetonitrile.

2.7 Experimental

General experimental details and sources of chemicals are outlined in Appendices A and B respectively.

2.7.1 Synthesis of $[\text{Cu}_2\{\mu\text{-(Ph}_2\text{P)}_2\text{py}\}_3](\text{PF}_6)_2$ (1)

The ligand 2,6-Bis(diphenylphosphino)pyridine (100 mg; 0.223 mmol) was added as a solid to a stirred solution of $[\text{Cu}(\text{MeCN})_4](\text{PF}_6)$ (55 mg; 0.149 mmol) in acetonitrile (10 ml). The mixture was stirred for 12 hours during which time all of the $(\text{Ph}_2\text{P})_2\text{py}$ ligand dissolved as the reaction took place. The solution remained colourless throughout the reaction. The volume of acetonitrile was then concentrated to *ca.* 3 ml under reduced pressure and the solution filtered through glass microfibre filter paper. A white crystalline precipitate was obtained upon addition of diethyl ether and cooling to -10°C for 12 hours. This precipitate was filtered, washed with diethyl ether and dried *in vacuo*. (yield 70-80%)

2.7.2 Synthesis of $[\text{Cu}_2\{\mu\text{-(Ph}_2\text{P)}_2\text{py}\}_2(\text{n}^2\text{-bipy})_2](\text{PF}_6)_2$ (2)

Bipyridine (42 mg; 0.268 mmol) in acetone (2 ml) was added dropwise to a stirred solution of $[\text{Cu}(\text{MeCN})_4](\text{PF}_6)$ (100 mg; 0.268 mmol) in acetone (5 ml). A dark red solution forms after stirring for 1 hour. The solution was filtered through glass microfibre filter paper and added dropwise to $(\text{Ph}_2\text{P})_2\text{py}$ (120 mg; 0.268 mmol) in acetone (5 ml). The solution turned a light green colour once the addition was completed and a yellow precipitate formed after further stirring for 2 hours. The precipitate was filtered off, washed with acetone and dried *in vacuo* for 1 hour to give an analytically pure sample. Yellow crystals were obtained by dissolving the precipitate in a minimum amount of acetonitrile, addition of diethyl ether and cooling to -10°C for 12 hours. (yield 75-80%) Anal. Calcd for $\text{Cu}_2\text{C}_{78}\text{H}_{62}\text{F}_{12}\text{N}_6\text{P}_6$: C, 57.70; H, 3.85; N, 5.18. Found: C, 57.32; H, 3.76; N, 5.84.

2.7.3 Synthesis of $[\text{Ag}_2\{\mu\text{-(Ph}_2\text{P)}_2\text{py}\}_3](\text{BF}_4)_2$ (3)

The 2,6-Bis(diphenylphosphino)pyridine ligand (100 mg; 0.223 mmol) was added as a solid to a stirred solution of $[\text{Ag}(\text{COD})_2](\text{BF}_4)$ (61 mg; 0.149 mmol) in acetonitrile (10 ml). The mixture was stirred for 12 hours during which time all of the $(\text{Ph}_2\text{P})_2\text{py}$ ligand dissolved as the reaction took place. The solution remained colourless throughout the reaction. The acetonitrile was then removed under reduced pressure and the white residue dissolved in a minimum of dichloromethane. Diethyl ether was added and the mixture cooled to -10°C for 12 hours. Colourless crystals formed which were filtered off, washed with diethyl ether and dried *in vacuo* for 1 hour to give an analytically pure sample. (yield 70-80%) Anal. Calcd for $\text{Ag}_2\text{C}_{87}\text{H}_{69}\text{F}_{12}\text{N}_3\text{P}_8$ (complex 3 with PF_6^- as counterion): C, 56.58; H, 3.77; N, 2.28. Found: C, 56.24; H, 4.18; N, 2.32.

2.7.4 Synthesis of $[\text{Ag}_2\{\mu\text{-(Ph}_2\text{P)}_2\text{py}\}_2(\text{n}^2\text{-bipy})_2](\text{BF}_4)_2$ (4)

Bipyridine (38 mg; 0.243 mmol) in acetonitrile (2 ml) was added dropwise to a stirred solution of $[\text{Ag}(\text{COD})_2](\text{BF}_4)$ (100 mg; 0.243 mmol) in acetonitrile (5 ml). A brown solution forms which changes to colourless after stirring for 1 hour. The solution was left to stir for a further 12 hours after which $(\text{Ph}_2\text{P})_2\text{py}$ (109 mg; 0.243 mmol) was added as a solid. The mixture was left to stir for a further 6 hours during which time the $(\text{Ph}_2\text{P})_2\text{py}$ ligand dissolved as the reaction took place. The volume of acetonitrile was then concentrated to *ca.* 3 ml under reduced pressure and the solution filtered through glass microfibre. A white crystalline precipitate was obtained upon addition of diethyl ether and cooling to -10°C for 12 hours. This precipitate was filtered, washed with diethyl ether and dried *in vacuo* for 1 hour to give an analytically pure sample. (yield 75-80%) Anal. Calcd for $\text{Ag}_2\text{C}_{78}\text{H}_{62}\text{B}_2\text{F}_8\text{N}_6\text{P}_4$: C, 58.71; H, 3.92; N, 5.27. Found: C, 57.99; H, 3.73; N, 5.33.

TABLE 1: Spectroscopic Data (Ph₂P)₂py and Its Complexes

Complex	Infrared Spectroscopic Data ^a cm ⁻¹	¹ H NMR ^b δ	³¹ P{ ¹ H} NMR ^c δ
(Ph ₂ P) ₂ py	[1579(vw), 1550(w), 1541(s)] v(C-Npy) [1474(w), 1429(s), 1419(s)] v(P-Cpy, Ph)	7.6-7.2 (m, 21H) 7.0 (d, 2H)	-3.5 (s)
[Cu ₂ {μ-(Ph ₂ P) ₂ py} ₃](PF ₆) ₂ (1)	[1560(vw), 1545(vw)] v(C-Npy) [1491(w), 1436(s), 1430(s)] v(P-Cpy, Ph) [839(vs)] v(P-F)	7.6-6.9 (m, 69H)	5.1 (b)
[Cu ₂ {μ-(Ph ₂ P) ₂ py} ₂ (η ² -bipy) ₂](PF ₆) ₂ (2)	[1597(m), 1560(w), 1552(m)] v(C-Npy) [1481(m), 1460(m), 1439(s)] v(P-Cpy, Ph) [839(vs)] v(P-F)	8.0-7.0 (m, 54H)	0.9 (b)
[Ag ₂ {μ-(Ph ₂ P) ₂ py} ₃](BF ₄) ₂ (3)	[1560(vw), 1545(w)] v(C-Npy) [1481(w), 1435(s), 1430(s)] v(P-Cpy, Ph) [1057(vs)] v(B-F)	7.6-6.9 (m, 69H)	14.3 (ct)
[Ag ₂ {μ-(Ph ₂ P) ₂ py} ₂ (η ² -bipy) ₂](BF ₄) ₂ (4)	[1593(w), 1562(w), 1545(w)] v(C-Npy) [1482(w), 1437(s), 1427(s)] v(P-Cpy, Ph) [1059(vs)] v(B-F)	8.0-7.0 (m, 54H)	11.0 (bs)

a. All infrared spectra run as KBr discs. vw = very weak, w = weak, m = medium, s = strong, vs = very strong

b. (Ph₂P)₂py run in CD₃OD, 1 run in CD₂Cl₂, 2 run in CD₃CN, 3 run in CD₂Cl₂ and 4 in CD₃CN. d = doublet, m = multiplet

c. All samples run in CH₃Cl₂ on external lock. All values relative to H₃PO₄. b = broad, bs = broad singlet, ct = coarse triplet

2.7.5 Single Crystal X-ray Diffraction Study of $[\text{Cu}_2\{\mu-(\text{Ph}_2\text{P})_2\text{py}\}_3](\text{PF}_6)_2$ (1)

Colourless bipyramidal shaped crystals (1) were grown by slow vapour diffusion of diethyl ether into a concentrated solution of (1) in dichloroethane. The general approach used for the intensity data collection and structure solution is described in Appendix A. The crystallographic data is given in Table 2, the fractional coordinates are given in Table 3, the anisotropic thermal parameters in Table 4, the interatomic distances in Table 5 and the interatomic angles in Table 6. The observed and calculated structure factors may be found on microfiche in an envelope fixed to the inside back cover.

2.7.6 Single Crystal X-ray Diffraction Study of $[\text{Cu}_2\{\mu-(\text{Ph}_2\text{P})_2\text{py}\}_2(\eta^2\text{-bipy})_2](\text{PF}_6)_2$ (2)

Yellow triangular shaped crystals (2) were grown by slow vapour diffusion of diethyl ether into a concentrated solution of (2) in acetonitrile. The general approach used for the intensity data collection and structure solution is described in Appendix A. The crystallographic data is given in Table 7, the fractional coordinates are given in Table 8, the anisotropic thermal parameters in Table 9, the interatomic distances in Table 10 and the interatomic angles in Table 11. The observed and calculated structure factors may be found on microfiche in an envelope fixed to the inside back cover.

2.7.7 Single Crystal X-ray Diffraction Study of $[\text{Ag}_2\{\mu-(\text{Ph}_2\text{P})_2\text{py}\}_3](\text{BF}_4)_2$ (3)

Colourless bipyramidal shaped crystals (1) were grown by cooling of a saturated acetonitrile-ethanol (1:1, vol:vol) solution of the compound. The general approach used for the intensity data collection and structure solution is described in Appendix A. The crystallographic data is given in Table 12, the fractional coordinates are given in Table 13, the anisotropic thermal parameters in Table 14, the interatomic distances in Table 15 and the interatomic angles in Table 16. The observed and calculated structure factors may be found on microfiche in an envelope fixed to the inside back cover.

Table 2.
Crystal Data and Details of the Crystallographic Analysis for
[Cu₂{μ-(Ph₂P)₂py}₃](PF₆)₂ (1)

Formula	Cu ₂ C ₈₇ H ₆₉ F ₁₂ N ₃ P ₈
Molecular Mass	1757.18
Crystal System	Triclinic
Space Group	P1
a (Å)	14.742 (3)
b (Å)	18.523 (3)
c (Å)	18.980 (8)
α (°)	100.55 (2)
β (°)	96.63 (3)
γ (°)	112.39 (1)
V (Å ³)	4612.12
Z	2
D _c (g.cm ⁻³)	1.27
F(000)	1796
λ(Mo - Kα) (Å)	0.71069
Scan Mode	ω - 2θ
ω scan angle	0.51 + 0.35 tanθ
Horizontal Aperture width (mm)	2.7 + 0.1 tanθ
Scattering range (°)	2 ≤ θ ≤ 23
μ (cm ⁻¹)	6.90
Absorption corrections	Semi empirical ⁶⁶
Measured intensities	12755
Unique intensities	9170
Unique intensities with [I > 3σ(I)]	5178
Structure solution	Direct & Fourier methods
Weighting scheme	1/(σ ² F + 0.00351F ²)
R = Σ(F _o - F _c)/ΣF _o	0.092
R _w = Σ _w ^{1/2} (F _o - F _c)/Σ _w ^{1/2} F _o	0.099
(Δ/σ) _{max}	0.328
Δρ _{max} (eÅ ⁻³)	1.242
Number of parameters	433

**Table 3. Fractional Coordinates ($\times 10^4$) and Isotropic Thermal Factors (\AA^2 , $\times 10^3$) for
 $[\text{Cu}_2\{\mu\text{-(Ph}_2\text{P)}_2\text{py}\}_3](\text{PF}_6)_2$**

	x/a	y/b	z/c	U_{eq}
Cu(1)	441(2)	3193(1)	1751(1)	51(1)
Cu(2)	-2042(1)	1439(1)	2765(1)	45
P(1)	1579(3)	3214(3)	2661(3)	55(1)
P(2)	-1227(3)	713(3)	3133(2)	52(1)
P(3)	92(3)	2271(2)	690(2)	49(1)
P(4)	-3182(3)	957(2)	1687(2)	45(1)
P(5)	-147(4)	4145(2)	1839(2)	52(1)
P(6)	-2072(3)	2482(2)	3596(2)	51(1)
N(1)	362(9)	1857(7)	2862(6)	48(3)*
N(2)	-1684(8)	1535(7)	994(6)	42(3)*
N(3)	-1083(9)	3509(7)	2823(7)	47(3)*
C(1)	1815(12)	3770(10)	3584(10)	64(5)*
C(2)	1853(14)	4546(12)	3685(11)	83(6)*
C(3)	2164(16)	5041(14)	4428(13)	102(7)*
C(4)	2377(15)	4748(13)	5046(12)	93(6)*
C(5)	2337(16)	3962(14)	4925(12)	101(7)*
C(6)	2024(15)	3477(12)	4167(12)	88(6)*
C(7)	2788(12)	3567(10)	2408(10)	59(5)*
C(8)	2805(16)	3425(13)	1704(12)	97(7)*
C(9)	3706(19)	3753(15)	1450(13)	112(8)*
C(10)	4568(18)	4220(14)	1952(14)	106(7)*
C(11)	4610(23)	4318(18)	2653(18)	154(11)*
C(12)	3651(19)	4070(15)	2899(13)	116(8)*
C(13)	1280(11)	2200(9)	2736(8)	48(4)*
C(14)	1952(12)	1830(10)	2706(9)	60(5)*
C(15)	1585(13)	1018(10)	2793(10)	69(5)*
C(16)	645(12)	682(9)	2920(9)	55(4)*

Table 3. / Cont.

C(17)	56(12)	1112(9)	2961(8)	54(4)*
C(18)	-1690(11)	-357(9)	2688(9)	54(4)*
C(19)	-1867(12)	-570(10)	1930(9)	63(5)*
C(20)	-2253(13)	-1399(11)	1571(10)	76(5)*
C(21)	-2456(15)	-1974(12)	1960(12)	87(6)*
C(22)	-2277(16)	-1761(13)	2734(12)	97(7)*
C(23)	-1912(15)	-934(12)	3132(11)	86(6)*
C(24)	-1048(14)	768(11)	4126(10)	72(5)*
C(25)	-1927(15)	630(12)	4386(12)	89(6)*
C(26)	-1806(19)	652(15)	5178(14)	115(8)*
C(27)	-863(18)	829(13)	5546(12)	104(7)*
C(28)	16(18)	1018(14)	5319(13)	113(8)*
C(29)	-93(16)	953(12)	4522(12)	93(6)*
C(30)	512(13)	2684(10)	-75(9)	65(5)*
C(31)	1107(15)	3512(12)	103(11)	86(6)*
C(32)	1460(19)	3854(16)	-517(16)	128(9)*
C(33)	1202(19)	3331(17)	-1167(14)	117(8)*
C(34)	637(17)	2554(14)	-1346(12)	103(7)*
C(35)	295(13)	2188(11)	-775(10)	74(5)*
C(36)	532(11)	1470(9)	669(8)	46(4)*
C(37)	1369(12)	1532(9)	394(9)	56(4)*
C(38)	1721(13)	907(11)	442(10)	73(5)*
C(39)	1267(13)	300(10)	772(9)	66(5)*
C(40)	399(13)	257(10)	1042(9)	64(5)*
C(41)	42(12)	853(10)	1009(9)	59(5)*
C(42)	-1296(12)	1759(9)	428(9)	53(4)*
C(43)	-1859(13)	1696(10)	-239(9)	63(5)*
C(44)	-2889(14)	1356(11)	-321(10)	71(5)*
C(45)	-3334(12)	1126(10)	240(9)	63(5)*

Table 3. / Cont.

C(46)	-2685(11)	1207(9)	882(8)	46(4)*
C(47)	-3845(12)	-117(10)	1429(9)	59(5)*
C(48)	-3985(14)	-603(12)	727(10)	79(6)*
C(49)	-4512(16)	-1456(13)	580(12)	96(7)*
C(50)	-4896(16)	-1796(13)	1123(12)	97(7)*
C(51)	-4729(15)	-1326(13)	1840(12)	93(6)*
C(52)	-4189(13)	-470(11)	1977(10)	70(5)*
C(53)	-4176(11)	1320(9)	1631(8)	46(4)*
C(54)	-5171(13)	805(10)	1539(9)	63(5)*
C(55)	-5892(15)	1119(12)	1506(11)	83(6)*
C(56)	-5579(15)	1969(12)	1578(11)	85(6)*
C(57)	-4597(15)	2454(11)	1678(10)	79(6)*
C(58)	-3862(13)	2149(10)	1715(9)	65(5)*
C(59)	789(12)	5138(9)	1901(9)	56(4)*
C(60)	486(13)	5771(10)	1883(9)	67(5)*
C(61)	1286(14)	6580(11)	1995(10)	74(5)*
C(62)	2240(14)	6684(11)	2092(10)	75(5)*
C(63)	2578(15)	6065(12)	2115(11)	86(6)*
C(64)	1786(14)	5269(11)	1996(10)	71(5)*
C(65)	-1220(12)	4024(9)	1182(9)	52(4)*
C(66)	-2043(15)	4062(11)	1343(10)	78(6)*
C(67)	-2868(17)	3961(13)	785(13)	102(7)*
C(68)	-2811(17)	3791(13)	76(13)	102(7)*
C(69)	-1957(20)	3794(15)	-95(14)	123(8)*
C(70)	-1110(19)	3913(15)	438(14)	120(8)*
C(71)	-518(10)	4242(9)	2717(8)	43(4)*
C(72)	-229(12)	4953(9)	3226(9)	56(4)*
C(73)	-505(12)	4912(10)	3897(9)	60(5)*
C(74)	-1034(12)	4186(10)	4058(9)	62(5)*

Table 3. / Cont.

C(75)	-1335(11)	3487(9)	3472(8)	49(4)*
C(76)	-1562(11)	2626(9)	4575(8)	46(4)*
C(77)	-2182(14)	2615(11)	5079(11)	78(5)*
C(78)	-1684(15)	2745(12)	5833(11)	86(6)*
C(79)	-738(15)	2871(11)	5998(11)	81(6)*
C(80)	-142(14)	2864(11)	5503(11)	82(6)*
C(81)	-594(13)	2748(10)	4743(10)	65(5)*
C(82)	-3335(13)	2426(11)	3589(10)	71(5)*
C(83)	-4058(16)	1664(13)	3527(11)	93(6)*
C(84)	-5097(21)	1625(18)	3581(15)	139(9)*
C(85)	-5215(19)	2307(18)	3642(14)	125(9)*
C(86)	-4522(24)	3067(19)	3666(16)	154(11)*
C(87)	-3482(19)	3159(15)	3646(13)	119(8)*
P(7)	7499(6)	879(3)	7423(3)	88(2)
F(1)	7332(24)	1328(11)	6890(8)	248(11)
F(2)	7692(17)	1591(8)	8087(7)	200(7)
F(3)	7609(21)	404(11)	7970(9)	236(10)
F(4)	7319(14)	175(8)	6770(8)	173(6)
F(5)	6424(17)	585(18)	7442(15)	297(12)
F(6)	8531(15)	1197(19)	7381(14)	339(12)
P(8)	7510(5)	5812(5)	2846(4)	109(2)
F(7)	8412(11)	5736(11)	2478(9)	179(7)
F(8)	8128(14)	5722(12)	3507(9)	197(7)
F(9)	8068(13)	6712(9)	3113(18)	323(13)
F(10)	6651(12)	5788(11)	3192(10)	209(7)
F(11)	6983(13)	4888(11)	2603(14)	242(9)
F(12)	7004(15)	5838(20)	2159(11)	292(13)

* isotropic temperature factor.

$$U_{eq} = \frac{1}{3} \sum_i \sum_j U_{ij} a_i^* a_j^* (a_i \cdot a_j)$$

Table 4. Anisotropic Temperature Factors (\AA^2 , $\times 10^3$) for $[\text{Cu}_2\{\mu\text{-(Ph}_2\text{P)}_2\text{py}\}_3](\text{PF}_6)_2$

	U(11)	U(22)	U(33)	U(23)	U(13)	U(12)
Cu(1)	69(1)	38(1)	52(1)	7(1)	16(1)	29(1)
Cu(2)	58(1)	38(1)	39(1)	9(1)	7(1)	20(1)
P(1)	64(3)	43(3)	58(3)	7(2)	11(2)	26(2)
P(2)	65(3)	47(3)	47(3)	13(2)	5(2)	28(2)
P(3)	67(3)	38(2)	51(3)	13(2)	21(2)	28(2)
P(4)	49(3)	45(2)	40(3)	10(2)	7(2)	19(2)
P(5)	82(3)	42(2)	42(3)	12(2)	18(2)	36(2)
P(6)	69(3)	41(3)	41(3)	7(2)	10(2)	22(2)
P(7)	148(6)	53(3)	71(4)	23(3)	46(4)	39(4)
F(1)	544(43)	168(16)	99(12)	69(12)	75(18)	200(23)
F(2)	435(28)	99(10)	77(9)	21(8)	62(13)	119(15)
F(3)	488(37)	165(15)	161(16)	90(13)	96(19)	215(21)
F(4)	284(20)	107(10)	117(11)	-7(9)	41(12)	87(12)
F(5)	176(20)	383(36)	294(29)	13(28)	109(20)	90(22)
F(6)	129(16)	434(41)	254(27)	-57(27)	87(17)	-47(20)
P(8)	87(5)	126(6)	108(5)	59(5)	8(4)	29(4)
F(7)	119(11)	263(20)	202(16)	136(15)	74(11)	82(12)
F(8)	239(19)	234(19)	145(14)	64(13)	-14(13)	132(16)
F(9)	143(14)	65(10)	675(50)	21(18)	-67(22)	26(10)
F(10)	127(13)	217(18)	231(19)	-9(14)	99(13)	26(12)
F(11)	147(15)	134(15)	394(34)	10(18)	80(19)	23(12)
F(12)	207(19)	584(48)	168(17)	230(24)	32(15)	192(26)

Table 5. Interatomic Distances (Å) for [Cu₂{μ-(Ph₂P)₂py}₃](PF₆)₂

Cu(1)-P(1)	2.249(5)	Cu(1)-P(3)	2.250(4)
Cu(1)-P(5)	2.231(6)	Cu(2)-P(2)	2.264(6)
Cu(2)-P(4)	2.280(4)	Cu(2)-P(6)	2.277(5)
P(1)-C(1)	1.78(2)	P(1)-C(7)	1.81(2)
P(1)-C(13)	1.80(2)	P(2)-C(17)	1.84(2)
P(2)-C(18)	1.82(2)	P(2)-C(24)	1.85(2)
P(3)-C(30)	1.83(2)	P(3)-C(36)	1.83(2)
P(3)-C(42)	1.86(2)	P(4)-C(46)	1.83(2)
P(4)-C(47)	1.79(2)	P(4)-C(53)	1.83(2)
P(5)-C(59)	1.80(2)	P(5)-C(65)	1.81(2)
P(5)-C(71)	1.81(2)	P(6)-C(75)	1.84(2)
P(6)-C(76)	1.85(2)	P(6)-C(82)	1.82(2)
N(1)-C(13)	1.33(2)	N(1)-C(17)	1.34(2)
N(2)-C(42)	1.33(2)	N(2)-C(46)	1.34(2)
N(3)-C(71)	1.36(2)	N(3)-C(75)	1.33(2)
C(1)-C(2)	1.39(3)	C(1)-C(6)	1.37(3)
C(2)-C(3)	1.45(3)	C(3)-C(4)	1.43(4)
C(4)-C(5)	1.41(4)	C(5)-C(6)	1.47(3)
C(7)-C(8)	1.32(3)	C(7)-C(12)	1.36(3)
C(8)-C(9)	1.42(4)	C(9)-C(10)	1.36(3)
C(10)-C(11)	1.30(4)	C(11)-C(12)	1.47(4)
C(13)-C(14)	1.40(3)	C(14)-C(15)	1.44(3)
C(15)-C(16)	1.36(3)	C(16)-C(17)	1.38(3)
C(18)-C(19)	1.39(2)	C(18)-C(23)	1.45(3)
C(19)-C(20)	1.42(2)	C(20)-C(21)	1.37(3)
C(21)-C(22)	1.42(3)	C(22)-C(23)	1.44(3)
C(24)-C(25)	1.39(3)	C(24)-C(29)	1.40(3)
C(25)-C(26)	1.49(4)	C(26)-C(27)	1.37(4)
C(27)-C(28)	1.35(4)	C(28)-C(29)	1.48(3)

Table 5. / Cont.

C(30)-C(31)	1.40(3)	C(30)-C(35)	1.39(2)
C(31)-C(32)	1.49(4)	C(32)-C(33)	1.33(4)
C(33)-C(34)	1.31(3)	C(34)-C(35)	1.42(3)
C(36)-C(37)	1.37(3)	C(36)-C(41)	1.41(2)
C(37)-C(38)	1.45(3)	C(38)-C(39)	1.37(3)
C(39)-C(40)	1.41(3)	C(40)-C(41)	1.40(3)
C(42)-C(43)	1.39(2)	C(43)-C(44)	1.38(3)
C(44)-C(45)	1.36(3)	C(45)-C(46)	1.41(2)
C(47)-C(48)	1.41(3)	C(47)-C(52)	1.37(3)
C(48)-C(49)	1.43(3)	C(49)-C(50)	1.37(3)
C(50)-C(51)	1.41(3)	C(51)-C(52)	1.43(3)
C(53)-C(54)	1.38(2)	C(53)-C(58)	1.40(2)
C(54)-C(55)	1.39(3)	C(55)-C(56)	1.44(3)
C(56)-C(57)	1.35(3)	C(57)-C(58)	1.40(3)
C(59)-C(60)	1.41(3)	C(59)-C(64)	1.38(3)
C(60)-C(61)	1.47(2)	C(61)-C(62)	1.33(3)
C(62)-C(63)	1.42(4)	C(63)-C(64)	1.45(2)
C(65)-C(66)	1.31(3)	C(65)-C(70)	1.43(3)
C(66)-C(67)	1.45(3)	C(67)-C(68)	1.35(4)
C(68)-C(69)	1.33(4)	C(69)-C(70)	1.43(4)
C(71)-C(72)	1.36(2)	C(72)-C(73)	1.39(3)
C(73)-C(74)	1.39(2)	C(74)-C(75)	1.43(2)
C(76)-C(77)	1.39(3)	C(76)-C(81)	1.35(3)
C(77)-C(78)	1.46(3)	C(78)-C(79)	1.31(3)
C(79)-C(80)	1.36(3)	C(80)-C(81)	1.46(3)
C(82)-C(83)	1.38(3)	C(82)-C(87)	1.44(4)
C(83)-C(84)	1.52(4)	C(84)-C(85)	1.33(5)
C(85)-C(86)	1.38(4)	C(86)-C(87)	1.48(5)
P(7)-F(1)	1.48(2)	P(7)-F(2)	1.56(2)

Table 5. / Cont.

P(7)-F(3)	1.51(2)	P(7)-F(4)	1.54(2)
P(7)-F(5)	1.47(3)	P(7)-F(6)	1.43(2)
P(8)-F(7)	1.61(2)	P(8)-F(8)	1.54(2)
P(8)-F(9)	1.50(2)	P(8)-F(10)	1.48(2)
P(8)-F(11)	1.54(2)	P(8)-F(12)	1.44(3)

Table 6. Interatomic Angles (°) for [Cu₂{μ-(Ph₂P)₂py}₃](PF₆)₂

P(1)-Cu(1)-P(3)	116.5(2)	P(1)-Cu(1)-P(5)	121.6(2)
P(3)-Cu(1)-P(5)	121.3(2)	P(2)-Cu(2)-P(4)	121.2(2)
P(2)-Cu(2)-P(6)	119.4(2)	P(4)-Cu(2)-P(6)	117.3(2)
Cu(1)-P(1)-C(1)	124.0(7)	Cu(1)-P(1)-C(7)	108.4(6)
C(1)-P(1)-C(7)	104.3(7)	Cu(1)-P(1)-C(13)	108.7(5)
C(1)-P(1)-C(13)	103.6(8)	C(7)-P(1)-C(13)	106.7(9)
Cu(2)-P(2)-C(17)	109.5(6)	Cu(2)-P(2)-C(18)	119.4(6)
C(17)-P(2)-C(18)	102.1(8)	Cu(2)-P(2)-C(24)	114.8(8)
C(17)-P(2)-C(24)	104.3(8)	C(18)-P(2)-C(24)	105.0(8)
Cu(1)-P(3)-C(30)	115.0(5)	Cu(1)-P(3)-C(36)	119.1(5)
C(30)-P(3)-C(36)	103.7(9)	Cu(1)-P(3)-C(42)	105.9(6)
C(30)-P(3)-C(42)	106.1(8)	C(36)-P(3)-C(42)	106.0(7)
Cu(2)-P(4)-C(46)	115.9(5)	Cu(2)-P(4)-C(47)	114.0(6)
C(46)-P(4)-C(47)	104.3(7)	Cu(2)-P(4)-C(53)	116.8(5)
C(46)-P(4)-C(53)	99.9(8)	C(47)-P(4)-C(53)	103.9(8)
Cu(1)-P(5)-C(59)	114.1(7)	Cu(1)-P(5)-C(65)	120.8(6)
C(59)-P(5)-C(65)	105.5(8)	Cu(1)-P(5)-C(71)	106.2(6)
C(59)-P(5)-C(71)	103.5(7)	C(65)-P(5)-C(71)	105.1(8)
Cu(2)-P(6)-C(75)	114.8(6)	Cu(2)-P(6)-C(76)	118.4(6)
C(75)-P(6)-C(76)	100.1(6)	Cu(2)-P(6)-C(82)	112.8(5)
C(75)-P(6)-C(82)	105.5(9)	C(76)-P(6)-C(82)	103.6(8)
C(13)-N(1)-C(17)	118(2)	C(42)-N(2)-C(46)	115.7(13)
C(71)-N(3)-C(75)	117.7(12)	P(1)-C(1)-C(2)	116(2)
P(1)-C(1)-C(6)	122(2)	C(2)-C(1)-C(6)	121(2)
C(1)-C(2)-C(3)	117(2)	C(2)-C(3)-C(4)	123(2)
C(3)-C(4)-C(5)	119(2)	C(4)-C(5)-C(6)	117(2)
C(1)-C(6)-C(5)	123(2)	P(1)-C(7)-C(8)	117.5(13)
P(1)-C(7)-C(12)	123(2)	C(8)-C(7)-C(12)	119(2)
C(7)-C(8)-C(9)	122(2)	C(8)-C(9)-C(10)	118(2)

Table 6. / Cont.

C(9)-C(10)-C(11)	123(3)	C(10)-C(11)-C(12)	117(3)
C(7)-C(12)-C(11)	120(2)	P(1)-C(13)-N(1)	111.6(14)
P(1)-C(13)-C(14)	124.2(11)	N(1)-C(13)-C(14)	124(2)
C(13)-C(14)-C(15)	116(2)	C(14)-C(15)-C(16)	118(2)
C(15)-C(16)-C(17)	121(2)	P(2)-C(17)-N(1)	113.5(14)
P(2)-C(17)-C(16)	123.9(12)	N(1)-C(17)-C(16)	123(2)
P(2)-C(18)-C(19)	117.2(14)	P(2)-C(18)-C(23)	119.1(12)
C(19)-C(18)-C(23)	124(2)	C(18)-C(19)-C(20)	118(2)
C(19)-C(20)-C(21)	121(2)	C(20)-C(21)-C(22)	121(2)
C(21)-C(22)-C(23)	121(2)	C(18)-C(23)-C(22)	115(2)
P(2)-C(24)-C(25)	113(2)	P(2)-C(24)-C(29)	119(2)
C(25)-C(24)-C(29)	128(2)	C(24)-C(25)-C(26)	113(2)
C(25)-C(26)-C(27)	117(2)	C(26)-C(27)-C(28)	131(2)
C(27)-C(28)-C(29)	113(2)	C(24)-C(29)-C(28)	117(2)
P(3)-C(30)-C(31)	115.4(14)	P(3)-C(30)-C(35)	121.3(13)
C(31)-C(30)-C(35)	123(2)	C(30)-C(31)-C(32)	116(2)
C(31)-C(32)-C(33)	116(2)	C(32)-C(33)-C(34)	129(3)
C(33)-C(34)-C(35)	118(2)	C(30)-C(35)-C(34)	118(2)
P(3)-C(36)-C(37)	119.3(13)	P(3)-C(36)-C(41)	117.5(14)
C(37)-C(36)-C(41)	123(2)	C(36)-C(37)-C(38)	117(2)
C(37)-C(38)-C(39)	122(2)	C(38)-C(39)-C(40)	119(2)
C(39)-C(40)-C(41)	120(2)	C(36)-C(41)-C(40)	119(2)
P(3)-C(42)-N(2)	110.6(11)	P(3)-C(42)-C(43)	124.7(13)
N(2)-C(42)-C(43)	124(2)	C(42)-C(43)-C(44)	117(2)
C(43)-C(44)-C(45)	121(2)	C(44)-C(45)-C(46)	116(2)
P(4)-C(46)-N(2)	114.1(11)	P(4)-C(46)-C(45)	120.3(12)
N(2)-C(46)-C(45)	125(2)	P(4)-C(47)-C(48)	124.4(14)
P(4)-C(47)-C(52)	115.8(12)	C(48)-C(47)-C(52)	120(2)
C(47)-C(48)-C(49)	120(2)	C(48)-C(49)-C(50)	119(2)

Table 6. / Cont.

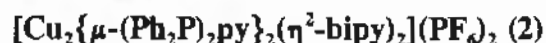
C(49)-C(50)-C(51)	122(2)	C(50)-C(51)-C(52)	118(2)
C(47)-C(52)-C(51)	121(2)	P(4)-C(53)-C(54)	121.6(14)
P(4)-C(53)-C(58)	116.0(12)	C(54)-C(53)-C(58)	122(2)
C(53)-C(54)-C(55)	119(2)	C(54)-C(55)-C(56)	119(2)
C(55)-C(56)-C(57)	120(2)	C(56)-C(57)-C(58)	122(2)
C(53)-C(58)-C(57)	118(2)	P(5)-C(59)-C(60)	119.0(13)
P(5)-C(59)-C(64)	120(2)	C(60)-C(59)-C(64)	122(2)
C(59)-C(60)-C(61)	117(2)	C(60)-C(61)-C(62)	120(2)
C(61)-C(62)-C(63)	125(2)	C(62)-C(63)-C(64)	115(2)
C(59)-C(64)-C(63)	122(2)	P(5)-C(65)-C(66)	125.4(14)
P(5)-C(65)-C(70)	115(2)	C(66)-C(65)-C(70)	119(2)
C(65)-C(66)-C(67)	122(2)	C(66)-C(67)-C(68)	119(2)
C(67)-C(68)-C(69)	119(2)	C(68)-C(69)-C(70)	123(3)
C(65)-C(70)-C(69)	116(2)	P(5)-C(71)-N(3)	111.4(10)
P(5)-C(71)-C(72)	124.7(12)	N(3)-C(71)-C(72)	123.8(14)
C(71)-C(72)-C(73)	117(2)	C(72)-C(73)-C(74)	122(2)
C(73)-C(74)-C(75)	116(2)	P(6)-C(75)-N(3)	116.1(10)
P(6)-C(75)-C(74)	120.5(13)	N(3)-C(75)-C(74)	123.4(14)
P(6)-C(76)-C(77)	119.1(13)	P(6)-C(76)-C(81)	115.8(13)
C(77)-C(76)-C(81)	125(2)	C(76)-C(77)-C(78)	114(2)
C(77)-C(78)-C(79)	122(2)	C(78)-C(79)-C(80)	125(2)
C(79)-C(80)-C(81)	116(2)	C(76)-C(81)-C(80)	119(2)
P(6)-C(82)-C(83)	115(2)	P(6)-C(82)-C(87)	118.3(14)
C(83)-C(82)-C(87)	127(2)	C(82)-C(83)-C(84)	115(2)
C(83)-C(84)-C(85)	117(2)	C(84)-C(85)-C(86)	129(3)
C(85)-C(86)-C(87)	117(3)	C(82)-C(87)-C(86)	115(2)
F(1)-P(7)-F(2)	92.3(10)	F(1)-P(7)-F(3)	177(2)
F(2)-P(7)-F(3)	87.6(10)	F(1)-P(7)-F(4)	88.0(10)
F(2)-P(7)-F(4)	179.4(13)	F(3)-P(7)-F(4)	92.2(10)

Table 6. / Cont.

F(1)-P(7)-F(5)	88(2)	F(2)-P(7)-F(5)	88.1(14)
F(3)-P(7)-F(5)	89(2)	F(4)-P(7)-F(5)	92.4(13)
F(1)-P(7)-F(6)	88(2)	F(2)-P(7)-F(6)	91.4(14)
F(3)-P(7)-F(6)	95(2)	F(4)-P(7)-F(6)	88.1(14)
F(5)-P(7)-F(6)	177(2)	F(7)-P(8)-F(8)	81.0(11)
F(7)-P(8)-F(9)	91.9(12)	F(8)-P(8)-F(9)	89.0(13)
F(7)-P(8)-F(10)	173.5(12)	F(8)-P(8)-F(10)	96.1(12)
F(9)-P(8)-F(10)	93.8(13)	F(7)-P(8)-F(11)	86.9(11)
F(8)-P(8)-F(11)	87.9(13)	F(9)-P(8)-F(11)	177(2)
F(10)-P(8)-F(11)	87.2(12)	F(7)-P(8)-F(12)	91.0(13)
F(8)-P(8)-F(12)	171(2)	F(9)-P(8)-F(12)	95(2)
F(10)-P(8)-F(12)	91.5(13)	F(11)-P(8)-F(12)	88(2)

Table 7.

Crystal Data and Details of the Crystallographic Analysis for



Formula	$\text{Cu}_2\text{C}_{78}\text{H}_{62}\text{F}_{12}\text{N}_6\text{P}_6$
Molecular Mass	1622.19
Crystal System	Triclinic
Space Group	$\text{P}\bar{1}$
a (Å)	11.622 (6)
b (Å)	12.719 (6)
c (Å)	14.429 (8)
α (°)	108.36 (4)
β (°)	109.63 (4)
γ (°)	90.49 (4)
V (Å ³)	1891.14
Z	1
D _c (g.cm ⁻³)	1.43
F(000)	828
$\lambda(\text{Mo - K}\alpha)$ (Å)	0.71069
Scan Mode	$\omega - 2\theta$
ω scan angle	$1.5 + 0.35 \tan\theta$
Horizontal Aperture width (mm)	$2.7 + 0.1 \tan\theta$
Scattering range (°)	$2 \leq \theta \leq 23$
μ (cm ⁻¹)	7.61
Absorption corrections	Semi empirical ⁶⁸
Measured intensities	5472
Unique intensities	3995
Unique intensities with [I > 3 σ (I)]	1985
Structure solution	Direct & Fourier methods
Weighting scheme	$1/(\sigma^2F + 0.00284F^2)$
$R = \Sigma(F_o - F_c)/\Sigma F_o$	0.080
$R_w = \Sigma_w^{1/2} (F_o - F_c)/\Sigma_w^{1/2} F_o$	0.081
(Δ/σ) _{max}	0.078
$\Delta\rho_{\text{max}}$ (eÅ ⁻³)	0.616
Number of parameters	259

**Table 8. Fractional Coordinates ($\times 10^4$) and Isotropic Thermal Factors (\AA^2 , $\times 10^3$) for
 $[\text{Cu}_2\{\mu\text{-(Ph}_2\text{P)}_2\text{py}\}_2(\eta^2\text{-bipy})](\text{PF}_6)_2$**

	x/a	y/b	z/c	U_{eq}
Cu	10195(2)	12257(2)	12110(2)	29(1)
P(1)	8352(4)	11357(4)	11783(3)	30(1)
P(2)	8157(4)	8571(4)	8033(3)	32(1)
N(1)	8126(12)	9796(11)	9950(10)	33(3)*
N(2)	10679(12)	13788(11)	13356(10)	31(3)*
N(3)	9721(12)	13352(11)	11290(11)	37(4)*
C(1)	7082(16)	11998(14)	11178(13)	39(5)*
C(2)	7101(15)	13144(14)	11685(13)	35(4)*
C(3)	6193(20)	13754(17)	11239(17)	64(6)*
C(4)	5273(22)	13186(20)	10234(19)	77(7)*
C(5)	5231(20)	12088(19)	9769(17)	71(7)*
C(6)	6146(19)	11439(17)	10185(16)	58(6)*
C(7)	8074(16)	11267(14)	12911(14)	41(5)*
C(8)	6842(16)	11137(15)	12901(14)	42(5)*
C(9)	6677(19)	10971(17)	13787(16)	59(6)*
C(10)	7685(19)	10937(17)	14611(16)	57(6)*
C(11)	8867(19)	11048(17)	14642(16)	58(6)*
C(12)	9082(17)	11233(15)	13779(14)	48(5)*
C(13)	8088(14)	9894(13)	10899(12)	26(4)*
C(14)	7989(15)	9025(13)	11272(12)	31(4)*
C(15)	7928(16)	7940(14)	10575(14)	42(5)*
C(16)	8023(15)	7811(14)	9602(13)	35(4)*
C(17)	8093(15)	8754(14)	9302(13)	35(4)*
C(18)	7916(15)	9882(14)	7861(13)	35(4)*
C(19)	6759(19)	10338(17)	7759(16)	58(6)*
C(20)	6534(20)	11282(18)	7494(17)	62(6)*

Table 8. / Cont.

C(21)	7449(20)	11842(18)	7318(17)	63(6)*
C(22)	8598(19)	11427(17)	7413(15)	57(6)*
C(23)	8814(17)	10451(16)	7667(15)	50(5)*
C(24)	6701(15)	7706(13)	7050(13)	32(4)*
C(25)	5893(18)	7179(16)	7329(15)	51(5)*
C(26)	4828(22)	6474(20)	6517(19)	82(7)*
C(27)	4672(20)	6327(18)	5493(18)	70(7)*
C(28)	5473(20)	6933(18)	5226(17)	62(6)*
C(29)	6532(19)	7644(17)	6039(16)	59(6)*
C(30)	11195(16)	13896(15)	14362(14)	43(5)*
C(31)	11576(17)	14984(16)	15114(15)	49(5)*
C(32)	11410(19)	15909(17)	14763(16)	57(6)*
C(33)	10874(17)	15773(15)	13760(15)	46(5)*
C(34)	10450(15)	14656(14)	13022(13)	34(4)*
C(35)	9858(16)	14439(15)	11892(14)	42(5)*
C(36)	9361(18)	15235(17)	11492(16)	54(5)*
C(37)	8686(24)	14934(22)	10411(22)	94(8)*
C(38)	8511(22)	13781(20)	9762(19)	78(7)*
C(39)	9089(17)	13067(15)	10255(15)	46(5)*
P(3)	7344(6)	7264(5)	3073(5)	64(2)
F(1)	6704(16)	8223(12)	2808(12)	122(5)
F(2)	6953(13)	6613(11)	1852(9)	90(4)
F(3)	7762(16)	7910(13)	4286(10)	118(5)
F(4)	8544(13)	7781(14)	3033(11)	113(5)
F(5)	8069(20)	6312(15)	3305(13)	156(7)
F(6)	6169(17)	6703(17)	3097(14)	157(7)

* isotropic temperature factor.

$$U_{eq} = \frac{1}{3} \sum_i \sum_j U_{ij} a_i^* a_j^* (a_i \cdot a_j)$$

**Table 9. Anisotropic Temperature Factors for (\AA^2 , $\times 10^3$) for
 $[\text{Cu}_2\{\mu\text{-(Ph}_2\text{P)}_2\text{py}\}_2(\eta^2\text{-bipy})](\text{PF}_6)_2$**

	U(11)	U(22)	U(33)	U(23)	U(13)	U(12)
Cu	29(1)	23(1)	28(1)	0(1)	10(1)	2(1)
P(1)	27(3)	34(3)	23(3)	-1(2)	11(2)	1(2)
P(2)	30(3)	31(3)	28(3)	1(2)	12(2)	0(2)
P(3)	74(4)	75(5)	58(4)	37(4)	27(4)	14(4)
F(1)	164(15)	93(11)	106(12)	42(10)	36(11)	70(11)
F(2)	113(11)	88(10)	51(8)	14(7)	16(8)	-7(8)
F(3)	175(16)	129(13)	48(9)	16(8)	49(10)	15(11)
F(4)	72(10)	171(16)	85(11)	38(10)	20(8)	-32(10)
F(5)	254(23)	142(15)	112(14)	86(13)	73(15)	97(16)
F(6)	141(16)	184(19)	155(17)	32(14)	88(14)	-54(14)

Table 10. Interatomic Distances (Å) for [Cu₂{μ-(Ph₂P)₂py}₂(η²-bipy)](PF₆)₂

Cu-Cu'	6.806(2)	Cu-P(1)	2.249(5)
Cu'-P(2)	2.223(6)	Cu-N(2)	2.107(13)
Cu-N(3)	2.063(13)	P(1)-C(1)	1.79(2)
P(1)-C(7)	1.80(2)	P(1)-C(13)	1.85(2)
P(2)-C(17)	1.80(2)	P(2)-C(18)	1.77(2)
P(2)-C(24)	1.86(2)	N(1)-C(13)	1.35(2)
N(1)-C(17)	1.35(2)	N(2)-C(30)	1.33(2)
N(2)-C(34)	1.33(2)	N(3)-C(35)	1.36(2)
N(3)-C(39)	1.35(2)	C(1)-C(2)	1.41(2)
C(1)-C(6)	1.43(2)	C(2)-C(3)	1.42(2)
C(3)-C(4)	1.43(3)	C(4)-C(5)	1.34(3)
C(5)-C(6)	1.44(3)	C(7)-C(8)	1.44(2)
C(7)-C(12)	1.41(2)	C(8)-C(9)	1.43(3)
C(9)-C(10)	1.37(3)	C(10)-C(11)	1.36(3)
C(11)-C(12)	1.44(3)	C(13)-C(14)	1.39(2)
C(14)-C(15)	1.41(2)	C(15)-C(16)	1.40(2)
C(16)-C(17)	1.41(2)	C(18)-C(19)	1.45(2)
C(18)-C(23)	1.42(2)	C(19)-C(20)	1.37(3)
C(20)-C(21)	1.41(3)	C(21)-C(22)	1.42(3)
C(22)-C(23)	1.40(3)	C(24)-C(25)	1.38(2)
C(24)-C(29)	1.38(2)	C(25)-C(26)	1.43(3)
C(26)-C(27)	1.38(3)	C(27)-C(28)	1.42(3)
C(28)-C(29)	1.43(3)	C(30)-C(31)	1.42(2)
C(31)-C(32)	1.41(3)	C(32)-C(33)	1.32(2)
C(33)-C(34)	1.44(2)	C(34)-C(35)	1.47(2)
C(35)-C(36)	1.36(2)	C(36)-C(37)	1.41(3)
C(37)-C(38)	1.44(3)	C(38)-C(39)	1.37(3)
P(3)-F(1)	1.518(14)	P(3)-F(2)	1.591(13)
P(3)-F(3)	1.579(14)	P(3)-F(4)	1.563(14)
P(3)-F(5)	1.54(2)	P(3)-F(6)	1.55(2)

Table 11. Interatomic Angles (°) for [Cu₂{μ-(Ph₂P)₂py}₂(η²-bipy)](PF₆)₂

P(1)-Cu-N(2)	113.9(4)	P(1)-Cu-N(3)	102.4(4)
N(2)-Cu-N(3)	79.8(5)	Cu-P(1)-C(1)	113.2(6)
P(2)-Cu'-P(1')	90.4(1)	P(2)-Cu'-N(2')	112.0(5)
P(2)-Cu'-N(3')	114.1(5)		
Cu-P(1)-C(7)	115.4(6)	C(1)-P(1)-C(7)	103.9(8)
Cu-P(1)-C(13)	113.4(5)	C(1)-P(1)-C(13)	105.4(8)
C(7)-P(1)-C(13)	104.5(8)	C(17)-P(2)-C(18)	104.9(8)
C(17)-P(2)-C(24)	107.1(8)	C(18)-P(2)-C(24)	100.5(8)
C(13)-N(1)-C(17)	117.1(14)	Cu-N(2)-C(30)	124.8(11)
Cu-N(2)-C(34)	112.1(11)	C(30)-N(2)-C(34)	123(2)
Cu-N(3)-C(35)	114.8(11)	Cu-N(3)-C(39)	125.7(12)
C(35)-N(3)-C(39)	118(2)	P(1)-C(1)-C(2)	116.3(13)
P(1)-C(1)-C(6)	123.6(14)	C(2)-C(1)-C(6)	120(2)
C(1)-C(2)-C(3)	121(2)	C(2)-C(3)-C(4)	118(2)
C(3)-C(4)-C(5)	120(2)	C(4)-C(5)-C(6)	123(2)
C(1)-C(6)-C(5)	117(2)	P(1)-C(7)-C(8)	120.8(13)
P(1)-C(7)-C(12)	118.9(13)	C(8)-C(7)-C(12)	120(2)
C(7)-C(8)-C(9)	118(2)	C(8)-C(9)-C(10)	120(2)
C(9)-C(10)-C(11)	124(2)	C(10)-C(11)-C(12)	119(2)
C(7)-C(12)-C(11)	120(2)	P(1)-C(13)-N(1)	113.3(11)
P(1)-C(13)-C(14)	119.8(12)	N(1)-C(13)-C(14)	126.5(14)
C(13)-C(14)-C(15)	115.5(14)	C(14)-C(15)-C(16)	119(2)
C(15)-C(16)-C(17)	120(2)	P(2)-C(17)-N(1)	119.2(12)
P(2)-C(17)-C(16)	119.4(13)	N(1)-C(17)-C(16)	122(2)
P(2)-C(18)-C(19)	123.0(14)	P(2)-C(18)-C(23)	119.5(13)
C(19)-C(18)-C(23)	117(2)	C(18)-C(19)-C(20)	122(2)
C(19)-C(20)-C(21)	120(2)	C(20)-C(21)-C(22)	120(2)
C(21)-C(22)-C(23)	120(2)	C(18)-C(23)-C(22)	121(2)
P(2)-C(24)-C(25)	121.9(13)	P(2)-C(24)-C(29)	113.5(14)

Table 11. / Cont.

C(25)-C(24)-C(29)	125(2)	C(24)-C(25)-C(26)	118(2)
C(25)-C(26)-C(27)	119(2)	C(26)-C(27)-C(28)	122(2)
C(27)-C(28)-C(29)	119(2)	C(24)-C(29)-C(28)	117(2)
N(2)-C(30)-C(31)	119(2)	C(30)-C(31)-C(32)	119(2)
C(31)-C(32)-C(33)	121(2)	C(32)-C(33)-C(34)	119(2)
N(2)-C(34)-C(33)	120(2)	N(2)-C(34)-C(35)	119(2)
C(33)-C(34)-C(35)	122(2)	N(3)-C(35)-C(34)	114(2)
N(3)-C(35)-C(36)	122(2)	C(34)-C(35)-C(36)	123(2)
C(35)-C(36)-C(37)	120(2)	C(36)-C(37)-C(38)	119(2)
C(37)-C(38)-C(39)	116(2)	N(3)-C(39)-C(38)	125(2)
F(1)-P(3)-F(2)	88.1(8)	F(1)-P(3)-F(3)	92.4(9)
F(2)-P(3)-F(3)	178.8(9)	F(1)-P(3)-F(4)	89.0(10)
F(2)-P(3)-F(4)	87.7(8)	F(3)-P(3)-F(4)	91.3(9)
F(1)-P(3)-F(5)	175.4(11)	F(2)-P(3)-F(5)	90.1(9)
F(3)-P(3)-F(5)	89.3(9)	F(4)-P(3)-F(5)	86.7(11)
F(1)-P(3)-F(6)	93.0(11)	F(2)-P(3)-F(6)	91.2(9)
F(3)-P(3)-F(6)	89.8(10)	F(4)-P(3)-F(6)	177.7(11)
F(5)-P(3)-F(6)	91.2(12)		

Table 12.
Crystal Data and Details of the Crystallographic Analysis for
 $[\text{Ag}_2\{\mu\text{-(Ph}_2\text{P)}_2\text{py}\}_3](\text{BF}_4)_2$ (3)

Formula	$\text{Ag}_2\text{C}_{87}\text{H}_{69}\text{B}_2\text{F}_8\text{N}_3\text{P}_6$
Molecular Mass	1731.71
Crystal System	Triclinic
Space Group	$\text{P}\bar{1}$
a (Å)	14.793 (4)
b (Å)	18.136 (5)
c (Å)	18.883 (4)
α (°)	76.37 (2)
β (°)	83.88 (2)
γ (°)	67.56 (2)
V (Å ³)	4605.33
Z	2
D_c (g.cm ⁻³)	1.25
F(000)	1756
λ (Mo - K α) (Å)	0.71069
Scan Mode	$\omega - 2\theta$
ω scan angle	$0.60 + 0.35 \tan\theta$
Horizontal Aperture width (mm)	$2.7 + 0.1 \tan\theta$
Scattering range (°)	$2 \leq \theta \leq 23$
μ (cm ⁻¹)	5.80
Absorption corrections	Semi empirical ⁶⁸
Measured intensities	13218
Unique intensities	9322
Unique intensities with $[I > 3\sigma(I)]$	4769
Structure solution	Direct & Fourier methods
Weighting scheme	$1/(\sigma^2F + 0.02077F^2)$
$R = \Sigma(F_o - F_c)/\Sigma F_o$	0.100
$R_w = \Sigma_w^{1/2} (F_o - F_c)/\Sigma_w^{1/2} F_o$	0.109
$(\Delta/\sigma)_{\text{max}}$	0.116
$\Delta\rho_{\text{max}}$ (eÅ ⁻³)	2.616
Number of parameters	470

**Table 13. Fractional Coordinates ($\times 10^4$) and Isotropic Thermal Factors (\AA^2 , $\times 10^3$)
for $[\text{Ag}_2\{\mu\text{-(Ph}_2\text{P)}_2\text{py}\}_3](\text{BF}_4)_2$**

	x/a	y/b	z/c	U_{eq}
Ag(1)	2262(1)	3247(1)	3221(1)	45(1)
Ag(2)	1568(1)	1417(1)	2219(1)	43(1)
P(1)	647(5)	4278(4)	3120(3)	44(2)
P(2)	463(5)	2519(4)	1309(3)	48(2)
P(3)	3457(5)	3212(4)	2230(4)	50(2)
P(4)	3150(5)	580(4)	1786(4)	57(2)
P(5)	2849(4)	2272(4)	4374(3)	42(2)
P(6)	856(5)	896(4)	3374(3)	46(2)
N(1)	411(13)	3589(11)	2098(9)	41(5)
N(2)	3586(15)	1803(13)	2018(11)	54(6)
N(3)	1788(12)	1511(11)	4067(10)	38(5)
C(1)	514(17)	5312(14)	3098(13)	46(6)*
C(2)	1357(20)	5475(17)	2997(15)	63(8)*
C(3)	1265(26)	6324(23)	2911(19)	98(11)*
C(4)	365(24)	6938(20)	2964(18)	85(10)*
C(5)	-504(23)	6732(20)	3128(18)	85(10)*
C(6)	-394(20)	5918(17)	3144(15)	63(8)*
C(7)	-256(19)	4079(16)	3732(14)	55(7)*
C(8)	-1155(24)	4199(20)	3509(18)	83(10)*
C(9)	-1894(24)	3977(21)	4084(20)	91(10)*
C(10)	-1686(28)	3768(23)	4773(22)	104(12)*
C(11)	-810(36)	3704(29)	5041(26)	141(16)*
C(12)	1(28)	3775(24)	4506(21)	108(12)*
C(13)	185(17)	4323(15)	2232(13)	47(6)*
C(14)	-221(18)	5022(15)	1748(14)	52(7)*
C(15)	-423(20)	5002(17)	1036(15)	68(8)*
C(16)	-226(18)	4209(16)	912(14)	54(7)*

Table 13. / Cont.

C(17)	196(16)	3512(13)	1437(12)	37(6)*
C(18)	806(16)	2612(14)	350(12)	43(6)*
C(19)	1641(19)	2743(17)	135(15)	61(7)*
C(20)	1958(20)	2836(17)	-586(16)	67(8)*
C(21)	1454(23)	2757(19)	-1075(17)	75(9)*
C(22)	659(25)	2672(21)	-897(18)	88(10)*
C(23)	234(20)	2606(17)	-155(15)	64(8)*
C(24)	-702(21)	2442(18)	1371(15)	67(8)*
C(25)	-656(23)	1627(20)	1399(17)	80(9)*
C(26)	-1594(42)	1480(34)	1462(30)	168(20)*
C(27)	-2405(33)	2218(30)	1358(24)	127(15)*
C(28)	-2519(39)	2985(35)	1311(29)	165(20)*
C(29)	-1560(27)	3101(23)	1358(20)	100(11)*
C(30)	4341(17)	3565(14)	2450(13)	44(6)*
C(31)	4715(24)	4072(20)	1912(18)	85(10)*
C(32)	5492(31)	4384(27)	2074(25)	126(15)*
C(33)	5674(32)	4112(28)	2774(27)	129(15)*
C(34)	5378(30)	3617(26)	3365(23)	118(13)*
C(35)	4699(24)	3299(21)	3116(18)	89(10)*
C(36)	3143(21)	3760(18)	1283(16)	70(8)*
C(37)	2363(25)	4495(21)	1221(19)	89(10)*
C(38)	2158(28)	4982(24)	454(22)	103(12)*
C(39)	2559(24)	4737(21)	-61(19)	85(10)*
C(40)	3338(25)	3932(22)	39(19)	94(11)*
C(41)	3604(22)	3450(19)	706(18)	76(9)*
C(42)	4172(18)	2160(15)	2109(13)	49(6)*
C(43)	5184(19)	1797(17)	2165(15)	61(7)*
C(44)	5588(19)	985(17)	2085(15)	60(7)*
C(45)	5024(18)	603(15)	1968(14)	54(7)*

Table 13. / Cont.

C(46)	4032(17)	1026(15)	1929(12)	44(6)*
C(47)	3770(19)	-508(16)	2200(15)	58(7)*
C(48)	3794(22)	-694(19)	2943(17)	79(9)*
C(49)	4198(26)	-1547(23)	3364(20)	96(11)*
C(50)	4545(31)	-2065(27)	2935(26)	125(14)*
C(51)	4622(38)	-1866(34)	2151(31)	161(19)*
C(52)	4161(27)	-1072(24)	1754(21)	101(11)*
C(53)	3285(24)	670(20)	822(18)	81(9)*
C(54)	3895(27)	866(23)	343(22)	104(12)*
C(55)	3846(26)	875(22)	-429(20)	95(11)*
C(56)	3155(36)	711(29)	-631(26)	136(16)*
C(57)	2460(35)	514(29)	-248(27)	138(16)*
C(58)	2504(34)	542(28)	537(26)	135(15)*
C(59)	2888(17)	2681(14)	5124(13)	44(6)*
C(60)	3115(20)	2246(17)	5795(16)	67(8)*
C(61)	3088(23)	2652(21)	6415(17)	83(9)*
C(62)	2829(29)	3482(26)	6232(24)	113(13)*
C(63)	2634(28)	3898(25)	5652(24)	108(12)*
C(64)	2630(27)	3541(23)	5018(20)	100(11)*
C(65)	4025(15)	1456(13)	4331(12)	36(5)*
C(66)	4164(17)	866(15)	3990(13)	49(6)*
C(67)	5121(18)	260(15)	3928(14)	53(7)*
C(68)	5809(20)	339(17)	4189(15)	61(7)*
C(69)	5737(19)	941(17)	4533(15)	63(8)*
C(70)	4818(20)	1507(17)	4624(15)	63(8)*
C(71)	1987(17)	1749(15)	4607(14)	47(6)*
C(72)	1509(19)	1706(16)	5316(14)	58(7)*
C(73)	773(20)	1437(17)	5417(15)	66(8)*
C(74)	544(18)	1167(15)	4795(14)	54(7)*

Table 13. / Cont.

C(75)	1064(16)	1210(13)	4160(12)	40(6)*
C(76)	1293(18)	-175(16)	3623(14)	54(7)*
C(77)	1357(22)	-580(20)	3096(17)	79(9)*
C(78)	1696(31)	-1490(27)	3213(23)	122(14)*
C(79)	2096(24)	-1958(21)	3891(19)	89(10)*
C(80)	2098(26)	-1567(23)	4462(20)	101(11)*
C(81)	1695(20)	-657(18)	4338(15)	67(8)*
C(82)	-467(19)	1215(17)	3391(15)	63(8)*
C(83)	-984(20)	2032(17)	3314(15)	61(7)*
C(84)	-1969(25)	2367(21)	3357(18)	89(10)*
C(85)	-2461(25)	1782(22)	3426(19)	94(11)*
C(86)	-1919(23)	933(20)	3477(17)	80(9)*
C(87)	-874(21)	655(19)	3467(16)	72(8)*
B(1)	9204(37)	692(71)	8038(63)	432(90)*
F(1)	2015(37)	155(71)	8029(63)	160(10)*
F(2)	989(37)	1106(71)	7124(63)	196(12)*
F(3)	1994(37)	1480(71)	7703(63)	249(17)*
F(4)	2647(37)	600(71)	6905(63)	240(16)*
B(2)	6805(10)	5706(8)	2142(7)	238(39)*
F(5)	6431(10)	5569(8)	2866(7)	134(8)*
F(6)	7301(10)	4944(8)	1934(7)	145(9)*
F(7)	7458(10)	6114(8)	2111(7)	170(10)*
F(8)	6031(10)	6197(8)	1658(7)	212(14)*

* isotropic temperature factor.

$$U_{eq} = \frac{1}{3} \sum_i \sum_j U_{ij} a_i^* a_j^* (a_i \cdot a_j)$$

Table14. Anisotropic Temperature Factors (\AA^2 , $\times 10^3$) for $[\text{Ag}_2\{\mu\text{-(Ph}_2\text{P)}_2\text{py}\}_3](\text{BF}_4)_2$

	U(11)	U(22)	U(33)	U(23)	U(13)	U(12)
Ag(1)	41(1)	40(1)	49(1)	-3(1)	-7(1)	-9(1)
Ag(2)	46(1)	39(1)	39(1)	-5(1)	3(1)	-15(1)
P(1)	43(4)	41(4)	37(4)	-2(3)	-5(3)	-6(3)
P(2)	63(5)	42(4)	37(4)	-1(3)	0(3)	-23(4)
P(3)	48(4)	47(4)	52(4)	-6(3)	-4(3)	-16(3)
P(4)	57(5)	48(4)	58(5)	-15(4)	8(4)	-12(4)
P(5)	38(4)	39(4)	42(4)	-4(3)	-4(3)	-9(3)
P(6)	49(4)	45(4)	43(4)	-4(3)	-1(3)	-20(3)
N(1)	49(12)	42(12)	34(11)	-6(9)	4(9)	-21(10)
N(2)	65(14)	57(14)	53(14)	-31(11)	14(11)	-27(12)
N(3)	28(10)	41(12)	45(12)	-15(10)	-14(9)	-6(9)

Table 15. Interatomic Distances (Å) for [Ag₂{μ-(Ph₂P)₂py}₃](BF₄)₂

Ag(1)-P(1)	2.422(6)	Ag(1)-P(3)	2.443(7)
Ag(1)-P(5)	2.459(6)	Ag(2)-P(2)	2.479(7)
Ag(2)-P(4)	2.451(7)	Ag(2)-P(6)	2.468(7)
P(1)-C(1)	1.80(3)	P(1)-C(7)	1.77(3)
P(1)-C(13)	1.85(3)	P(2)-C(17)	1.76(2)
P(2)-C(18)	1.82(2)	P(2)-C(24)	1.79(3)
P(3)-C(30)	1.80(3)	P(3)-C(36)	1.84(3)
P(3)-C(42)	1.85(3)	P(4)-C(46)	1.86(3)
P(4)-C(47)	1.84(3)	P(4)-C(53)	1.79(3)
P(5)-C(59)	1.76(2)	P(5)-C(65)	1.83(2)
P(5)-C(71)	1.84(3)	P(6)-C(75)	1.81(2)
P(6)-C(76)	1.76(3)	P(6)-C(82)	1.84(3)
N(1)-C(13)	1.32(3)	N(1)-C(17)	1.37(3)
N(2)-C(42)	1.32(3)	N(2)-C(46)	1.35(3)
N(3)-C(71)	1.30(3)	N(3)-C(75)	1.37(3)
C(1)-C(2)	1.39(3)	C(1)-C(6)	1.40(3)
C(2)-C(3)	1.46(4)	C(3)-C(4)	1.39(4)
C(4)-C(5)	1.47(4)	C(5)-C(6)	1.41(4)
C(7)-C(8)	1.38(4)	C(7)-C(12)	1.47(4)
C(8)-C(9)	1.56(4)	C(9)-C(10)	1.30(4)
C(10)-C(11)	1.41(5)	C(11)-C(12)	1.52(6)
C(13)-C(14)	1.34(3)	C(14)-C(15)	1.42(4)
C(15)-C(16)	1.43(4)	C(16)-C(17)	1.38(3)
C(18)-C(19)	1.36(3)	C(18)-C(23)	1.35(3)
C(19)-C(20)	1.39(4)	C(20)-C(21)	1.32(4)
C(21)-C(22)	1.26(4)	C(22)-C(23)	1.47(4)
C(24)-C(25)	1.44(4)	C(24)-C(29)	1.38(4)
C(25)-C(26)	1.51(6)	C(26)-C(27)	1.41(6)
C(27)-C(28)	1.32(6)	C(28)-C(29)	1.54(6)

Table 15. / Cont.

C(30)-C(31)	1.42(4)	C(30)-C(35)	1.33(4)
C(31)-C(32)	1.56(5)	C(32)-C(33)	1.32(5)
C(33)-C(34)	1.41(5)	C(34)-C(35)	1.50(5)
C(36)-C(37)	1.39(4)	C(36)-C(41)	1.35(4)
C(37)-C(38)	1.50(5)	C(38)-C(39)	1.17(4)
C(39)-C(40)	1.47(5)	C(40)-C(41)	1.35(4)
C(42)-C(43)	1.41(3)	C(43)-C(44)	1.40(4)
C(44)-C(45)	1.34(3)	C(45)-C(46)	1.39(3)
C(47)-C(48)	1.36(4)	C(47)-C(52)	1.39(4)
C(48)-C(49)	1.48(4)	C(49)-C(50)	1.30(5)
C(50)-C(51)	1.44(6)	C(51)-C(52)	1.40(6)
C(53)-C(54)	1.30(5)	C(53)-C(58)	1.45(5)
C(54)-C(55)	1.46(5)	C(55)-C(56)	1.30(5)
C(56)-C(57)	1.32(6)	C(57)-C(58)	1.50(6)
C(59)-C(60)	1.33(3)	C(59)-C(64)	1.43(4)
C(60)-C(61)	1.51(4)	C(61)-C(62)	1.37(5)
C(62)-C(63)	1.17(5)	C(63)-C(64)	1.49(5)
C(65)-C(66)	1.31(3)	C(65)-C(70)	1.41(3)
C(66)-C(67)	1.45(3)	C(67)-C(68)	1.26(3)
C(68)-C(69)	1.36(4)	C(69)-C(70)	1.39(4)
C(71)-C(72)	1.45(3)	C(72)-C(73)	1.35(4)
C(73)-C(74)	1.49(4)	C(74)-C(75)	1.36(3)
C(76)-C(77)	1.35(4)	C(76)-C(81)	1.47(4)
C(77)-C(78)	1.50(5)	C(78)-C(79)	1.41(5)
C(79)-C(80)	1.43(5)	C(80)-C(81)	1.49(4)
C(82)-C(83)	1.37(4)	C(82)-C(87)	1.34(4)
C(83)-C(84)	1.37(4)	C(84)-C(85)	1.48(5)
C(85)-C(86)	1.43(4)	C(86)-C(87)	1.45(4)
B(2)-F(5)	1.424(0)	B(2)-F(6)	1.423(0)
B(2)-F(7)	1.423(0)	B(2)-F(8)	1.424(0)

Table 16. Interatomic Angles (°) for [Ag₂{μ-(Ph₂P)₂py}₃](BF₄)₂

P(1)-Ag(1)-P(3)	121.9(2)	P(1)-Ag(1)-P(5)	121.7(2)
P(3)-Ag(1)-P(5)	116.0(2)	P(2)-Ag(2)-P(4)	117.9(2)
P(2)-Ag(2)-P(6)	118.0(2)	P(4)-Ag(2)-P(6)	120.4(2)
Ag(1)-P(1)-C(1)	117.8(8)	Ag(1)-P(1)-C(7)	117.7(9)
C(1)-P(1)-C(7)	106.4(12)	Ag(1)-P(1)-C(13)	106.6(8)
C(1)-P(1)-C(13)	104.7(11)	C(7)-P(1)-C(13)	101.6(12)
Ag(2)-P(2)-C(17)	114.6(8)	Ag(2)-P(2)-C(18)	119.1(8)
C(17)-P(2)-C(18)	102.3(11)	Ag(2)-P(2)-C(24)	110.8(10)
C(17)-P(2)-C(24)	103.1(12)	C(18)-P(2)-C(24)	105.4(12)
Ag(1)-P(3)-C(30)	109.7(8)	Ag(1)-P(3)-C(36)	123.4(10)
C(30)-P(3)-C(36)	103.8(13)	Ag(1)-P(3)-C(42)	112.3(8)
C(30)-P(3)-C(42)	104.1(11)	C(36)-P(3)-C(42)	101.6(12)
Ag(2)-P(4)-C(46)	107.2(8)	Ag(2)-P(4)-C(47)	122.9(9)
C(46)-P(4)-C(47)	101.9(12)	Ag(2)-P(4)-C(53)	115.6(11)
C(46)-P(4)-C(53)	99.2(14)	C(47)-P(4)-C(53)	106.6(14)
Ag(1)-P(5)-C(59)	117.0(8)	Ag(1)-P(5)-C(65)	116.1(7)
C(59)-P(5)-C(65)	106.0(11)	Ag(1)-P(5)-C(71)	104.4(8)
C(59)-P(5)-C(71)	107.6(11)	C(65)-P(5)-C(71)	104.8(11)
Ag(2)-P(6)-C(75)	115.1(8)	Ag(2)-P(6)-C(76)	113.3(9)
C(75)-P(6)-C(76)	104.5(12)	Ag(2)-P(6)-C(82)	115.3(9)
C(75)-P(6)-C(82)	102.3(12)	C(76)-P(6)-C(82)	105.1(13)
C(13)-N(1)-C(17)	120(2)	C(42)-N(2)-C(46)	115(2)
C(71)-N(3)-C(75)	119(2)	P(1)-C(1)-C(2)	116(2)
P(1)-C(1)-C(6)	121(2)	C(2)-C(1)-C(6)	122(2)
C(1)-C(2)-C(3)	118(3)	C(2)-C(3)-C(4)	121(3)
C(3)-C(4)-C(5)	120(3)	C(4)-C(5)-C(6)	117(3)
C(1)-C(6)-C(5)	122(3)	P(1)-C(7)-C(8)	123(2)
P(1)-C(7)-C(12)	117(2)	C(8)-C(7)-C(12)	121(3)
C(7)-C(8)-C(9)	119(3)	C(8)-C(9)-C(10)	119(3)

Table 16. / Cont.

C(9)-C(10)-C(11)	124(4)	C(10)-C(11)-C(12)	119(4)
C(7)-C(12)-C(11)	116(3)	P(1)-C(13)-N(1)	112(2)
P(1)-C(13)-C(14)	123(2)	N(1)-C(13)-C(14)	124(2)
C(13)-C(14)-C(15)	120(3)	C(14)-C(15)-C(16)	115(2)
C(15)-C(16)-C(17)	122(2)	P(2)-C(17)-N(1)	118(2)
P(2)-C(17)-C(16)	123(2)	N(1)-C(17)-C(16)	119(2)
P(2)-C(18)-C(19)	118(2)	P(2)-C(18)-C(23)	122(2)
C(19)-C(18)-C(23)	120(2)	C(18)-C(19)-C(20)	123(3)
C(19)-C(20)-C(21)	119(3)	C(20)-C(21)-C(22)	120(3)
C(21)-C(22)-C(23)	126(3)	C(18)-C(23)-C(22)	113(3)
P(2)-C(24)-C(25)	113(2)	P(2)-C(24)-C(29)	124(3)
C(25)-C(24)-C(29)	123(3)	C(24)-C(25)-C(26)	118(3)
C(25)-C(26)-C(27)	112(4)	C(26)-C(27)-C(28)	133(5)
C(27)-C(28)-C(29)	113(5)	C(24)-C(29)-C(28)	119(4)
P(3)-C(30)-C(31)	121(2)	P(3)-C(30)-C(35)	119(2)
C(31)-C(30)-C(35)	120(3)	C(30)-C(31)-C(32)	123(3)
C(31)-C(32)-C(33)	107(4)	C(32)-C(33)-C(34)	137(5)
C(33)-C(34)-C(35)	111(4)	C(30)-C(35)-C(34)	122(3)
P(3)-C(36)-C(37)	114(2)	P(3)-C(36)-C(41)	123(2)
C(37)-C(36)-C(41)	123(3)	C(36)-C(37)-C(38)	115(3)
C(37)-C(38)-C(39)	124(4)	C(38)-C(39)-C(40)	119(4)
C(39)-C(40)-C(41)	122(3)	C(36)-C(41)-C(40)	117(3)
P(3)-C(42)-N(2)	110(2)	P(3)-C(42)-C(43)	124(2)
N(2)-C(42)-C(43)	127(2)	C(42)-C(43)-C(44)	115(3)
C(43)-C(44)-C(45)	121(3)	C(44)-C(45)-C(46)	119(3)
P(4)-C(46)-N(2)	112(2)	P(4)-C(46)-C(45)	124(2)
N(2)-C(46)-C(45)	124(2)	P(4)-C(47)-C(48)	115(2)
P(4)-C(47)-C(52)	120(2)	C(48)-C(47)-C(52)	125(3)
C(47)-C(48)-C(49)	122(3)	C(48)-C(49)-C(50)	112(4)

Table 16. / Cont.

C(49)-C(50)-C(51)	126(5)	C(50)-C(51)-C(52)	121(5)
C(47)-C(52)-C(51)	113(4)	P(4)-C(53)-C(54)	133(3)
P(4)-C(53)-C(58)	111(3)	C(54)-C(53)-C(58)	116(4)
C(53)-C(54)-C(55)	121(4)	C(54)-C(55)-C(56)	118(4)
C(55)-C(56)-C(57)	131(5)	C(56)-C(57)-C(58)	110(5)
C(53)-C(58)-C(57)	123(4)	P(5)-C(59)-C(60)	125(2)
P(5)-C(59)-C(64)	119(2)	C(60)-C(59)-C(64)	117(3)
C(59)-C(60)-C(61)	121(3)	C(60)-C(61)-C(62)	116(3)
C(61)-C(62)-C(63)	127(4)	C(62)-C(63)-C(64)	121(4)
C(59)-C(64)-C(63)	119(3)	P(5)-C(65)-C(66)	122(2)
P(5)-C(65)-C(70)	118(2)	C(66)-C(65)-C(70)	120(2)
C(65)-C(66)-C(67)	121(2)	C(66)-C(67)-C(68)	117(3)
C(67)-C(68)-C(69)	126(3)	C(68)-C(69)-C(70)	117(3)
C(65)-C(70)-C(69)	119(3)	P(5)-C(71)-N(3)	114(2)
P(5)-C(71)-C(72)	121(2)	N(3)-C(71)-C(72)	125(2)
C(71)-C(72)-C(73)	118(3)	C(72)-C(73)-C(74)	117(3)
C(73)-C(74)-C(75)	120(2)	P(6)-C(75)-N(3)	115(2)
P(6)-C(75)-C(74)	124(2)	N(3)-C(75)-C(74)	122(2)
P(6)-C(76)-C(77)	117(2)	P(6)-C(76)-C(81)	125(2)
C(77)-C(76)-C(81)	118(3)	C(76)-C(77)-C(78)	124(3)
C(77)-C(78)-C(79)	118(4)	C(78)-C(79)-C(80)	120(4)
C(79)-C(80)-C(81)	120(3)	C(76)-C(81)-C(80)	119(3)
P(6)-C(82)-C(83)	116(2)	P(6)-C(82)-C(87)	120(2)
C(83)-C(82)-C(87)	124(3)	C(82)-C(83)-C(84)	124(3)
C(83)-C(84)-C(85)	115(3)	C(84)-C(85)-C(86)	121(3)
C(85)-C(86)-C(87)	118(3)	C(82)-C(87)-C(86)	118(3)
F(5)-B(2)-F(6)	-21.6(0)	F(5)-B(2)-F(7)	-21.6(0)
F(6)-B(2)-F(7)	-21.7(0)	F(5)-B(2)-F(8)	-21.6(0)
F(6)-B(2)-F(8)	-21.6(0)	F(7)-B(2)-F(8)	-21.6(0)

CHAPTER 3

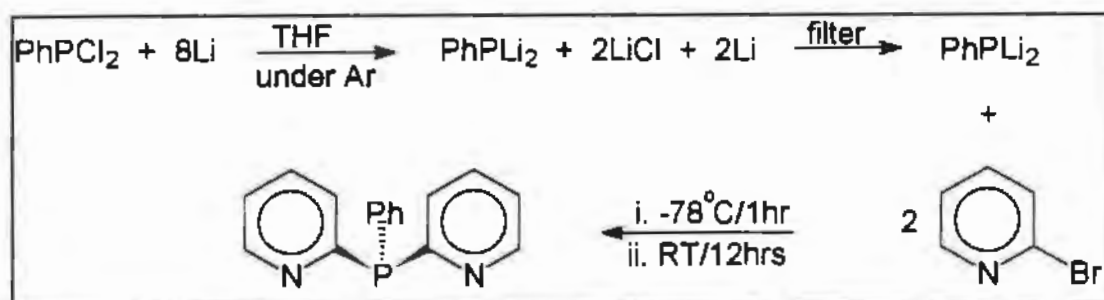
Dinuclear Phenylbis(2-pyridyl)phosphine Ligand-Bridged Complex of Cu(I).

3.1 Aims

The aim of the work described in this chapter was to synthesise dinuclear complexes of copper(I), silver(I) and gold(I) bridged by the ligand $\text{PhP}(\text{py})_2$ and to investigate the type of coordination that the $\text{PhP}(\text{py})_2$ ligand adopts when bonded to these transition metals.

3.2 Synthesis of Phenylbis(2-pyridyl)phosphine

The synthesis of $\text{PhP}(\text{py})_2$ was based on the method used by Newkome¹ *et al.* for the synthesis of the ligand Ph_2Ppy . There are no reports in the literature of the $\text{PhP}(\text{py})_2$ being synthesised in this way and earlier reports have the synthesis of the ligand based on the method used by Schmidbauer² *et al.*. Improved yields were obtained using Newkomes method. The synthesis is outlined in Scheme 7.



Scheme 7. Synthesis of the $\text{PhP}(\text{py})_2$ ligand.

The synthesis of the ligand is performed under an atmosphere of argon, and a white air-sensitive crystalline solid is isolated.

Characterisation data obtained for the ligand were in good agreement with those reported in the literature² (see experimental section). The solid state infrared spectrum was, as expected

dominated by modes resulting from vibrations associated with the phenyl moieties, P-C bond vibrations. The ^1H NMR consisted of a broad series of multiplets ranging from δ 8.8 - 7.0. The $^{31}\text{P}\{^1\text{H}\}$ NMR spectrum of $(\text{Ph}_2\text{P})_2\text{py}$ shows a sharp singlet at δ -3.7, which is characteristic of these types of ligands^{2,3,4}. Elemental analysis is in good agreement with the ligand's formulation.

3.3 Synthesis and Characterisation of $[\text{Cu}_2\{\mu\text{-PhP(py)}_2\}_2(\text{MeCN})_2](\text{PF}_6)_2$ (**5**)

3.3.1 Reaction of $[\text{Cu}(\text{MeCN})_4](\text{PF}_6)$ with PhP(py)_2 : Synthesis $[\text{Cu}_2\{\mu\text{-}(\text{Ph}_2\text{P})_2\text{py}\}_2(\text{MeCN})_2](\text{PF}_6)_2$ (**5**)

Addition of PhP(py)_2 as a suspension to a stirred solution of $[\text{Cu}(\text{MeCN})_4](\text{PF}_6)$ in acetonitrile in a 1:1 molar ratio was found to afford a product characterised as the dinuclear complex $[\text{Cu}_2(\mu\text{-PhP(py)}_2)_2(\text{MeCN})_2](\text{PF}_6)_2$ (**5**). The PhP(py)_2 ligand dissolves as the reaction takes place to give a pale yellow solution. Compound **5** is precipitated by addition of diethyl ether to give a white microcrystalline material which is unstable with respect to air and light and on prolonged exposure to either of the two, decomposes to give a dark brown product.

The solid state infrared spectrum of **5** indicates the presence of PF_6^- (Table 17). The ligand peaks are very weak once the ligand is coordinated and do not seem to show up in the infrared spectrum. The fact that the phosphorus atom of the ligand is coordinated is indicated by a $^{31}\text{P}\{^1\text{H}\}$ NMR spectrum which gives a broad peak centred at δ 20.5, which is shifted downfield from the free ligand which shows a sharp singlet at δ -3.7. The ^1H NMR spectrum of **5** is similar to that of the free ligand with a broad series of multiplets ranging from δ 8.1 to 7.2, the coordinated acetonitrile being indicated by a singlet at δ 2.4. Elemental analysis was not possible to obtain due to the instability of the product.

3.3.2 Crystal Structure of $[\text{Cu}_2\{\mu\text{-PhP(py)}_2\}_2(\text{MeCN})_2](\text{PF}_6)_2 \cdot 2\{(\text{CH}_3)_2\text{CO}\}$

Single crystals of **5** were obtained by cooling a concentrated solution of **5** in a 1:1 acetone:diethyl ether mixture, and an X-ray crystal structure analysis confirmed that the

complex is indeed $[\text{Cu}_2\{\mu\text{-PhP(py)}_2\}_2(\text{MeCN})_2](\text{PF}_6)_2$. The crystal structure consists of well-separated dinuclear $[\text{Cu}_2\{\mu\text{-PhP(py)}_2\}_2(\text{MeCN})_2]^{2+}$ cations, PF_6^- anions and two molecules of acetone. The molecular structure of the cation, showing the atom labelling scheme, is illustrated in Figure 24. The cation possesses a crystallographically imposed centre of symmetry with the two copper atoms in the dinuclear cation bridged by two PhP(py)_2 ligands with the phosphorus atom of the ligand coordinated to the one copper atom and the nitrogen atoms of the pyridine rings coordinated to the other copper atom. The coordination around each copper atom is completed by one acetonitrile group coordinating to each copper atom. The geometry around each copper atom is pseudo-tetrahedral with the smallest angle being the $\text{N}(1)\text{CuN}(2)$ angle of $92.6(4)^\circ$ and the largest angle being the $\text{P}(1)\text{CuN}(2)$ angle of $123.3(3)^\circ$. The $\text{Cu}\cdots\text{Cu}'$ distance is $3.458(2) \text{ \AA}$ which indicates that there is no $\text{Cu}\text{-Cu}$ interaction. The $\text{Cu}\text{-P}$ distance is $2.196(4) \text{ \AA}$ which is in the normal range for $\text{Cu}\text{-P}$ distances in these types of complexes⁴⁴⁻⁴⁷. The $\text{Cu}\text{-N}$ distances range from $2.025(14)$ to $2.090(10) \text{ \AA}$ which are expected distances for $\text{Cu}\text{-N}$ bonds⁴⁸⁻⁵⁰. The angle between the planes defined by the pyridine rings of the ligand is 114° .

3.4 Reaction of PhP(py)_2 with Silver(I) and Gold(I)

Reaction of PhP(py)_2 with $[\text{Ag}(\text{COD})_2](\text{BF}_4)$ or $[\text{Au}(\text{MeCN})_2](\text{SbF}_6)$ affords mixtures of ill-defined products that decompose rapidly upon formation to give dark brown oils. The reactions were repeated in a variety of solvents as well as in the absence of light with the same results. Characterisation data that were obtained on the decomposition products did not shed any light on the possible structures of the complexes formed.

3.5 Conclusion

Complex **5** is the first example of PhP(py)_2 coordinating to a transition metal as a bridging ligand that has been verified x-ray crystallographically and as such extends the type of known modes of coordination that the PhP(py)_2 ligand may adopt when reacted with a transition metal.

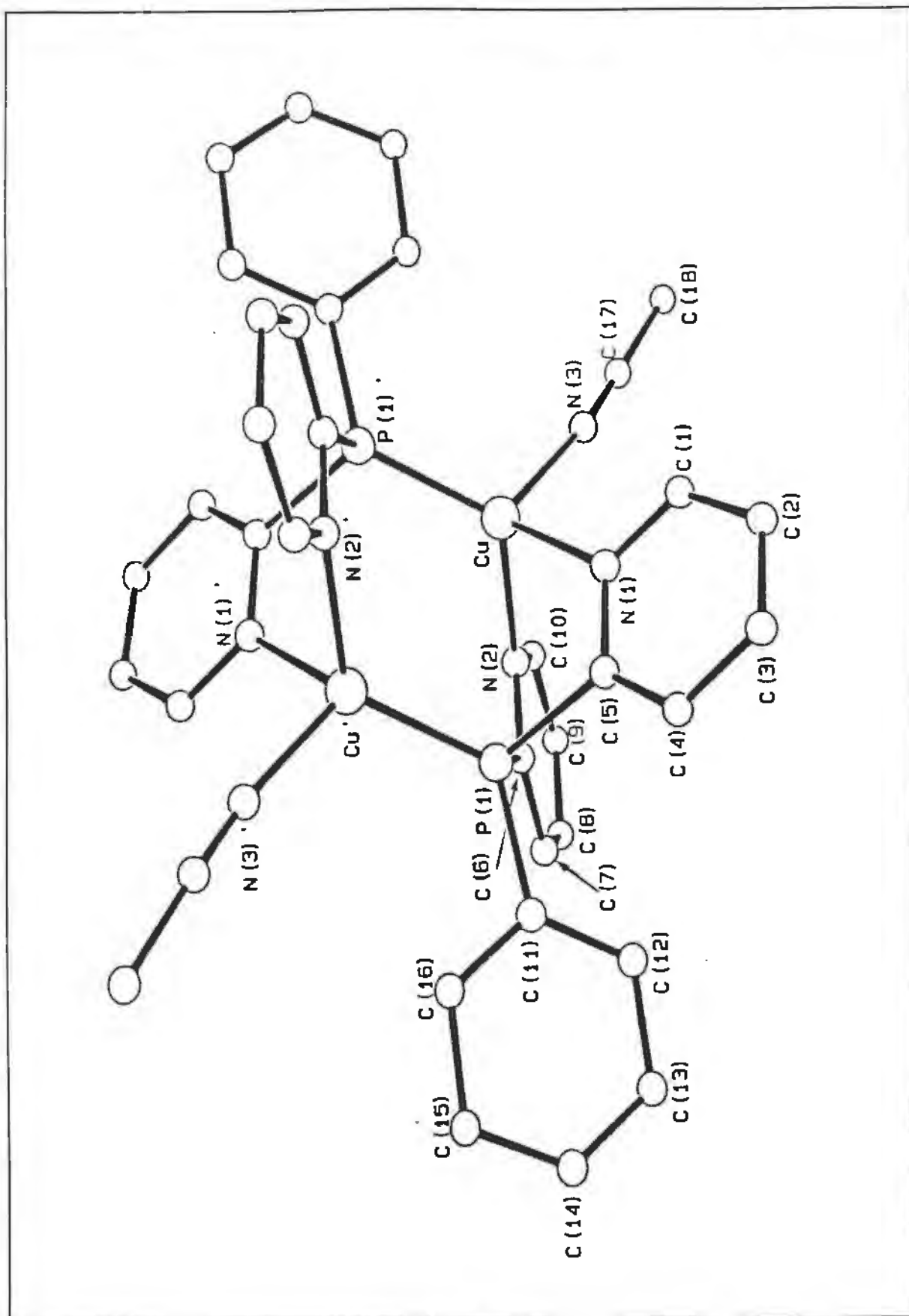


Figure 24. Molecular structure of the $[\text{Cu}_2\{\mu\text{-PhP(py)}_2\}_2(\text{MeCN})_2]^{2+}$ cation.

3.6 Experimental

General experimental details and sources of chemicals are outlined in Appendices A and B respectively.

3.6.1 Synthesis of $[\text{Cu}_2\{\mu\text{-PhP}(\text{py})_2\}_2(\text{MeCN})_2](\text{PF}_6)_2$ (5)

The Phenylbis(2-pyridyl)phosphine ligand (100 mg; 0.378 mmol) was added as a solid to a stirred solution of $[\text{Cu}(\text{MeCN})_4](\text{PF}_6)$ (141 mg; 0.378 mmol) in acetonitrile (10 ml). The mixture was stirred for 12 hours during which time all of the $\text{PhP}(\text{py})_2$ ligand dissolved as the reaction took place. The solution changed colour from colourless to pale yellow. The volume of acetonitrile was then concentrated to *ca.* 1 ml under reduced pressure and the solution filtered through glass microfibre filter paper. A white crystalline precipitate was obtained upon addition of diethyl ether and cooling to -10°C for 12 hours. This precipitate was filtered, washed with diethyl ether and dried *in vacuo*. (yield 50-60%)

3.6.2 Reaction of $\text{PhP}(\text{py})_2$ with $[\text{Ag}(\text{COD})_2](\text{BF}_4)$

The Phenylbis(2-pyridyl)phosphine ligand (100 mg; 0.378 mmol) was added as a solid to a stirred solution of $[\text{Ag}(\text{COD})_2](\text{BF}_4)$ (155 mg; 0.378 mmol) in acetonitrile (10 ml). The reaction was kept in the dark at all times. The mixture was stirred for 12 hours during which time all of the $\text{PhP}(\text{py})_2$ ligand dissolved. The solution changed colour from colourless to yellow. The volume of acetonitrile was then concentrated to *ca.* 1 ml under reduced pressure during which time the solution becomes a dark orange colour. Diethyl ether was added and the mixture cooled to -10°C for 1 hour. The solution became very dark and a dark brown oil formed that consisted of a number of ill-defined products.

3.6.3 Reaction of $\text{PhP}(\text{py})_2$ with $[\text{Au}(\text{MeCN})_2](\text{SbF}_6)$

An excess of gold metal (149 mg; 0.756 mmol) was added as a solid to a stirred solution of NOSbF_6 (100 mg; 0.378 mmol) in acetonitrile (10 ml). This was left to stir for 12 hours which

resulted in the formation of $[\text{Au}(\text{MeCN})_2](\text{SbF}_6)$ which could not be isolated as a solid. The solution containing the $[\text{Au}(\text{MeCN})_2](\text{SbF}_6)$ complex was filtered through glass microfibre filter paper to remove unreacted gold metal and added dropwise to a stirred suspension of $\text{PhP}(\text{py})_2$ (100 mg; 0.378 mmol) in acetonitrile (5 ml). The solution turned yellow as the $[\text{Au}(\text{MeCN})_2](\text{SbF}_6)$ complex was added. This was left to stir for 6 hours during which time all of the $\text{PhP}(\text{py})_2$ ligand dissolved. The volume of acetonitrile was concentrated to *ca.* 1 ml under reduced pressure during which time the solution becomes a dark orange colour. Diethyl ether was added and the mixture cooled to -10°C for 1 hour. The solution became very dark and a dark brown oil formed that consisted of a number of ill-defined products.

TABLE 17: Spectroscopic Data for PhP(py)₂ and Its Complexes

Complex	Infrared Spectroscopic Data ^a cm ⁻¹	¹ H NMR ^b δ	³¹ P{ ¹ H} NMR ^c δ
PhP(py) ₂	[1580(m), 1570(w)] ν(C-Npy) [1477(s), 1431(s)] ν(P-Cpy,Ph)	8.8-7.0 (m,13H)	-3.7 (s)
[Cu ₂ {μ-PhP(py) ₂ }(MeCN) ₂](PF ₆) ₂ (5)	[833(vs)] ν(P-F)	8.1-7.2 (m,32H)	20.5 (b)

a. All infrared spectra run as KBr discs. w = weak, m = medium, s = strong, vs = very strong

b. PhP(py)₂ run in CD₃OD and **5** in CD₃CN, m = multiplet

c. PhP(py)₂ run in CHCl₃ and **5** run in MeCN on external lock. All values relative to H₃PO₄. b = broad, s = singlet

3.6.4 Single crystal X-ray diffraction study of $[\text{Cu}_2\{\mu\text{-PhP}(\text{py})_2\}_2(\text{MeCN})_2](\text{PF}_6)_2 \cdot 2\{(\text{CH}_3)_2\text{CO}\}$

Colourless rectangular shaped crystals (**5**) were grown by cooling a saturated acetone-diethyl ether (1:1, vol:vol) solution of the compound. The general approach used for the intensity data collection and structure solution is described in Appendix A. The crystallographic data is given in Table 18, the fractional coordinates are given in Table 19, the anisotropic thermal parameters in Table 20, the interatomic distances in Table 21 and the interatomic angles in Table 22. The observed and calculated structure factors may be found on microfiche in an envelope fixed to the inside back cover.

Table 18.
Crystal Data and Details of the Crystallographic Analysis for
[Cu₂{μ-PhP(py)₂}₂(MeCN)₂](PF₆)₂·2{(CH₃)₂CO} (5)

Formula	Cu ₂ C ₃₆ H ₃₂ F ₁₂ N ₆ P ₄
Molecular Mass	1027.66
Crystal System	Triclinic
Space Group	P $\bar{1}$
a (Å)	9.077 (2)
b (Å)	9.354 (2)
c (Å)	14.878 (2)
α (°)	80.89 (1)
β (°)	81.42 (2)
γ (°)	86.11 (2)
V (Å ³)	1231.99
Z	1
D _c (g.cm ⁻³)	1.38
F(000)	516
λ(Mo - Kα) (Å)	0.71069
Scan Mode	ω - 2θ
ω scan angle	0.40 + 0.35 tanθ
Horizontal Aperture width (mm)	2.7 + 0.1 tanθ
Scattering range (°)	2 ≤ θ ≤ 23
μ (cm ⁻¹)	11.03
Absorption corrections	Semi empirical ⁶⁸
Measured intensities	3574
Unique intensities	2785
Unique intensities with [I > 3σ(I)]	1944
Structure solution	Direct & Fourier methods
Weighting scheme	1/(σ ² F + F ²)
R = Σ(F _o - F _c)/ΣF _o	0.090
R _w = Σ _w ^{1/2} (F _o - F _c)/Σ _w ^{1/2} F _o	0.090
(Δ/σ) _{max}	0.520
Δρ _{max} (eÅ ⁻³)	1.376
Number of parameters	195

Table 19. Fractional Coordinates ($\times 10^4$) and Isotropic Thermal Factors ($\text{\AA}^2, \times 10^3$) for $[\text{Cu}_2\{\mu\text{-PhP(py)}_2\}_2(\text{MeCN})_2](\text{PF}_6)_2 \cdot 2\{(\text{CH}_3)_2\text{CO}\}$

	x/a	y/b	z/c	U_{eq}
Cu	5136(2)	846(2)	5935(1)	54(1)
P(1)	5844(4)	1290(4)	3744(3)	56(1)
N(1)	4220(11)	2543(10)	5099(7)	46(3)
N(2)	7288(13)	1185(11)	5239(8)	56(3)
N(3)	5296(13)	1836(13)	7031(9)	63(3)
C(1)	3269(15)	3513(14)	5478(10)	51(4)*
H(1)	3002(15)	3368(14)	6218(10)	134(17)*
C(2)	2590(16)	4656(16)	4949(10)	64(4)*
H(2)	1873(16)	5405(16)	5316(10)	134(17)*
C(3)	2856(16)	4784(16)	4023(10)	61(4)*
H(3)	2210(16)	5593(16)	3626(10)	134(17)*
C(4)	3869(15)	3805(15)	3623(10)	56(4)*
H(4)	4074(15)	3909(15)	2883(10)	134(17)*
C(5)	4537(14)	2712(14)	4177(9)	48(3)*
C(6)	7463(15)	1475(14)	4318(10)	51(4)*
C(7)	8843(17)	1894(16)	3834(11)	65(4)*
H(5)	9090(17)	2045(16)	3093(11)	134(17)*
C(8)	9972(18)	2016(16)	4324(11)	70(4)*
H(6)	11076(18)	2250(16)	3968(11)	134(17)*
C(9)	9788(17)	1743(16)	5256(11)	66(4)*
H(7)	10678(17)	1849(16)	5646(11)	134(17)*
C(10)	8402(17)	1316(15)	5692(11)	60(4)*
H(8)	8166(17)	1118(15)	6434(11)	134(17)*
C(11)	6465(17)	2025(16)	2545(10)	64(4)*
C(12)	6919(19)	3451(19)	2282(12)	83(5)*
H(9)	6580(19)	4296(19)	2698(12)	134(17)*
C(13)	7474(22)	3884(23)	1348(14)	104(6)*
H(10)	7854(22)	4974(23)	1155(14)	134(17)*
C(14)	7494(24)	2940(25)	728(16)	118(7)*
H(11)	8031(24)	3327(25)	43(16)	134(17)*
C(15)	7167(24)	1510(26)	971(16)	124(8)*
H(12)	7202(24)	792(26)	467(16)	134(17)*

Table 19. / Cont.

C(16)	6620(20)	1064(21)	1922(13)	93(6)*
H(13)	6465(20)	-70(21)	2181(13)	134(17)*
C(17)	5339(19)	2237(19)	7675(13)	73(5)*
C(18)	5351(24)	2800(23)	8542(14)	111(7)*
H(14)	5012(24)	1771(23)	8930(14)	134(17)*
H(15)	4540(24)	3642(23)	8724(14)	134(17)*
H(16)	6426(24)	3035(23)	8697(14)	134(17)*
P(2)	10240(7)	2808(13)	7903(5)	153(3)
F(1)	-357(21)	3861(27)	8531(13)	245(9)
F(2)	10890(20)	1616(20)	7274(13)	197(7)
F(3)	8192(16)	-2936(23)	1974(14)	221(8)
F(4)	1319(19)	-2659(31)	2362(14)	279(11)
F(5)	10417(21)	3910(20)	7030(11)	227(7)
F(6)	9905(29)	1593(29)	8710(12)	288(11)
O(1)	2255(26)	1772(25)	2232(15)	230(10)*
C(19)	2652(26)	1449(25)	960(15)	366(32)*
C(20)	3302(26)	1023(25)	686(15)	289(26)*
C(21)	1451(26)	2364(25)	497(15)	517(45)*

* isotropic temperature factor.

$$U_{eq} = \frac{1}{3} \sum_i \sum_j U_{ij} a_i^* a_j^* (a_i \cdot a_j)$$

**Table 20. Anisotropic Temperature Factors ($\text{\AA}^2, \times 10^3$) for
 $[\text{Cu}_2\{\mu\text{-PhP(py)}_2\}_2(\text{MeCN})_2](\text{PF}_6)_2 \cdot 2\{(\text{CH}_3)_2\text{CO}\}$**

	U(11)	U(22)	U(33)	U(23)	U(13)	U(12)
Cu	57(1)	40(1)	56(1)	4(1)	14(1)	-2(1)
P(1)	65(3)	38(2)	56(3)	1(2)	20(2)	-2(2)
N(1)	49(7)	36(6)	51(7)	-4(5)	1(5)	-2(5)
N(2)	56(8)	43(7)	60(8)	0(6)	12(6)	5(6)
N(3)	58(8)	65(8)	60(9)	5(7)	2(7)	-7(6)
P(2)	71(5)	282(11)	80(5)	31(6)	6(4)	8(6)
F(1)	181(17)	368(30)	147(14)	-46(17)	71(13)	76(18)
F(2)	185(17)	207(18)	183(17)	21(14)	-23(14)	-21(14)
F(3)	92(11)	308(24)	301(23)	-158(20)	-45(13)	26(13)
F(4)	126(15)	503(39)	198(19)	16(22)	-68(14)	-12(19)
F(5)	232(19)	220(18)	160(15)	60(13)	65(13)	78(15)
F(6)	357(32)	342(31)	124(15)	79(17)	0(16)	-51(25)

Table 21. Interatomic Distances (Å) for [Cu₂{μ-PhP(py)₂}₂(MeCN)₂](PF₆)₂·2{(CH₃)₂CO}

Cu-Cu'	3.458(2)	Cu-P(1')	2.196(4)
Cu-N(1)	2.064(10)	Cu-N(2)	2.090(10)
Cu-N(3)	2.025(14)	P(1)-C(5)	1.850(13)
P(1)-C(6)	1.837(14)	P(1)-C(11)	1.83(2)
N(1)-C(1)	1.34(2)	N(1)-C(5)	1.34(2)
N(2)-C(6)	1.34(2)	N(2)-C(10)	1.32(2)
N(3)-C(17)	1.09(2)	C(1)-C(2)	1.39(2)
C(2)-C(3)	1.35(2)	C(3)-C(4)	1.39(2)
C(4)-C(5)	1.38(2)	C(6)-C(7)	1.40(2)
C(7)-C(8)	1.36(2)	C(8)-C(9)	1.36(2)
C(9)-C(10)	1.38(2)	C(11)-C(12)	1.40(2)
C(11)-C(16)	1.38(2)	C(12)-C(13)	1.41(2)
C(13)-C(14)	1.37(3)	C(14)-C(15)	1.37(3)
C(15)-C(16)	1.43(3)	C(17)-C(18)	1.47(2)
P(2)-F(1)	1.49(2)	P(2)-F(2)	1.59(2)
P(2)-F(5)	1.52(2)	P(2)-F(6)	1.53(2)
O(1)-C(19)	1.940(0)	C(19)-C(20)	.789(0)
C(19)-C(21)	1.519(0)	C(20)-C(21)	2.055(0)

Table 22. Interatomic Angles (°) for [Cu₂{μ-PhP(py)₂}]₂(MeCN)₂(PF₆)₂·2{(CH₃)₂CO}

P(1')-Cu-N(1)	104.5(6)	P(1')-Cu-N(2)	123.3 (3)
P(1')-Cu-N(3)	115.7 (4)	Cu-P(1')-C(5')	111.5(2)
Cu-P(1')-C(6')	115.2(2)	Cu-P(1')-C(11')	119.1(2)
N(1)-Cu-N(2)	92.6(4)	N(1)-Cu-N(3)	99.9(4)
N(2)-Cu-N(3)	98.2(5)	C(5)-P(1)-C(6)	101.1(6)
C(5)-P(1)-C(11)	104.5(6)	C(6)-P(1)-C(11)	103.4(7)
Cu-N(1)-C(1)	119.6(9)	Cu-N(1)-C(5)	122.3(8)
C(1)-N(1)-C(5)	118.2(11)	Cu-N(2)-C(6)	118.0(10)
Cu-N(2)-C(10)	120.7(10)	C(6)-N(2)-C(10)	120.5(12)
Cu-N(3)-C(17)	172.6(13)	N(1)-C(1)-C(2)	122.1(13)
C(1)-C(2)-C(3)	119.6(14)	C(2)-C(3)-C(4)	118.7(14)
C(3)-C(4)-C(5)	119.4(13)	P(1)-C(5)-N(1)	113.8(9)
P(1)-C(5)-C(4)	124.2(10)	N(1)-C(5)-C(4)	121.9(12)
P(1)-C(6)-N(2)	117.6(10)	P(1)-C(6)-C(7)	122.6(11)
N(2)-C(6)-C(7)	119.8(13)	C(6)-C(7)-C(8)	118(2)
C(7)-C(8)-C(9)	122(2)	C(8)-C(9)-C(10)	117(2)
N(2)-C(10)-C(9)	122.6(14)	P(1)-C(11)-C(12)	122.0(13)
P(1)-C(11)-C(16)	116.6(13)	C(12)-C(11)-C(16)	121(2)
C(11)-C(12)-C(13)	118(2)	C(12)-C(13)-C(14)	120(2)
C(13)-C(14)-C(15)	124(2)	C(14)-C(15)-C(16)	116(2)
C(11)-C(16)-C(15)	121(2)	N(3)-C(17)-C(18)	178(2)
F(1)-P(2)-F(2)	177.1(12)	F(1)-P(2)-F(5)	96.0(13)
F(2)-P(2)-F(5)	86.9(9)	F(1)-P(2)-F(6)	88.3(12)
F(2)-P(2)-F(6)	88.9(14)	F(5)-P(2)-F(6)	172(2)
O(1)-C(19)-C(20)	1.4(0)	O(1)-C(19)-C(21)	-26.5(0)
C(20)-C(19)-C(21)	-8.5(0)	C(19)-C(20)-C(21)	-27.0(0)
C(19)-C(21)-C(20)	18.9(0)		

CHAPTER 4

Dinuclear 2,7-Bis(diphenylphosphino)-4-methylnaphthyridine Ligand-Bridged Complexes of Cu(I), Ag(I) and Au(I).

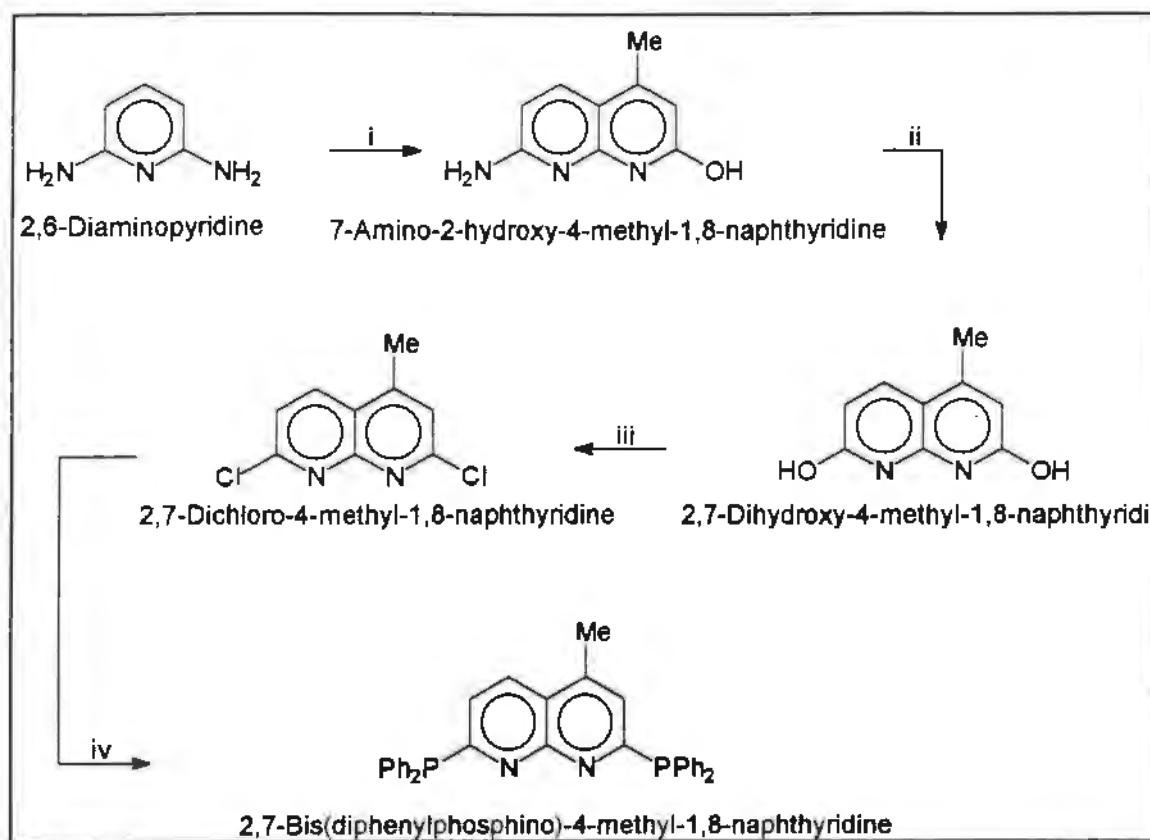
4.1 Aims

The aims of the work described in this chapter were to synthesise the novel ligand $(\text{Ph}_2\text{P})_2\text{menapy}$, to synthesise dinuclear complexes of copper(I), silver(I) and gold(I) bridged by the $(\text{Ph}_2\text{P})_2\text{menapy}$ ligand and to investigate the type of coordination that the $(\text{Ph}_2\text{P})_2\text{menapy}$ ligand adopts when bonded to these transition metals.

4.2 Synthesis of 2,7-Bis(diphenylphosphino)-4-methylnaphthyridine

The synthesis of $(\text{Ph}_2\text{P})_2\text{menapy}$ was based on the method used by Newkome ¹ *et al.* for the synthesis of the ligand Ph_2Ppy and is similar to the method used by Ziesel ³ for the synthesis of $(\text{Ph}_2\text{P})_2\text{napy}$. The synthesis requires 2,7-dichloro-4-methyl-1,8-naphthyridine as a starting material which is synthesised via a three step process in an adaption of the method used by Newkome ⁶⁰ *et al.* for the synthesis of 2,7-dichloro-1,8-naphthyridine. The synthesis of both 2,7-dichloro-4-methyl-1,8-naphthyridine and $(\text{Ph}_2\text{P})_2\text{menapy}$ is outlined in Scheme 8.

The first step involves heating 2,6-diaminopyridine with ethylacetoacetate at 90°C which leads to the formation of 2-amino-7-hydroxy-4-methyl-1,8-naphthyridine which is isolated as a pale yellow precipitate ²⁴. The second step is a diazotization in which the amino group of 2-amino-7-hydroxy-4-methyl-1,8-naphthyridine is converted to a hydroxy group affording 2,7-dihydroxy-4-methyl-1,8-naphthyridine as a pale yellow precipitate. The third step involves the chlorination of the hydroxy groups by PCl_5 and POCl_3 to afford 2,7-dichloro-4-methyl-1,8-naphthyridine as a pale yellow precipitate which can be purified further by sublimation under reduced pressure at 150°C to give a white solid. Finally 2,7-dichloro-4-methyl-1,8-



Scheme 8. i = ethylacetoacetate; ii = H_2SO_4 , NaNO_2 ; iii = PCl_5 , POCl_3 ; iv = $2 \times \text{Ph}_2\text{PLi}$.

naphthyridine is reacted with lithium diphenylphosphide to afford $(\text{Ph}_2\text{P})_2\text{menapy}$. Considerable difficulty was experienced in the purification of the product. When pure, $(\text{Ph}_2\text{P})_2\text{menapy}$ is a microcrystalline solid, which is expected to be essentially colourless, by comparison with the colourless $(\text{Ph}_2\text{P})_2\text{napy}$ ligand reported by Ziessel. Attempts at purification using procedures such as recrystallisation of the crude ligand from methanol-chloroform or purification by chromatography (alumina, dichloroethane/hexane), lead to the formation of red oils. Eventually a pale red solid was obtained by simply reducing an ether extract of the compound to dryness. Because of the reddish colour this material is probably not 100% pure but there was no evidence in the ^{31}P $\{^1\text{H}\}$ NMR spectrum for impurities, only two peaks appearing at δ 0.2 and -1.4 corresponding to the pure ligand (discussed below). Handling of the ligand is complicated by its extreme sensitivity to oxygen; even when kept in an inert atmosphere glove box it was found to oxidise over a period of days to $\text{Ph}_2\text{POmenapyPPh}_2$ and $(\text{Ph}_2\text{PO})_2\text{menapy}$. As a result satisfactory microanalytical results for %C, %H and %N could

not be obtained.

Characterisation data obtained for the ligand $(\text{Ph}_2\text{P})_2\text{menapy}$ are similar to those obtained for the ligand $(\text{Ph}_2\text{P})_2\text{napy}$ ³. The solid state infrared spectrum is, as expected, dominated by peaks resulting from vibrations associated with the phenyl moieties as well as peaks assigned to P-C bond vibrations (Table 23). The ¹H NMR spectrum consists of a broad multiplet ranging from δ 8.6 to 7.2 and a singlet at δ 2.55 corresponding to the methyl protons. The ³¹P{¹H} NMR spectrum exhibits two sharp singlets at δ 0.2 and -1.4. The two singlets arise because the two phosphorus atoms of the $(\text{Ph}_2\text{P})_2\text{menapy}$ ligand are chemically inequivalent due to the location of the methyl group. The chemical shifts obtained are characteristic of these types of ligands^{2,4}. Mass spectrophotometry showed a molecular ion peak of 512 mass units which is expected for this ligand.

4.3 Reactions Involving $[\text{Cu}(\text{MeCN})_4](\text{PF}_6)$ as Precursor

4.3.1 Reaction of $[\text{Cu}(\text{MeCN})_4](\text{PF}_6)$ with $(\text{Ph}_2\text{P})_2\text{menapy}$: Synthesis and Characterisation of $[\text{Cu}_2\{\mu-(\text{Ph}_2\text{P})_2\text{menapy}\}_2(\text{H}_2\text{O})_4](\text{PF}_6)_2$ (**6**)

Dropwise addition of a solution of $(\text{Ph}_2\text{P})_2\text{menapy}$ in acetonitrile to a stirred solution of an equimolar amount of $[\text{Cu}(\text{MeCN})_4](\text{PF}_6)$ in acetonitrile was found to lead to the immediate formation of a dark red solution from which a red crystalline solid could be isolated by the addition of diethyl ether. As described below this product was characterised as $[\text{Cu}_2\{\mu-(\text{Ph}_2\text{P})_2\text{menapy}\}_2(\text{H}_2\text{O})_4](\text{PF}_6)_2$ (**6**).

The solid state infrared spectrum of **6** indicates the presence of both the ligand $(\text{Ph}_2\text{P})_2\text{menapy}$ and the counterion PF_6^- (Table 23). Both phosphorus atoms of the ligand are considered to be coordinated on the basis that the ³¹P{¹H} NMR spectrum affords a single broad peak centred at δ 2.4, which is downfield of the two sharp singlets at δ 0.2 and -1.4 exhibited by the free ligand. The ¹H NMR spectrum of **6** shows a broad series of multiplets ranging from δ 7.9 to 6.5 corresponding to the phenyl and naphthyridine protons and a broad peak centred at δ 2.2 arising from the overlapping of the peak corresponding to the methyl protons of the

naphthyridine and the peak corresponding to the protons of the coordinated H_2O groups. Elemental analysis for %C, %H and %N is consistent with the proposed formula for **6**. It is proposed that the source of water is from the solvents used. The proposed structure of **6** is shown in figure 24.

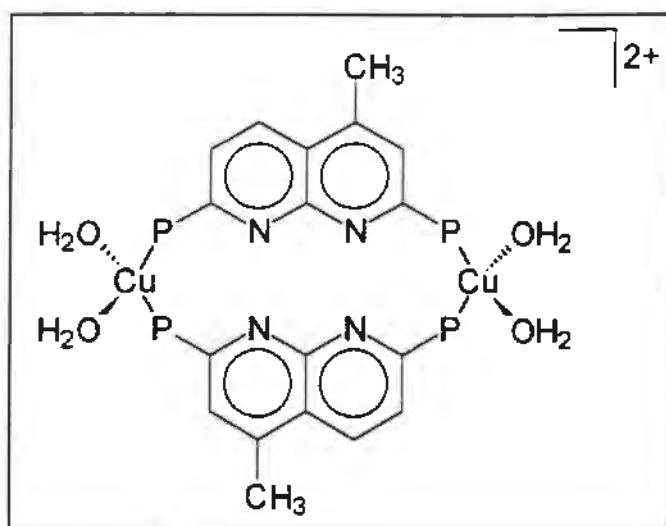


Figure 24. Proposed structure of $[\text{Cu}_2\{\mu\text{-(Ph}_2\text{P)}_2\text{menapy}\}_2(\text{H}_2\text{O})_4]^{2+}$.

4.3.2 Reaction of $[\text{Cu}(\text{MeCN})_4](\text{PF}_6)$ with a mixture of $(\text{Ph}_2\text{P})_2\text{menapy}$ and $\text{Ph}_2\text{POmenapyPPh}_2$: Synthesis and Crystal Structure of $[\text{Cu}_2(\mu\text{-Ph}_2\text{POmenapyPPh}_2)_2(\text{MeCN})_2](\text{PF}_6)_2$ (**7**)

Dropwise addition of a solution of a mixture of $(\text{Ph}_2\text{P})_2\text{menapy}$ and the oxidised ligand $\text{Ph}_2\text{POmenapyPPh}_2$ in acetonitrile to a stirred solution of $[\text{Cu}(\text{MeCN})_4](\text{PF}_6)$ in acetonitrile led to the formation of mixture of products from which a red as well as a yellow crystalline solid could be isolated by the addition of diethyl ether. As described below these products were characterised as **6** and $[\text{Cu}_2(\mu\text{-Ph}_2\text{POmenapyPPh}_2)_2(\text{MeCN})_2](\text{PF}_6)_2$ (**7**).

The two compounds could not be separated from each other and characterisation data were obtained on a mixture of the two (Table 23). The only data that showed any significant difference from that of a sample of **6** was the $^{31}\text{P}\{^1\text{H}\}$ NMR spectrum which showed in addition to the broad peak centred at δ 2.4 a sharp singlet at δ 17.0. The peak at δ 17.0 is

thought to correspond to the phosphorus bonded to the oxygen atom, as a downfield shift is expected when phosphorus is bonded to oxygen¹. Elemental analysis was not possible because the two products could not be separated from each other, at least not beyond the separation of a few single crystals by hand (*vide infra*).

A single crystal of **7** was obtained by hand selection from a crop of crystals containing both **6** and **7**, and an X-ray crystal structure analysis (by P. Fanwick)⁶³ established that the complex is indeed $[\text{Cu}_2(\mu\text{-Ph}_2\text{POMenapyPPh}_2)_2(\text{MeCN})_2](\text{PF}_6)_2$. The crystal structure consists of well-separated dinuclear $[\text{Cu}_2(\mu\text{-Ph}_2\text{POMenapyPPh}_2)_2(\text{MeCN})_2]^{2+}$ cations and PF_6^- anions. The structure of the cation, showing the atom labelling scheme, is illustrated in Figure 25. The cation possesses a crystallographically imposed centre of symmetry with the two copper atoms in the dinuclear cation being bridged by two $\text{Ph}_2\text{POMenapyPPh}_2$ ligands in a head-to-tail fashion. Each ligand coordinates to one copper atom through the unoxidised phosphorus atom and to the other copper atom through the oxygen atom and the nitrogen atom of the naphthyridine ring. The coordination around each copper atom is completed by an acetonitrile group. The geometry around each copper atom is pseudo tetrahedral with the smallest angle being the O-Cu-N(1) angle of $80.7(2)^\circ$ and the largest angle being the P(1)-Cu-N(1) angle of $122.4(2)^\circ$. The Cu...Cu separation is $5.405(1) \text{ \AA}$ which obviously indicates the absence of any Cu...Cu interaction. The Cu-P(1) distance is $2.178(3) \text{ \AA}$ which is in the expected range for Cu-P distances⁴⁴⁻⁴⁷. The Cu-N(1) distance is $2.072(7) \text{ \AA}$ and the Cu-N(3) distance is $1.964(9) \text{ \AA}$ again distances that are close to literature values⁴⁸⁻⁵⁰. The Cu-O distance is $2.312(6) \text{ \AA}$ also a value within the range of Cu-O distances found in the literature⁶¹⁻⁶².

4.4 Reaction of $[\text{Ag}(\text{COD})_2](\text{BF}_4)$ with $(\text{Ph}_2\text{P})_2\text{menapy}$: Synthesis and Characterisation of $[\text{Ag}_2\{\mu\text{-}(\text{Ph}_2\text{P})_2\text{menapy}\}_2(\text{H}_2\text{O})_4](\text{BF}_4)_2$ (**8**)

Dropwise addition of a solution of $(\text{Ph}_2\text{P})_2\text{menapy}$ in acetonitrile to a stirred solution of an equimolar amount of $[\text{Ag}(\text{COD})_2](\text{BF}_4)$ in acetonitrile resulted in the formation of a yellow solution from which a pale yellow crystalline solid could be isolated by addition of diethyl ether. As described below this compound was characterised as $[\text{Ag}_2\{\mu\text{-}(\text{Ph}_2\text{P})_2\text{menapy}\}_2(\text{H}_2\text{O})_4](\text{BF}_4)_2$ (**8**).

The solid state infrared spectrum of **8** indicates the presence of both the ligand $(\text{Ph}_2\text{P})_2\text{menapy}$ and the cation BF_4^- (Table 23). The fact that both phosphorus atoms of the ligand are coordinated is indicated by a ^{31}P $\{^1\text{H}\}$ NMR spectrum which shows two multiplets centered at δ 18.0 and 7.9, which is downfield from the free ligand which shows two sharp singlets at δ 0.2 and -1.4. This complex spectrum arises due to spin-spin coupling of the phosphorus atoms to $^{107,109}\text{Ag}$: naturally abundant silver consists in fact of two isotopes having spin $1/2$, ^{107}Ag (51% abundance) and ^{109}Ag (49% abundance). The spectrum is further complicated by the fact that the phosphorus atoms are not equivalent due to the location of a methyl group on the naphthyridyl ligand. The ^1H NMR spectrum of **8** is similar to that of the free ligand with a broad series of multiplets ranging from δ 6.6 to 8.3, a broad peak at δ 2.6 corresponding to the methyl group of the ligand and a broad peak at δ 1.25 with an intensity equivalent to eight protons which corresponds to the protons of the coordinated H_2O groups. Elemental analysis is consistent with the proposed formula for **8**. It is proposed that the source of water is as for complex **6** discussed above where it must have entered the reaction through the solvent. The proposed structure of **8** is shown in Figure 26.

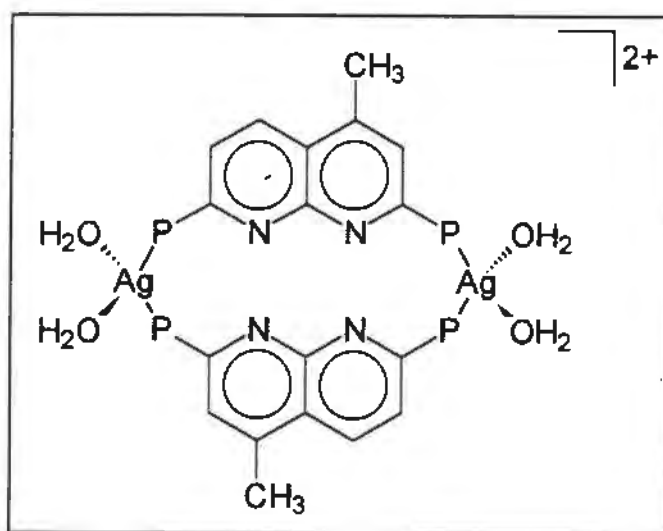


Figure 26. Proposed structure of $[\text{Ag}_2\{\mu\text{-(Ph}_2\text{P)}_2\text{menapy}\}_2(\text{H}_2\text{O})_4]^{2+}$.

4.5 Reaction of $(\text{Ph}_2\text{P})_2\text{menapy}$ with Gold(I)

Reaction of $(\text{Ph}_2\text{P})_2\text{menapy}$ with $[\text{Au}(\text{MeCN})_2](\text{SbF}_6)$ afforded an ill-defined yellow product

that decomposed after a few days to give a black oil. Due to the problems associated with the synthesis of the ligand (discussed above) this reaction could not be studied fully owing to the unavailability of ligand. It is considered that further study of this reaction is appropriate as initial studies showed promise.

4.6 Conclusion

The products isolated for the reactions of $(\text{Ph}_2\text{P})_2\text{menapy}$ with copper and silver precursors (complexes **6** and **8**) are the first examples of compounds containing coordinated $(\text{Ph}_2\text{P})_2\text{menapy}$. As is the case for the $[\text{Rh}_2\{\mu\text{-(Ph}_2\text{P)}_2\text{napy}\}_2(\text{COD})_2](\text{BF}_4)_2$ complex ³, which contains the related $(\text{Ph}_2\text{P})_2\text{napy}$ ligand, the $(\text{Ph}_2\text{P})_2\text{menapy}$ ligand in these complexes adopts a bridging mode of coordination with coordination to the transition metal taking place solely through the phosphorus atoms of the ligand. As for $[\text{Rh}_2\{\mu\text{-(Ph}_2\text{P)}_2\text{napy}\}_2(\text{COD})_2](\text{BF}_4)_2$ there is a degree of uncertainty about the structures of **6** and **8** as one can only be certain about the structures of the complexes once a single crystal X-ray structure determination has been done. Single crystals of both **6** and **8** were grown but they were too small to be useful for X-ray structure analysis.

In the case of complex **7** the oxidised ligand behaves as both a chelating as well as a bridging ligand. This is due to the phosphorus-oxygen bond relieving the steric strain through the formation of a five membered ring upon chelation, instead of a strained four membered ring that would result if the phosphorus rather than the oxygen atom was bonded to the metal.

4.7 Experimental

General experimental details and sources of chemicals are outlined in Appendices A and B respectively.

4.7.1 Synthesis of 2-Amino-7-hydroxy-4-methyl-1,8-naphthyridine ²⁴

A solution of 2,6-Diaminopyridine (50 g), ethylacetoacetate (56 g) and concentrated HCl (10 ml) was heated to 85°C with stirring for six hours. A light yellow precipitate formed which was separated by filtration. This was washed thoroughly with water and diethyl ether, and dried under reduced pressure. (Yield 50%); ¹H NMR (Me₂SO-d₆) δ 2.30 (s, 3H, Me), 3.30 (m, 1H, OH), 6.00 (s, 1H, 3-napy), 6.30 (d, 1H, 5-napy), 6.60 (s, 2H, NH₂), 7.70 (d, 1H, 6-napy).

4.7.2 Synthesis of 2,7-Dihydroxy-4-methyl-1,8-naphthyridine ⁶⁰

2-Amino-7-hydroxy-4-methyl-1,8-naphthyridine (10 g; 571 mmol) was ground to a fine powder and then dissolved in H₂SO₄ (50 ml; 50%). The mixture was cooled to 5°C and an aqueous solution of NaNO₂ (6 g; 870 mmol) was added dropwise. A small amount of diethyl ether (20 ml) was added to the solution to prevent foaming. The mixture was stirred for twenty minutes and then poured over crushed ice to afford a pale yellow precipitate. This was filtered off, washed with water, methanol and diethyl ether, and dried under reduced pressure. (Yield 90%) ¹H NMR (Me₂SO-d₆) δ 2.35 (s, 3H, Me), 3.45 (m, 2H, OH), 6.20 (s, 1H, 3-napy), 6.35 (d, 1H, 5-napy), 7.90 (d, 1H, 6-napy).

4.7.3 Synthesis of 2,7-Dichloro-4-methyl-1,8-naphthyridine ⁶⁰

2,7-Dihydroxy-4-methyl-1,8-naphthyridine (5 g; 284 mmol) and PCl₅ (14 g; 672 mmol) were added together and the mixture ground to a fine powder and added to POCl₃ (20 ml). The mixture was heated to 65°C whereupon the solid dissolved. Once all the solid had dissolved the solution was left to cool to room temperature, and crushed ice was added to decompose the

excess POCl_3 . At this point a pale yellow precipitate separated which was filtered off and washed with water. The product was crystallised from acetone to give 2,7-dichloro-4-methyl-1,8-naphthyridine as a white microcrystalline solid. (Yield 90%) $^1\text{H NMR}$ ($\text{Me}_2\text{SO}-d_6$) δ 2.60 (s, 3H, Me), 7.35 (s, 1H, 3-napy), 7.50 (d, 1H, 5-napy), 8.30 (d, 1H, 6-napy).

4.7.4 Synthesis of 2,7-Bis(diphenylphosphino)-4-methyl-1,8-naphthyridine $\{(\text{Ph}_2\text{P})_2\text{menapy}\}$

A solution of chlorodiphenylphosphine (1.9 ml; 10.33 mmol) in tetrahydrofuran (20 ml) was added dropwise over 1 hour to a stirred suspension of lithium metal (0.5 g) in tetrahydrofuran. The solution turned red after about twenty minutes. It was refluxed for a further 1 hour after the addition of all of the chlorodiphenylphosphine. The mixture was allowed to cool after which the solution was filtered through a frit and added dropwise over 30 minutes to a stirred suspension of 2,7-dichloro-4-methyl-1,8-naphthyridine (1 g, 4.69 mmol) in tetrahydrofuran (20 ml) at 0°C . The solution turned dark green once all the lithiumdiphenylphosphine was added. The mixture was allowed to heat to room temperature and stirred for a further 12 hours. The green solution was then acidified with conc. HCl (10 ml) and 3N HCl (10 ml) and washed with diethyl ether (3×25 ml). It was then basified with conc. NH_3 to a $\text{pH} > 9$ and then extracted with diethyl ether (3×40 ml). The diethyl ether was dried over MgSO_4 , filtered and evaporated to dryness under reduced pressure, affording $(\text{Ph}_2\text{P})_2\text{menapy}$ as a pale red solid. The solid was not analytically pure and rapidly oxidised when not kept under inert conditions. (yield 45%)

4.7.5 Synthesis of $[\text{Cu}_2\{\mu-(\text{Ph}_2\text{P})_2\text{menapy}\}_2(\text{H}_2\text{O})_4](\text{PF}_6)_2$ (6)

A solution of 2,7-Bis(diphenylphosphino)-4-methylnaphthyridine ligand (25 mg; 0.049 mmol) in acetonitrile (4 ml) was added dropwise to a stirred solution of $[\text{Cu}(\text{MeCN})_4](\text{PF}_6)$ (18 mg; 0.049 mmol) in acetonitrile (4 ml). The solution turned red as soon as the $(\text{Ph}_2\text{P})_2\text{menapy}$ ligand was added. The mixture was stirred for 12 hours after which the volume of acetonitrile was concentrated to *ca.* 1 ml under reduced pressure and the solution filtered through glass microfibre filter paper. A red crystalline precipitate was obtained upon addition of diethyl ether and cooling to -10°C for 12 hours. This precipitate was filtered, washed with diethyl

ether and dried *in vacuo* for 1 hour to give an analytically pure sample. (yield 50-60%) Anal. Calcd for $\text{Cu}_2\text{C}_{66}\text{H}_{60}\text{F}_{12}\text{N}_4\text{O}_4\text{P}_6$: C, 52.35; H, 3.99; N, 3.70. Found: C, 53.09; H, 3.81; N, 3.90.

4.7.6 Synthesis of $[\text{Cu}_2\{\mu\text{-(PhP-menapy-OPPh)}\}_2(\text{MeCN})_2](\text{PF}_6)_2$ (7)

A solution of a mixture of the 2,7-Bis(diphenylphosphino)-4-methylnaphthyridine and the oxidised ($\text{Ph}_2\text{POmenapyPPH}_2$) ligands (25 mg) in acetonitrile (4 ml) was added dropwise to a stirred solution of $[\text{Cu}(\text{MeCN})_4](\text{PF}_6)$ (18 mg; 0.049 mmol) in acetonitrile (4 ml). It turned red as soon as the ligands were added. The mixture was stirred for 12 hours after which the volume of acetonitrile was concentrated to *ca.* 1 ml under reduced pressure and the solution filtered through glass microfibre filter paper. A mixture of a red crystalline precipitate and yellow crystals were obtained upon addition of diethyl ether and cooling to -10°C for 12 hours. The yellow crystals were complex 7.

4.7.7 Synthesis of $[\text{Ag}_2\{\mu\text{-(Ph}_2\text{P)}_2\text{menapy}\}_2(\text{H}_2\text{O})_4](\text{BF}_4)_2$ (8)

A solution of 2,7-Bis(diphenylphosphino)-4-methylnaphthyridine (25 mg; 0.049 mmol) in acetonitrile (4 ml) was added dropwise to a stirred solution of $[\text{Ag}(\text{COD})_2](\text{BF}_4)$ (21 mg; 0.049 mmol) in acetonitrile (4 ml). The solution turned yellow as soon as the ligand was added. The mixture was stirred for 12 hours after which the volume of acetonitrile was concentrated to *ca.* 1 ml under reduced pressure and the solution filtered through glass microfibre filter paper. A pale yellow crystalline precipitate was obtained upon addition of diethyl ether and cooling to -10°C for 12 hours. This precipitate was filtered, washed with diethyl ether and dried *in vacuo* for 1 hour to give an analytically pure sample. (yield 50-60%) Anal. Calcd for $\text{Ag}_2\text{C}_{66}\text{H}_{60}\text{B}_2\text{F}_8\text{N}_4\text{O}_4\text{P}_4$: C, 53.33; H, 4.07; N, 3.77. Found: C, 53.91; H, 3.84; N, 3.64.

4.7.8 Reaction of $(\text{Ph}_2\text{P})_2\text{menapy}$ with $[\text{Au}(\text{MeCN})_2](\text{SbF}_6)$

An excess of gold metal (19 mg; 0.098 mmol) was added as a solid to a stirred solution of NOSbF_6 (13 mg; 0.049 mmol) in acetonitrile (2 ml). This was left to stir for 12 hours which

resulted in the formation of $[\text{Au}(\text{MeCN})_2](\text{SbF}_6)$ which could not be isolated as a solid. The solution containing the $[\text{Au}(\text{MeCN})_2](\text{SbF}_6)$ complex was then filtered through glass microfibre filter paper to remove unreacted gold metal and added dropwise to a stirred solution of $(\text{Ph}_2\text{P})_2\text{menapy}$ (25 mg; 0.049 mmol) in acetonitrile (2 ml). The solution turned yellow as the $[\text{Au}(\text{MeCN})_2](\text{SbF}_6)$ complex was added. This was left to stir for 2 hours after which the volume of acetonitrile was concentrated to *ca.* 1 ml under reduced pressure. Diethyl ether was added and the mixture cooled to -10°C for a few hours. The solution became dark and a black oil formed that consisted of a number of ill-defined products.

TABLE 23: Spectroscopic Data for $(\text{Ph}_2\text{P})_2\text{menapy}$ and Its Complexes

Complex	Infrared Spectroscopic Data ^a cm ⁻¹	¹ H NMR ^b δ	³¹ P{ ¹ H} NMR ^c δ
$(\text{Ph}_2\text{P})_2\text{menapy}$	[1591(m), 1576(s)] ν(C-Nnapy) [1491(w), 1481(w), 1434(s)] ν(P-C)	8.6-7.2 (m,23H) 2.55 (s,3H)	0.2 (s) -1.4 (s)
$[\text{Cu}_2\{\mu-(\text{Ph}_2\text{P})_2\text{menapy}\}_2(\text{H}_2\text{O})_4](\text{PF}_6)_2$ (6)	[1591(m), 1576(m)] ν(C-Nnapy) [1496(w), 1484(w), 1437(m)] ν(P-C) [843(vs)] ν(P-F)	7.9-6.5 (m,46H) 2.2 (b,14H)	2.4 (b)
A mixture of $[\text{Cu}_2(\mu-\text{Ph}_2\text{POmenapyPPh}_2)_2(\text{MeCN})_2](\text{PF}_6)_2$ (7) and (6)	[1591(m), 1576(m)] ν(C-Nnapy) [1496(w), 1484(w), 1437(m)] ν(P-C) [843(vs)] ν(P-F)	7.9-6.5 (m) 2.2 (b)	2.4 (b) 17.0 (s)
$[\text{Ag}_2\{\mu-(\text{Ph}_2\text{P})_2\text{menapy}\}_2(\text{H}_2\text{O})_4](\text{BF}_4)_2$ (8)	[1592(m), 1580(m)] ν(C-Nnapy) [1493(w), 1482(w), 1438(s)] ν(P-C) [1084(vs), 1061(vs)] ν(B-F)	8.3-6.6 (m,46H) 2.6 (b,6H) 1.25 (b,8H)	18.0 (m) 7.9 (m)

a. All infrared spectra run as KBr discs. w = weak, m = medium, s = strong, vs = very strong

b. $(\text{Ph}_2\text{P})_2\text{menapy}$ run in CDCl_3 , **6** and **7** in CD_3CN and **8** in CD_2Cl_2 , m = multiplet, b = broad

c. $(\text{Ph}_2\text{P})_2\text{menapy}$ run in CHCl_3 , **6** and **8** run in MeCN on external lock. All values relative to H_3PO_4 . b = broad, s = singlet, m = multiplet.

APPENDIX A

General Experimental Details

1 Instrumentation

Carbon, hydrogen and nitrogen analyses were performed by Galbraith Laboratories, Knoxville, Tennessee, U.S.A.

Infrared spectra were recorded on a Shimadzu FT-1400 infrared spectrometer.

$^{31}\text{P}\{^1\text{H}\}$ NMR spectra were recorded on a Varian FT-80A spectrometer.

^1H NMR spectra were recorded on a Gemini 200 spectrometer. Deuterated solvents were employed in all cases.

Mass spectra were recorded on a Hewlett-Packard Gas Chromatographic-Mass Spectrometer (HP5988A).

Absorption spectra were recorded on a Shimadzu UV-2101PC UV-VIS Scanning Spectrophotometer.

Emission spectra were recorded on a Shimadzu RF-5000 recording spectrofluorophotometer at the University of Zululand.

2 Experimental Techniques

All reactions were performed under a dry nitrogen atmosphere using standard Schlenk techniques.

All solvents were freshly distilled and dried before use, using standard procedures. In the case of the synthesis of the ligands, the tetrahydrofuran was twice distilled before use. For emission

measurements AR grade solvents were degassed and then used.

3 Crystal Structure Determinations

(a) Data Collection

The intensities of the reflections were measured at 22°C with an Enraf-Nonius CAD-4 diffractometer using graphite monochromated Mo-K α radiation.

Cell constants were obtained by fitting the setting angles of 25 high-order reflections ($\theta > 12^\circ$). Three standard reflections were measured every hour to check any possible decomposition of the crystal. An $\omega - 2\theta$ scan with a variable speed up to a maximum of $5.49^\circ \cdot \text{min}^{-1}$ was used. The ω -angle changed as $a_\theta + b_\theta \tan \theta$ ($^\circ$), the horizontal aperture as $a_h + b_h \tan \theta$ (mm), but was limited to the range 1.3 - 5.9 mm. The vertical slit was fixed at 4 mm. Optimum values of a_θ , b_θ , a_h and b_h were determined for each crystal by a critical evaluation of peak shape for several reflections with different values of θ using the program OTPLOT (Omega-Theta plot; Enraf-Nonius diffractometer control program, 1988). Where applicable, a linear decay correction was applied using the mean value linear curves fitted through three intensity control reflections, measured at regular time intervals. Data were corrected for Lorentz and polarization effects, and where possible for absorption by the psi-scan (semi-empirical) method ⁶⁶.

(b) Structural Solution and Refinement

Direct methods or the Patterson function were used to solve the phase problem. Once a suitable phasing model was found, successive applications of Fourier and difference Fourier techniques allowed the location of the remaining non-hydrogen atoms. Hydrogen atoms were not located for any of the structures reported in this thesis. Weighted full-matrix least-squares methods were always used to refine the structure; the weighting scheme was chosen so as to find the smallest variation of the mean value of $\omega(F_o - F_c)^2$ as a function of the magnitude of F_o . R , R_w and the weighting scheme are defined as follows:

$$R = \frac{\sum |F_o - F_c|}{\sum |F_o|}, R_w = \frac{\sum \omega^{1/2} |F_o - F_c|}{\sum \omega^{1/2} |F_o|}$$

and $\omega = 1.0 / [\sigma(F)^2 + gF^2]$, where g is a variable.

Scattering factor data were taken from "International Tables for X-ray Crystallography", Kynoch Press, Birmingham, Vol. 4 (1974), pp94, 149. For all the structure solution calculations, the programs SHELX-76⁶⁷ and SHELX-86⁶⁸ were employed. Mean plane and torsion angle calculations were performed using the programs PLANE and TORSION of the SDP package⁶⁹. Plotting of structures was performed using the program ORTEP-II⁷⁰ while the tabulation of fractional coordinates, thermal parameters, interatomic distances and angles was achieved using the program TABLES⁷¹.

APPENDIX B

Sources of Chemicals

Chemical	Source
Li metal	Saarchem
2,2'-bipyridine	Fluka
POCl ₃	Merck
PCl ₅	Saarchem
NaNO ₂	Saarchem
Na ₂ CO ₃	Saarchem
MgSO ₄	Saarchem
NOSbF ₆	Strem
ethylacetoacetate	Merck
2,6-diaminopyridine	Merck
2-bromopyridine	Aldrich
chlorodiphenylphosphine	Strem
dichlorophenylphosphine	Fluka

All chemicals were used without further purification except for 2,6-diaminopyridine which was first distilled under reduced pressure at 150°C.

The starting materials [Cu(MeCN)₄](PF₆)⁶⁴ and [Ag(COD)₂](BF₄)⁶⁵ were prepared according to literature procedures.

REFERENCES

1. G.P. Newkome and C.J. Hager, *J. Org. Chem.*, 1978, **43**, 947.
2. I. Mittel, H. Schmidbaur and Y. Inoguchi, *Z. Naturforsch.*, 1980, **35b**, 1329.
3. R. Ziessel, *Tetrahedron Letters*, 1989, **30**, 463.
4. F.G. Mann and J. Watson, *J. Org. Chem.*, 1948, **13**, 502.
5. K. Issleib and D. Müller, *Chem. Ber.*, 1959, **92**, 3175.
6. G.R. Newkome, *Chem. Rev.*, 1993, 2067.
7. H. Christina, E. McFarlane, W. McFarlane and A.S. Muir, *Polyhedron*, 1990, **14**, 1757.
8. F.E. Wood, J. Hvoslef, H. Hope and A.L. Balch, *Inorg. Chem.*, 1984, **23**, 4309.
9. M. Olmstead, A. Maissonnet, J. Farr and A.L. Balch, *Inorg. Chem.*, 1981, **20**, 4060.
10. A.L. Balch, L.A. Fosset and M.M. Olmstead, *Inorg. Chem.*, 1986, **25**, 4526.
11. J.P. Farr, M.M. Olmstead, C.H. Hunt and A.L. Balch, *Inorg. Chem.*, 1981, **20**, 1182.
12. F.E. Wood, M.M. Olmstead and A.L. Balch, *J. Am. Chem. Soc.*, 1983, **105**, 6332.
13. F.E. Wood, J. Hvoslef and A.L. Balch, *J. Am. Chem. Soc.*, 1983, **105**, 6986.
14. A.L. Balch, H. Hope and F.E. Wood, *J. Am. Chem. Soc.*, 1985, **107**, 6936.
15. S. Shieh, D. Li, S. Peng and C. Che, *J. Chem. Soc., Dalton Trans.*, 1993, 195.
16. Y. Inoguchi, B. Milewski-Mahrla, D. Neugebauer, P.G. Jones and H. Schmidbaur, *Chem. Ber.*, 1983, **116**, 1487.
17. Y. Inoguchi, B. Milewski-Mahrla and H. Schmidbaur, *Chem. Ber.*, 1984, **115**, 3085.
18. G.R. Newkome, D.W. Evans and F.R. Fronczek, *Inorg. Chem.*, 1987, **26**, 3500.
19. K. Wajda-Hermanowicz and F. Pruchnik, *Transition Met. Chem.*, 1988, **13**, 101.
20. P. Espinet, P. Gómez-Elipé and F. Villafañe, *J. Organo. Met. Chem.*, 1993, 145.
21. M.G. Ehrlich, F.R. Fronczek, S.F. Watkins, G.R. Newkome and D.C. Hager, *Acta Cryst., C (Cr. Str. Comm.)*, **40**, 78, 1984.
22. W.W. Paulder and T.J. Kress, *J. Heterocycl. Chem.*, 1967, **4**, 284.
23. A. Reissert, *Ber.*, 1893, **26**, 2137.
24. E.V. Brown, *J. Org. Chem.*, 1965, **30**, 1607.
25. O. Seide, *Ber.*, 1926, **59**, 2465.
26. E.L. Enwall and K. Emerson, *Acta Cryst.*, 1979, **35**, 2562.

27. G.W. Bushnell, K.R. Dixon and M.A. Khan, *Can. J. Chem.*, 1978, **56**, 450.
28. J.L. Dewan, D.L. Kepert and A.H. White, *J. Chem. Soc., Dalton Trans.*, 1975, 490.
29. C. Mealli and L. Sacconi, *Acta. Cryst.*, 1977, **33**, 710.
30. J.M. Epstein, J.C. Dewan, D.L. Kepert and A.H. White, *J. Chem. Soc., Dalton Trans.*, 1974, 1949.
31. A. Clearfield and P. Singh, *J. Chem. Soc. Chem. Commun.*, 1970, 389.
32. P. Singh, A. Clearfield and I. Bernal, *J. Coord. Chem.*, 1971, **1**, 29.
33. A. Tiripichio, M.J. Camellini, R. Uson, L.A. Oro, M.A. Ciriano and F. Vigan, *J. Chem. Soc., Dalton Trans.*, 1984, 125.
34. C. Mealli and F. Zonobini, *J. Chem. Soc. Chem. Commun.*, 1982, 97.
35. D. Gatteschi, C. Mealli and L. Sacconi, *J. Am. Chem. Soc.*, 1973, **95**, 2736.
36. V. Jain, V. Jakkal and R. Bohra, *J. Organomet. Chem.*, 1990, **319**, 417.
37. J. Farr, M. Olmstead, F. Wood and A. Balch, *J. Am. Chem. Soc.*, 1983, **105**, 792.
38. N. Alcock, P. Moore, P. Lampe and K. Mok, *J. Chem. Soc., Dalton Trans.*, 1982, 207.
39. Y. Inguchi, B. Milewski-Mahrla, D. Neugebauer, P. Jones and H. Schmidbaur, *Chem. Ber.*, 1983, **16**, 1487.
40. J. Farr, M. Olmstead, C. Hunt and A. Balch, *Inorg. Chem.*, 1981, **20**, 1182.
41. Z. Tortorelli, C. Tucker, C. Woods and J. Bardner, *Inorg. Chem.*, 1986, **25**, 3534.
42. Z.Z. Zhong, H-S. Wong, X. Zhen, X-K. Yao and R-J. Wang, *J. Organomet. Chem.*, 1989, **376**, 123.
43. A. Maisonnnet, J. Farr, M. Olmstead and C. Hunt, *Inorg. Chem.*, 1982, **21**, 3961.
44. E. Lastra, M. Gamasa, J. Gimeno, M. Lanbrónchi and D. Tiripicchio, *J. Chem. Soc., Dalton Trans.*, 1989, 1499.
45. S.J. Berners-Price, L.A. Golguhoun, P.C. Healy, K.A. Byriel and J.V. Hanna, *J. Chem. Soc., Dalton Trans.*, 1992, 3357.
46. J. Diez, M.P. Gamasa, J. Gimerio, A. Tiripicchio and M.T. Gamellini, *J. Chem. Soc., Dalton Trans.*, 1987, 1275.
47. D.M. Ho, R. Bau, *Inorg. Chem.*, 1983, **22**, 4079.
48. S. Kitigawa and M. Munakata, *Inorg. chem.*, 1981, **20**, 2261.
49. K. Nilsson and Å. Oskarsson, *Acta. Chem. Scand.*, 1982, **36(A)**, 605.

50. K.D. Karlin, Y. Gultneh, J.P. Hitchinson and J. Zubieta, *J. Am. Chem. Soc.*, 1982, **104**, 5240.
51. D.M. Ho and R. Bau, *Inorg. Chem.*, 1983, **22**, 4073.
52. A.A.M. Aly, D. Neugebauer, O. Orama, U. Schakert and H. Schmidbaur, *Angew. Chem. Int. Ed. (Engl.)*, 1978, **17**, 125.
53. A.F.M.J. van der Ploeg, G. van Koten and A.L. Spek, *Inorg. Chem.*, 1979, **18**, 1052.
54. C. Che, H. Yip, W. Lo and S. Peng, *Polyhedron*, 1994, **13**, 887.
55. C. che, H. Kwong, V.W. Yam and K. Cho, *J. Chem. Soc., Chem. Commun.*, 1989, 885.
56. C. Che, H. Yip, D. Li, S. Peng, G. Lee, Y. Wang and S. Liu, *J. Chem. Soc., Chem. Commun.*, 1991, 1615.
57. V.W. Yam, T. Lai and C. Che, *J. Chem. Soc., Dalton Trans.*, 1990, 3747.
58. C. Che, H. Yip, V.W. Yam, P. Cheung, T. Lai, S. Shieh and S. Peng, *J. Chem. Soc., Dalton Trans.*, 1992, 427.
59. C. King, J.C. Wang, N.I.M. Khan and J.P. Fackler, *Inorg. Chem.*, 1989, **28**, 2145.
60. G.R. Newkome, S.J. Garbis, V.K. Majestic, F.R. Fronczek and G. Chiari, *J. Org. Chem.*, 1981, **46**, 833.
61. K.D. Karlin, J.C. Hayes, Y. Gultneh, R.W. Cruse, J.W. McKowan, J.P. Hutchinson and J. Zubieta, *J. Am. Chem. Soc.*, 1984, **106**, 2121.
62. K.D. Karlin, J.C. Hayes, Y. Gultneh, R.W. Cruse, and J. Zubieta, *J. Am. Chem. Soc.*, 1987, **109**, 2668.
63. P. Fanwick, Personal Communication. The triclinic cell parameters for $[\text{Cu}_2(\mu\text{-Ph}_2\text{POMenapyPPh}_2)_2(\text{MeCN})_2](\text{PF}_6)_2$ are (at 295 K) $a = 9.314(1)$, $b = 14.049(1)$, $c = 14.959 \text{ \AA}$, $\alpha = 95.22(1)$, $\beta = 101.09(1)$, $\gamma = 102.42(1)^\circ$, and $Z = 1$. There were no systematic absences; the space group was determined to be $P\bar{1}$. The structure was refined to $R = 0.052$ and the number of parameters was 451.
64. G.J. Kubas, *Inorg. Syn.*, 1979, **19**, 90.
65. A. Albinati, S.V. Mülle and G. Carturan, *J. Organomet. Chem.*, 1979, **182**, 269.
66. A.C.T. North, D.C. Philips and F.S. Mathews, *Acta Crystallogr., Sect. A.*, 1968, **24**, 351.
67. G. Sheldrick, SHELX-76, Program for Crystal Structure Determination, University of

Cambridge, 1976.

68. G. Sheldrick, SHELX-86, Program for Crystal Structure Determination, University of Göttingen, 1976.
69. Structure Determination Package, B.A. Frenze and Associates Inc., College Station, Texas 77480, USA; and Enraf-Nonius, Delft, Holland, 1985.
70. C. Johnson, ORTEP-II, A Fortran Thermal Epsiloid Programme for Crystal Structure Illustrations, Oak Ridge National Laboratory, Tennessee, 1976.
71. D. Liles. TABLES, Program for Tabulation of Crystallographic Data, Council for Scientific and Industrial Research (Pretoria), 1988.

